Volume 23, Number 4, 2023 ISSN 1562-8353

NONLINEAR DYNAMICS AND SYSTEMS THEORY
An International Journal of Research and Surveys

Volume 23 Number 4 2023

CONTENTS

ISSN 1562-8353 Printed in Ukraine
To receive contents and abstracts by e-mail, visit our Website at: **http://www.e-ndst.kiev.ua**

NONLINEAR DYNAMICS & SYSTEMS THEORY

Volume 23, No. 4, 2023

Nonlinear Dynamics and Systems Theory

An International Journal of Research and Surveys

InforMath Publishing Group
http://www.e-ndst.kiev.ua

Nonlinear Dynamics and Systems Theory
An International Journal of Research and Surveys

INSTRUCTIONS FOR CONTRIBUTORS

(1) General. Nonlinear Dynamics and Systems Theory (ND&ST) is an international journal devoted to publishing peer-refereed, high quality, original papers, brief notes and review articles focusing on nonlinear dynamics and systems theory and their practical applications in engineering, physical and life sciences. Submission of a manuscript is a representation that the submission has been approved by all of the authors and by the institution where the work was carried out. It also represents that the manuscript has not been previously published, has not been copyrighted, is not being submitted for publication elsewhere, and that the authors have agreed that the copyright in the article shall be assigned exclusively to InforMath Publishing Group by signing a transfer of copyright form. Before submission, the authors should visit the website:

http://www.e-ndst.kiev.ua

for information on the preparation of accepted manuscripts. Please download the archive Sample_NDST.zip containing example of article file (you can edit only the file Samplefilename.tex).

(2) Manuscript and Correspondence. Manuscripts should be in English and must meet common standards of usage and grammar. To submit a paper, send by e-mail a file in PDF format directly to

Professor A.A. Martynyuk, Institute of Mechanics,
Nesterov str.3, 03057, MSP 680, Kiev-57, Ukraine
e-mail: journalndst@gmail.com

or to one of the Regional Editors or to a member of the Editorial Board. Final version of the manuscript must typeset using LaTex program which is prepared in accordance with the style file of the Journal. Manuscript texts should contain the title of the article, name(s) of the author(s) and complete affiliations. Each article requires an abstract not exceeding 150 words. Formulas and citations should not be included in the abstract. AMS subject classifications and key words must be included in all accepted papers. Each article requires a running head (abbreviated form of the title) of no more than 30 characters. The sizes for regular papers, survey articles, brief notes, letters to editors and book reviews are: (i) 10-14 pages for regular papers, (ii) up to 24 pages for survey articles, and (iii) 2-3 pages for brief notes, letters to the editor and book reviews.

(3) Tables, Graphs and Illustrations. Each figure must be of a quality suitable for direct reproduction and must include a caption. Drawings should include all relevant details and should be drawn professionally in black ink on plain white drawing paper. In addition to a hard copy of the artwork, it is necessary to attach the electronic file of the artwork (preferably in PCX format).

(4) References. Each entry must be cited in the text by author(s) and number or by number alone. All references should be listed in their alphabetic order. Use please the following style:

Journal: [1] H. Poincare, Title of the article. *Title of the Journal* **volume** (issue) (year) pages. [Language]

Book: [2] A.M. Lyapunov, *Title of the Book.* Name of the Publishers, Town, year.

Proceeding: [3] R. Bellman, Title of the article. In: *Title of the Book.* (Eds.). Name of the Publishers, Town, year, pages. [Language]

(5) Proofs and Sample Copy. Proofs sent to authors should be returned to the Editorial Office with corrections within three days after receipt. The corresponding author will receive a sample copy of the issue of the Journal for which his/her paper is published.

(6) Editorial Policy. Every submission will undergo a stringent peer review process. An editor will be assigned to handle the review process of the paper. He/she will secure at least two reviewers' reports. The decision on acceptance, rejection or acceptance subject to revision will be made based on these reviewers' reports and the editor's own reading of the paper.

NONLINEAR DYNAMICS AND SYSTEMS THEORY
An International Journal of Research and Surveys
Published by InforMath Publishing Group since 2001

Volume 23 Number 4 2023

CONTENTS

Founded by A.A. Martynyuk in 2001.
Registered in Ukraine Number: KB No 5267 / 04.07.2001.

NONLINEAR DYNAMICS AND SYSTEMS THEORY
An International Journal of Research and Surveys

Impact Factor from SCOPUS for 2022: SJR – 0.293, SNIP – 0.784 and CiteScore – 1.5

Nonlinear Dynamics and Systems Theory (ISSN 1562–8353 (Print), ISSN 1813–7385 (Online)) is an international journal published under the auspices of the S.P. Timoshenko Institute of Mechanics of National Academy of Sciences of Ukraine and Curtin University of Technology (Perth, Australia). It aims to publish high quality original scientific papers and surveys in areas of nonlinear dynamics and systems theory and their real world applications.

AIMS AND SCOPE

Nonlinear Dynamics and Systems Theory is a multidisciplinary journal. It publishes papers focusing on proofs of important theorems as well as papers presenting new ideas and new theory, conjectures, numerical algorithms and physical experiments in areas related to nonlinear dynamics and systems theory. Papers that deal with theoretical aspects of nonlinear dynamics and/or systems theory should contain significant mathematical results with an indication of their possible applications. Papers that emphasize applications should contain new mathematical models of real world phenomena and/or description of engineering problems. They should include rigorous analysis of data used and results obtained. Papers that integrate and interrelate ideas and methods of nonlinear dynamics and systems theory will be particularly welcomed. This journal and the individual contributions published therein are protected under the copyright by International InforMath Publishing Group.

PUBLICATION AND SUBSCRIPTION INFORMATION

Nonlinear Dynamics and Systems Theory will have 5 issues in 2023, printed in hard copy (ISSN 1562–8353) and available online (ISSN 1813–7385), by InforMath Publishing Group, Nesterov str., 3, Institute of Mechanics, Kiev, MSP 680, Ukraine, 03057. Subscription prices are available upon request from the Publisher, EBSCO Information Services (`mailto:journals@ebsco.com`), or website of the Journal: `http://e-ndst.kiev.ua`. Subscriptions are accepted on a calendar year basis. Issues are sent by airmail to all countries of the world. Claims for missing issues should be made within six months of the date of dispatch.

ABSTRACTING AND INDEXING SERVICES

Papers published in this journal are indexed or abstracted in: Mathematical Reviews / MathSciNet, Zentralblatt MATH / Mathematics Abstracts, PASCAL database (INIST–CNRS) and SCOPUS.

Nonlinear Dynamics and Systems Theory, **23** (4) (2023) 359–366

A Novel Fractional-Order Chaotic System and Its Synchronization via Adaptive Control Method

Rami Amira [1] and Fareh Hannachi [2*]

[1] *Laboratory of Mathematics, Informatics and Systems (LAMIS), Echahid Cheikh Larbi Tebessi University, Tebessa, Algeria.*
[2] *Echahid Cheikh Larbi Tebessi University, Tebessa, Algeria.*

Received: May 8, 2023; Revised: September 27, 2023

Abstract: In this paper, the synchronization of a new fractional-order chaotic system via the adaptive control method is introduced. Firstly, the novel fractional-order system is presented and its dynamics is investigated throughout the Lyapunov exponents spectrum. Secondly, based on the stability theory of fractional-order systems, synchronization of the fractional-order system with fully uncertain parameters is realized by designing appropriate adaptive controllers and estimation laws. Finally, numerical simulations are implemented to demonstrate the effectiveness and flexibility of the synchronization controllers and the estimation laws for the unknown parameters.

Keywords: *chaotic system; strange attractor; Lyapunov exponent; Lyapunov stability theory; adaptive control; synchronization.*

Mathematics Subject Classification (2010): 34D08, 34C28, 37B55, 37B25, 37D45, 70K20, 93D05, 93D21

1 Introduction

Fractional chaotic dynamical systems are non-linear systems that allow sensitivity to initial conditions, those chaotic systems are widely used in several fields such as physics, chemistry, biology, economics, especially in secure communication and cryptography[1-2].

In 1990, Pecora and Carol [3] introduced for the first time a method of synchronization of two integer-order chaotic systems. After that, many research papers have addressed synchronization between integer-integer order chaotic systems [4-6]. Recently,

* Corresponding author: mailto:fareh.hannachi@univ-tebessa.dz

the synchronization of chaos within fractional chaotic systems has attracted a considerable attention and different techniques have been used to achieve different types of synchronization for these systems, among them, active control [7-8], backstepping control [10], and the modified projective synchronization [11], the hyprid projective synchronization [12], the full state hybrid projective synchronization [13], the inverse full state hybrid projective synchronization [14]. An adaptive control method [15-17] is one of the robust control methods used for chaos synchronization when parameters are unknown or initially uncertain. In an adaptive method, the control law and the parameter update law are designed so that the chaotic response system behaves like chaotic drive systems. Thus, the adaptive scheme maintains a system's consistent performance in the presence of uncertainty and variation in plant parameters. This control method differs from other control methods because it does not require advance information about the limits on these uncertain or time-varying parameters because it relates to a control law that changes itself. Several research papers study adaptive control in the case of integer-order systems, see F. Hannachi [15] and V. Sundarapandian [16-17]. However, the works presented and related to the synchronization between fractional-order chaotic systems remain limited, and finding new results using this method of control is required because of its important applications, especially in the fields of secure communication and encryption [18-20]. In this work, a novel fractional order system is presented and its chaoticity is confirmed using the Lyapunouv exponents tool. Moreover, the synchronization of the fractional-order system with unknown parameters is realized by designing appropriate adaptive controllers and estimation laws using the stability theory of fractional-order systems. Finally, the effectiveness of the proposed scheme for this type of synchronization is demonstrated by an illustrative example with numerical simulation in Matlab.

This paper is organized as follows. In Sections 2 and 3, basic tools of fractional calculus and a description of the novel fractional-order chaotic system are given. In Section 4, using the new chaotic system, chaos synchronization between fractional-fractional chaotic systems for commensurate orders via the adaptive control method and stability theory of fractional-order systems is investigated. In Section 5, numerical simulations are given to demonstrate the effectiveness and flexibility of the synchronization controllers and the estimation laws for the unknown parameters. The conclusion is given in Section 6.

2 Basics of Fractional Calculus

Definition 2.1 ([21]){Caputo fractional derivative}
The Caputo fractional derivative of order $q \in \mathbb{R}^+$ on the half axis $\mathbb{R}^+$ is defined as follows:

$$ {}_a^C D_t^q f(t) = \frac{1}{\Gamma(n-q)} \int_a^t \frac{f^{(n)}(\tau)}{(t-\tau)^{q-n+1}} d\tau, t > a, \tag{1} $$

with $n = \min\{k \in \mathbb{N}/k > q\}, q > 0$.

To simplify the notation, we replace ${}_a^C D_t^q f(t)$ by ${}^C D_t^q f(t)$.

Lemma 2.1 *The trivial solution of the following fractional-order system:*

$$ D_t^q X(t) = F(X(t)), $$

where D_t^q is the Caputo fractional derivative of order $q, 0 < q \leq 1, F : R^n \longrightarrow R^n$, is asymptotically stable if there exists a positive definite function $V(X(t))$ such that $D_t^q V(X(t)) < 0$ for all $t > 0$.

Lemma 2.2 *Let $x(t) \in \mathbb{R}$ be a continuous and derivable function. Then, for any time instant $t \geqslant t_0$,*

$$\frac{1}{2}{}^C D_t^\alpha x^2(t) \leqslant x(t){}_{t_0}^C D_t^\alpha x(t), \quad \forall \alpha \in (0,1).$$

3 Presentation of the New Fractional-Order System

Several works [24-26] have reported on a 3-D dynamic model of finance (the Ma system) and offered its simplified system equations. In this paper, we consider the fractional version of this simplified finance system [26] given by

$$\begin{cases} {}^C D_t^{q_1} x_1(t) = -a(x_1 + x_2), \\ {}^C D_t^{q_2} x_2 = -x_2 - c x_1 x_3, \\ {}^C D_t^{q_3} x_3 = b + a x_1 x_2, \end{cases} \tag{2}$$

where D^q is the Caputo derivative operator, a, b, c are positive reals parameters. The model describes the time variations of three state variables $x_i, i = \overline{1,3}$: the interest rate x_1, the investment demand x_2, and the price index x_3. With the chosen parameters $a = 4, b = 20, c = 4$ and with the orders $(q_1; q_2; q_3) = (0.9; 0.95; 0.98)$;$(x_1(0); x_2(0); x_3(0)) = (0.4; 0.5; 0.2)$, the Lyapunov exponents are computed using the Benettin–Wolf algorithm [23] in Matlab and given as follows:

$$L_1 = 1.2790; L_2 = -0.0001 \simeq 0; L_3 = -6.7482. \tag{3}$$

So, we have $L_1 > 0$, then the novel fractional system (2) is chaotic. The chaotic attractor and the Lyapynov spectrum are depicted in Fig.1. Indeed, the Kaplan-Yorke dimension for this chaotic system is calculated as

$$D_{KY} = 2 + \frac{L_1 + L_2}{|L_3|} = 2.1895. \tag{4}$$

4 Adaptive Synchronization of the Novel Fractional System with Commensurate Order

This section aims to design an adaptive control law for globally synchronizing the identical novel fractional chaotic system with unknown system parameters. The master system is given by

$$\begin{cases} {}^C D_t^{q} x_1(t) = -a(x_1 + x_2), \\ {}^C D_t^{q} x_2(t) = -x_2 - d x_1 x_3, \\ {}^C D_t^{q} x_3(t) = b + a x_1 x_2. \end{cases} \tag{5}$$

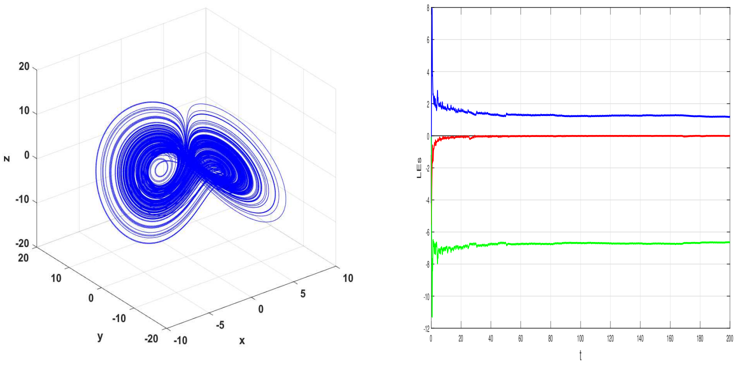

Figure 1: Lyapunov exponents spectrum.

The slave system is obtained as follows:

$$\begin{cases} {}^{C}D_t^q y_1(t) = -a(y_1 + y_2) + u_1, \\ \\ {}^{C}D_t^q y_2(t) = -y_2 - cy_1y_3 + u_2, \\ \\ {}^{C}D_t^q y_3(t) = b + ay_1y_2 + u_3. \end{cases} \tag{6}$$

In both systems (5) and (6), we have parameters a, b, c, which are unknown, and their estimates $a_1(t), b_1(t), c_1(t)$, respectively. We will later search for an adaptive feedback controls u_1, u_2, u_3. Define now the synchronization error between the systems (5) and (6) as

$$e_i = y_i - x_i, i = \overline{1,3}. \tag{7}$$

Equation (7) implies

$${}^{C}D_t^q e_i(t) = {}^{C}D_t^q y_i(t) - {}^{C}D_t^q x_i(t), i = \overline{1,3}. \tag{8}$$

Thus, the synchronization error dynamics between (5) and (6) is obtained as

$$\begin{cases} {}^{C}D_t^q e_1(t) = a(e_1 + e_2) + u_1, \\ \\ {}^{C}D_t^q e_2(t) = -e_2 + cx_1x_3 - cy_1y_3 + u_2, \\ \\ {}^{C}D_t^q e_3(t) = a(y_1y_2 - x_1x_2) + u_3. \end{cases} \tag{9}$$

We take the adaptive control law as follows:

$$\begin{cases} u_1 = -a_1(e_2 + e_2) - k_1e_1, \\ u_2 = e_2 - c_1x_1x_3 + c_1y_1y_3 - k_2e_2, \\ u_3 = -a_1(y_1y_2 - x_1x_2) - k_3e_3, \end{cases} \tag{10}$$

where $k_i > 0$, i=1,...,3, are the gains constants.

By substituting (10) into (9), we obtain the closed-loop error as

$$\begin{cases} {}^{C}\!D_t^q e_1(t) = (a - a_1)(e_2 + e_1) - k_1 e_1, \\ {}^{C}\!D_t^q e_2(t) = (c - c_1)(x_1 x_3 - y_1 y_3) - k_2 e_2, \\ {}^{C}\!D_t^q e_3(t) = (a - a_1)(y_1 y_2 - x_1 x_2) - k_3 e_3. \end{cases} \tag{11}$$

We can define the estimation errors for the parameters as

$$\begin{cases} e_a(t) = a - a_1(t), \\ e_b(t) = b - b_1(t), \\ e_c(t) = c - c_1(t). \end{cases} \tag{12}$$

Applying the Caputo derivative of order q in (12), we obtain

$$\begin{cases} {}^{C}\!D_t^q e_a(t) = -{}^{C}\!D_t^q a_1(t), \\ {}^{C}\!D_t^q e_b(t) = -{}^{C}\!D_t^q b_1(t), \\ {}^{C}\!D_t^q e_c(t) = -{}^{C}\!D_t^q c_1(t). \end{cases} \tag{13}$$

By using (12), we rewrite the closed-loop system (11) as

$$\begin{cases} {}^{C}\!D_t^q e_1(t) = e_a(e_2 + e_1) - k_1 e_1, \\ {}^{C}\!D_t^q e_2(t) = e_c(x_1 x_3 - y_1 y_3) - k_2 e_2, \\ {}^{C}\!D_t^q e_3(t) = e_a(y_1 y_2 - x_1 x_2) - k_3 e_3. \end{cases} \tag{14}$$

Our goal now is to lead the system (14) to zero. Let us choose the Lyapunov candidate function as follows:

$$V(e_1, e_2, e_3, e_a, e_c) = \frac{1}{2}\left(k_1 e_1^2 + k_2 e_2^2 + k_3 e_3^2 + e_a^2 + e_c^2\right), \tag{15}$$

which is a positive definite function on $\mathbb{R}^5$. Applying the Caputo operator of differentiation in V along the trajectories of the systems (13) and (14) and using Lemma 2.2, we obtain

$$\begin{cases} {}^{C}\!D_t^q V(e_1, e_2, e_3, e_a, e_c) = \frac{1}{2} D^q k_1 e_1^2 + \frac{1}{2} k_2 D^q e_2^2 + \frac{1}{2} k_3 D^q e_3^2 + \frac{1}{2} D^q e_a^2 + \frac{1}{2} D^q e_c^2 \\ \leq k_1 e_1 D^q e_1 + k_2 e_2 D^q e_2 + k_3 e_3 D^q e_3 + e_a D^q e_a + e_c D^q e_c \\ \leq -k_1^2 e_1^2 - k_2^2 e_2^2 - k_3^2 e_3^2 + e_a\left(k_1 e_1^2 + k_1 e_1 e_2 + k_3 e_3 y_1 y_2 - k_3 e_3 x_1 x_2 - D^q a_1(t)\right) \\ +e_c\left(k_2 e_2 x_1 x_3 - k_2 e_2 y_1 y_3 - D^q c_1(t)\right). \end{cases} \tag{16}$$

In view of (16), we take the parameter update law as follows:

$$\begin{cases} {}^{C}\!D_t^q a_1(t) = k_1 e_1^2 + k_1 e_1 e_2 + k_3 e_3 y_1 y_2 - k_3 e_3 x_1 x_2, \\ {}^{C}\!D_t^q c_1(t) = k_2 e_2 x_1 x_3 - k_2 e_2 y_1 y_3. \end{cases} \tag{17}$$

Substituting (17) into (16), we obtain

$$ {}^{C}\!D_t^q V(e_1, e_2, e_3, e_a, e_c) \leq -k_1^2 e_1^2 - k_2^2 e_2^2 - k_3^2 e_3^2 < 0.$$

Hence, the zero solution of the error system (16) is assymptoticlly stable and the following theorem is proved.

Theorem 4.1 *The novel fractional chaotic systems (5) and (6) with unknown parameters are globally synchronized for all initial conditions by the adaptive control law (10) and the parameter update law (17) with $k_i > 0$ gains constants.*

5 Numerical Simulation

In order to verify our results, we use the Adams-Bashforth-Moulton algorithm [22] for the fractional-order system to solve the systems of differential equations (5), (6), (14) and (17). The initial conditions are chosen as $(x_1(0), x_2(0), x_3(0)) = (0.4, 0.5, 0.2)$, $(y_1(0), y_2(0), y_3(0)) = (5.4, -4.5, 2.2)$, respectively. $(e_1(0), e_2(0), e_3(0)) = (5, -5, 2)$, $(a_1(0), c_1(0)(0)) = (5, 4.5)$. In Fig.2, the synchronization between the states x_i and y_i, $i = \overline{1,3}$, is depicted. In Fig.3, the time-history of the synchronization errors $e_1(t), e_2(t), e_3(t)$ is depicted.

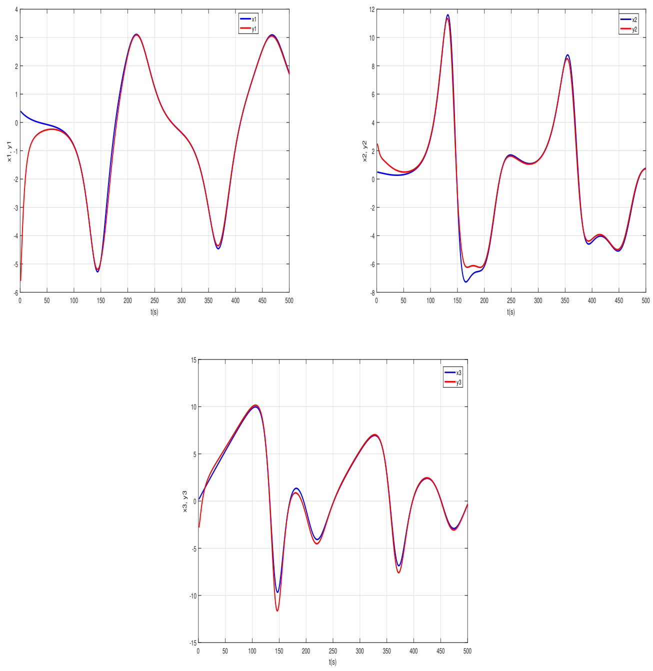

Figure 2: Synchronization between $x_i, y_i, i = 1, 2, 3$.

6 Conclusion

This paper reports on a new fractional-order chaotic system and its synchronization via the adaptive control method. The novel fractional-order system is presented and its chaoticity is confirmed using the Lyapunov exponents tool. Moreover, the synchronization of the fractional-order system with unknown parameters is realized by designing appropriate adaptive controllers and estimation laws using the stability theory of fractional-order systems. Numerical simulations are implemented to demonstrate the effectiveness and flexibility of the synchronization controllers and the estimation laws for the unknown parameters.

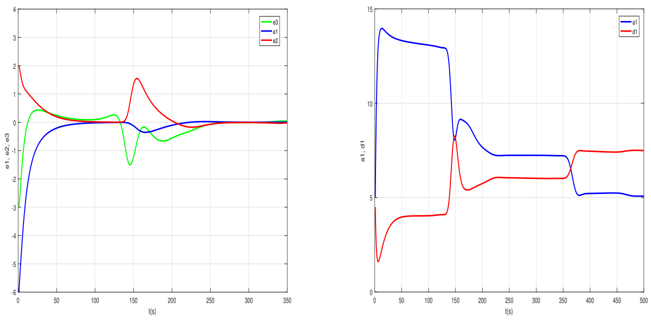

Figure 3: (a) The time-history of the synchronization errors $e_1(t), e_2(t), e_3(t)$ and (b) Parameters estimation.

7 Concluding remarks

The main important points in this work are:

- A novel fractional-order financial system is presented and its chaoticity is confirmed using the Lyapunov exponents.
- The synchronization between identical 3-D fractional-order financial systems with commensurate order and unknown parameters is achieved by designing appropriate adaptive controllers and estimation laws using the stability theory of fractional-order systems.

The results achieved through the study of the novel fractional-order financial system have wide-ranging applications. These include areas such as secure communication and signal encryption, making further research of the system particularly relevant. As such, they will be given due consideration in future work.

Acknowledgment

The author would like to thank the editor in chief and the referees for their valuable suggestions and comments.

References

[1] N. Smaoui and A. Kanso. Cryptography with chaos and shadowing. *Chaos, Solitons and Fractals* **42** (4) (2009) 2312–2321.

[2] A. A. Zaher and A. Abu-Rezq. On the design of chaos-based secure communication systems. *Communications in Nonlinear Science and Numerical Simulation* **16** (9) (2011) 3721–3737.

[3] L. M. Pecora and T. L. Caroll. Synchronization in chaotic systems. *Physical Review Letters* **64** (1990) 821–825.

[4] F. Hannachi. Analysis and Adaptive Control Synchronization of a Novel 3-D Chaotic System. *Nonlinear Dynamics and Systems Theory* **19** (1) (2019) 68–78.

[5] H. Adloo and M. Roopaei. Review article on adaptive synchronization of chaotic systems with unknown parameters. *Nonlinear Dynamics* **65** (1) (2011) 141–159.

[6] G. H. Li. Modified projective synchronization of chaotic system. *Chaos, Solitons and Fractals* **32** (5) (2007) 1786–1790.

[7] S. M. Hamidzadeh and R. Esmaelzadeh. Control and synchronization chaotic satellite using active control. *International Journal of Computer Applications* **94** (10) (2014) 29–33.

[8] S. Bhalekar. Synchronization of non-identical fractional order hyperchaotic systems using active control. *World Journal of Modelling and Simulation* **10** (1) (2014) 60–68.

[9] D. Hamri and F. Hannachi. A New Fractional-Order 3D Chaotic System Analysis and Synchronization. *Nonlinear Dynamics and Systems Theory* **21** (4) (2021) 381–392.

[10] S. Vaidyanathan, B. A. Idowu and A. T. Azar. Backstepping controller design for the global chaos synchronization of Sprott's jerk systems. *Chaos modeling and control systems design* (2015) 39–58.

[11] N. Boudjerida, M. S. Abdeloahab and R. Lozi . Modified projective synchronization of fractional-order hyperchaotic memristor-based Chua's circuit. *J. Innov. Appl. Math. Comput. Sci.* **2** (3) (2022) 69–82.

[12] N. Jia and T. Wang. Chaos control and hybrid projective synchronization for a class of new chaotic systems. *Computers and Mathematics with Applications* **62** (12) (2011) 4783–4795.

[13] S. Vaidyanathan, C. Volos. Analysis and adaptive control of a novel 3-D conservative no-equilibrium chaotic system. *Archives of Control Sciences* **25** (3) (2015) 333–353.

[14] A. Ouannas and G.Grassi. Inverse full state hybrid projective synchronization for chaotic maps with different dimensions. *Chinese Physics B* **25** (9) (2016) 090503.

[15] F. Hannachi. Analysis, dynamics and adaptive control synchronization of a novel chaotic 3-D system. *SN Applied Sciences* **1**:158 (2019).

[16] S. Vaidyanathan, Q. Zhu and A. T. Azar. Adaptive control of a novel nonlinear double convection chaotic system. In: *Fractional Order Control and Synchronization of Chaotic Systems*. Springer, Cham, 2017, 357–385.

[17] S. Vaidyanathan and Volos, C. Analysis and adaptive control of a novel 3-D conservative no-equilibrium chaotic system. *Archives of Control Sciences* **25** (3) (2015) 333–353.

[18] S. Banerjee. Chaos Synchronization and Cryptography for Secure Communications: Applications for Encryption. IGI global, 2010.

[19] C. K.Volos, I. M. Kyprianidis and I. N .Stouboulos. Image encryption process based on chaotic synchronization phenomena. *Signal Processing* **93** (5) (2013) 1328–1340.

[20] L. Keuninckx, M. C. Soriano, I. Fischer, C. R. Mirasso, R. M .Nguimdo and G. Van der Sande. Encryption key distribution via chaos synchronization. *Scientific reports* **7** (1) (2017) 1–14.

[21] I. Petras. *Fractional-Order Nonlinear Systems.* Springer, Berlin, 2011.

[22] K. Diethelm, N. J. Ford and A. D. Freed. A predictor-corrector approach for the numerical solution of fractional differential equations. *Nonlinear Dynamics* **29** (1) (2002) 3–22.

[23] M. F. Danca. Matlab code for Lyapunov exponents of fractional-order systems, part ii: the noncommensurate case. International Journal of *Bifurcation and Chaos* **31** (12) (2021) 2150187.

[24] J. H. Ma and Y. S. Chen. Study for the bifurcation topological structure and the global complicated character of a kind of nonlinear finance system (I). *Appl. Math. Mech.* (English Ed.) **22** (2001) 1240–1251.

[25] J. H. Ma and Y. S.Chen. Study for the bifurcation topological structure and the global complicated character of a kind of nonlinear finance system (II). Appl. Math. Mech. (English Ed.) **22** (2001) 1375–1382.

[26] J. Ding, W. Yang and H. Yao. A new modified hyperchaotic finance system and its control. *International Journal of Nonlinear Science* **8** (1) (2009) 59–66.

Nonlinear Dynamics and Systems Theory, **23** (4) (2023) 367–380

Analysis of Problems in Generalized Viscoplasticity under Dynamic Thermal Loading

I. Boukaroura * and A. Djabi

Applied Mathematics Laboratory, Ferhat Abbas-Setif 1 University, Setif,19000, Algeria

Received: May 6, 2023; Revised: October 19, 2023

Abstract: This paper examines two uncoupled quasistatic problems for thermo-viscoplastic materials, wherein the equation model considers the dependence of mechanical properties on a parameter θ, which represents the absolute temperature. Specifically, both the tensor of viscosity and the plastic deformation depend on this parameter. The boundary conditions for these problems are displacement traction and Signorini conditions. Our analysis establishes the existence of a unique solution to the problems, as well as the continuous dependence of the solution on the parameter θ. To provide a practical demonstration of our findings, we also present two one-dimensional examples that describe the processes involved in these problems.

Keywords: *viscoplastic; temperature; variational equality; Cauchy-Lipschitz method.*

Mathematics Subject Classification (2010): 35D30, 70K75, 74F05, 74M15, 74F05, 74C10, 93A30.

1 Introduction

Our study focuses on the analysis of two models designed for thermo-viscoplastic materials, which exhibit a unique coupling between their mechanical and thermal properties. Over the years, mathematicians, physicists, and engineers have extensively studied thermo-viscoplasticity laws to effectively model the influence of temperature on the behavior of various materials such as metals, magmas, and polymers. To gain further insight, we refer the interested readers to the sources such as [1, 2, 4, 5, 8, 11, 15]. Moreover, practical applications and mechanical interpretations of thermo-viscoplasticity can

* Corresponding author: mailto:ilyes.boukaroura@univ-setif.dz

be found in [13, 14]. To accurately describe the behavior of these materials in real-world scenarios, we employ a rate-type constitutive equation of the following form:

$$\dot{\sigma} = \xi\varepsilon(\dot{u}) + \mathcal{G}(\sigma, \varepsilon, \theta). \tag{1}$$

Here u, σ represent, respectively, the displacement field, θ is the absolute temperature, ξ is the fourth order elastic tensor and $\mathcal{G}$ is a nonlinear constitutive function, which describes the thermo-plastic behavior of the material and the stress field, $\varepsilon(u) = (\varepsilon_{ij}(u))$ is the linearised strain tensor,

$$\varepsilon_{ij}(u) = \frac{1}{2}(\nabla u \ + \nabla^T u).$$

For the heat flux q, a constitutive classical Fourier law is given by

$$q = K\nabla\theta. \tag{2}$$

In [15], existence and uniqueness results were obtained for problems (1)-(2) under classical displacement traction boundary conditions. However, the research in recent papers has been based on generalized thermo-viscoplastic theories with temperature-independent mechanical properties. In this paper, we aim to investigate the impact of temperature dependence of ξ on the behavior of the solution in generalized thermo-viscoplasticity. To accomplish this, we consider a rate-type constitutive equation of the form

$$\dot{\sigma} = \xi(\theta)\varepsilon\,(\dot{u}) + \mathcal{G}(\sigma, \varepsilon, \theta). \tag{3}$$

The paper is organized as follows. In Section 2, we describe the mathematical model for the problem. And we introduce some notations, list the assumptions on the problem's data, and derive the variational formulation of the model. In Section 3, we state our main existence and uniqueness result which is based on a Cauchy-Lipschitz technique and present the continuous dependence of the solution upon the parameter θ. We give two numerical examples in the last Section 4.

2 Problem Statement

Let Ω be a bounded domain in $\mathbb{R}^d (d = 1, 2, 3)$ with a smooth boundary Γ which is partitioned into three disjoint measurable parts Γ_1, Γ_2 and Γ_3 such that $eas\Gamma_1 > 0$. Let $T > 0$ and let $[0, T]$ denote the time interval of interest.

We consider the following mixed problem.

Problem P

Find a displacement field $u : \Omega \times (0, T) \to \mathbb{R}^d$, a stress field $\sigma : \Omega \times (0, T) \to \mathbb{S}_d$, a temperature $\theta : \Omega \to \mathbb{R}$, and the heat flux function $q : \Omega \to \mathbb{R}^d$ such that

$$\dot{\sigma} = \xi(\theta)\varepsilon(\dot{u}) + \mathcal{G}(\sigma, \varepsilon, \theta), \quad \text{in } \Omega \times (0,T), \tag{4}$$
$$Div\sigma + f_0 = 0, \quad \text{in } \Omega \times (0,T), \tag{5}$$
$$divq + r = \dot{\theta}, \quad \text{in } \Omega \times (0,T), \tag{6}$$
$$q = K\nabla\theta, \quad \text{in } \Omega \times (0,T), \tag{7}$$
$$u = 0 \quad \text{on } \Gamma_1 \times (0,T), \tag{8}$$
$$\sigma \cdot \nu = f_2, \quad \text{on } \Gamma_2 \times (0,T), \tag{9}$$
$$q \cdot \nu = \chi, \quad \text{on } \Gamma_2 \times (0,T), \tag{10}$$
$$\theta = 0 \quad \text{on } (\Gamma_1 \cup \Gamma_2) \times (0,T), \tag{11}$$
$$u(0) = u_0, \sigma(0) = \sigma_0, \quad \text{in } \Omega, \tag{12}$$
$$\theta(0) = \theta_0, \quad \text{in } \Omega. \tag{13}$$

Here $\mathbb{S}_d$ is the set of second order symmetric tensors on $\mathbb{R}^d$, $\nu = (\nu_i)$ is the unit outward normal to Ω and u_0, σ_0, θ_0 are the initial data.

We consider the following boundary conditions:

$$u_\nu \leq 0, \sigma_\nu \leq 0, \sigma_\tau = 0, \sigma_\nu . u_\nu = 0, \quad \text{on } \Gamma_3 \times (0,T). \tag{14}$$

In this way, we obtain two initial and boundary value problems $(\mathbf{P}_i)$ defined as follows.

Problem $\mathbf{P}_1$ Find the unknowns (u, σ, θ, q) such that (4)-(13) hold. This problem represents a displacement traction problem, in this case, $\Gamma_3 = \phi$.

Problem $\mathbf{P}_2$ Find the unknowns (u, σ, θ, q) such that (4)-(14) hold. This problem models the frictionless contact between the thermo-viscoplastic body and the rigid foundation, (14) represent the Signorini boundary conditions.

2.1 Variational formulation

For a weak formulation, we list the assumptions on the data and derive variational formulations for the contact problems $(\mathbf{P}_i)$. To this end, we need to introduce some notations and preliminary material. For more details, we refer the reader to [3,12]. We denote by $\mathbb{S}_d$ the space of second order symmetric tensors on $\mathbb{R}^d$ $(d = 2,3)$, while $\|\cdot\|$ denotes the Euclidean norm.

Let $\Omega \subset \mathbb{R}^d$ be a bounded domain with Lipschitz boundary Γ and let ν denote the unit outer normal on $\partial\Omega = \Gamma$. We shall use the notations

$$\begin{aligned} H = \tilde{H} = & \ \left[L^2(\Omega)\right]^d, \\ \mathcal{H} = & \ \tilde{\mathcal{H}} = \left[L^2(\Omega)\right]_s^{d\times d}, \\ Y = & \ \left[L^2(\Omega)\right]^M, M \in \mathbb{N}, \end{aligned}$$

and

$$\begin{aligned} H_1 = &\ \{u = (u_i) \in H : \varepsilon(u) \in \mathcal{H}\}, \\ \tilde{H}_1 = &\ \{\theta \in \tilde{H} : \nabla\theta \in \tilde{\mathcal{H}}\}, \\ \\ \mathcal{H}_1 = &\ \{\sigma \in \mathcal{H} : Div\sigma \in H\}, \\ \mathcal{V} = &\ \{\sigma \in \mathcal{H}_1 : Div\sigma = 0 \text{ in } \Omega, \sigma\nu = 0 \quad on\ \Gamma_1\}, \\ \\ \tilde{\mathcal{H}}_1 = &\ \left\{q \in \tilde{\mathcal{H}} : divq \in \tilde{H}\right\}, \\ \tilde{\mathcal{V}} = &\ \left\{q \in \tilde{\mathcal{H}}_1 : divq = 0 \text{ in } \Omega, q\nu = 0 \quad on\ \Gamma_1\right\}, \end{aligned}$$

where $\varepsilon : H \to \mathcal{H}$, $\nabla : \tilde{H} \to \tilde{\mathcal{H}}$, $Div : \mathcal{H} \to H$, and $div : \tilde{\mathcal{H}} \to \tilde{H}$ are the partial derivative operators of the first order, respectively, defined by

$$\begin{aligned} &\varepsilon(u) = (\varepsilon_{ij}(u)), \varepsilon_{ij}(u) = \tfrac{1}{2}(u_{i,j} + u_{j,i}), \\ &\nabla\theta = (\nabla_i\theta), \quad \nabla_i\theta = \tfrac{\partial\theta}{\partial x_i}, \\ &Div\sigma = (\tfrac{\partial\sigma_{ij}}{\partial x_j}), divq = (\tfrac{\partial q_i}{\partial x_i}). \end{aligned}$$

Here and below, the indices i and j run from 1 to d, the spaces H, H_1, $\mathcal{H}$, $\mathcal{H}_1$, $\tilde{H}$, $\tilde{H}_1$, $\tilde{\mathcal{H}}$ and $\tilde{\mathcal{H}}_1$ are real Hilbert spaces endowed with the canonical inner products given by

$$\begin{aligned} (u, v)_H &= \int_\Omega u_i v_i dx, \\ (u, v)_{H_1} &= (u, v)_H + (\varepsilon(u), \varepsilon(v))_{\mathcal{H}}, \\ (\sigma, \tau)_{\mathcal{H}} &= \int_\Omega \sigma_{ij}.\tau_{ij} dx, \\ (\sigma, \tau)_{\mathcal{H}_1} &= (\sigma, \tau)_{\mathcal{H}} + (Div\sigma, Div\tau)_H, \\ (\theta, \varphi)_{\tilde{H}} &= \int_\Omega \theta_i\varphi_i dx, \\ (\theta, \varphi)_{\tilde{H}_1} &= (\theta, \varphi)_{\tilde{H}} + (\nabla\theta, \nabla\varphi)_{\tilde{\mathcal{H}}}, \\ (q, p)_{\tilde{\mathcal{H}}} &= \int_\Omega q_{ij}.p_{ij} dx, \\ (q, p)_{\tilde{\mathcal{H}}_1} &= (q, p)_{\tilde{\mathcal{H}}} + (divq, divp)_{\tilde{H}}. \end{aligned}$$

The associated norms are denoted by $\|\cdot\|_H$, $\|\cdot\|_{H^1}$, $\|\cdot\|_{\mathcal{H}}$, $\|\cdot\|_{\mathcal{H}_1}$, $\|\cdot\|_{\tilde{H}}$, $\|\cdot\|_{\tilde{H}_1}$, $\|\cdot\|_{\tilde{\mathcal{H}}}$, and $\|\cdot\|_{\tilde{\mathcal{H}}_1}$, respectively. Also, for any real normed space X, we denote by X' the strong dual, by $\|\cdot\|_X$, $\|\cdot\|_{X'}$ the norms on X and X', respectively, and by $\langle,\rangle_{X',X}$ the canonical duality pairing between X and X', if in addition, X is a real Hilbert space and $A : X \to X$ is a continuous symmetric and positively definite linear operator, we denote by $\langle,\rangle_{A,X}$ and $\|\cdot\|_{A,X}$ the energetical product and the energetical norm induced by A on X.

Let

$$\begin{aligned} H_\Gamma &= (H^{1/2}(\Gamma))^d, \ \tilde{H}_\Gamma = (\tilde{H}^{1/2}(\Gamma))^d \\ \text{and } \gamma &: \ H_1(\Gamma)^d \to H_\Gamma, \ \tilde{\gamma} : \tilde{H}^1(\Gamma)^d \to \tilde{H}_\Gamma, \end{aligned}$$

be the trace map. We introduce the following closed sub-spaces of H_1 and $\tilde{H}_1$:

$$\begin{aligned} V = &\ \{u \in H_1 : \gamma u = 0 \quad on\ \ \Gamma_1\}, \\ \tilde{V} = &\ \left\{\theta \in \tilde{H}_1 : \tilde{\gamma}\theta = 0 \quad on\ \ \tilde{\Gamma}_1\right\}, \\ Q = &\ \left\{\eta \in H^1 : \eta = 0 \quad on\ \ \Gamma_1 \cup \Gamma_2\right\}. \end{aligned}$$

We introduce the following notations for the problems (P_i):

$$L(t,v) = \langle f_0(t), v\rangle + \langle f_2(t), \gamma v\rangle_{L^2(\Gamma_2)}$$

U_{ad}, and $\sum\limits_{ad}(t,v)$. For the problem P_1, we have

$$\begin{gathered} U_{ad} = V, \\ \sum_{ad}(t,v) = \{\tau \in \mathcal{H};\ \langle \tau, \varepsilon(w)\rangle = L(t,w);\quad \forall w \in V\} \\ (\sum_{ad} \text{ does not depend on } V). \end{gathered}$$

For the problem P_2, we have

$$\begin{gathered} U_{ad} = \{v \in V;\ v_\nu \leq 0 \text{ on } \Gamma_3\} \\ \sum_{ad}(t,v) = \{\tau \in \mathcal{H};\ \langle \tau, \varepsilon(w) - \varepsilon(v)\rangle \geq L(t, w-v);\quad \forall w \in V\}. \end{gathered}$$

In the study of the Problem $(\mathbf{P}_i)$, we consider the following assumptions.
The *operator* $\xi : \mathbb{R}^d \times \mathbb{S}_d \to \mathbb{S}_d$ satisfies

$$\left\{\begin{array}{l} \text{(a) There exists } L_\xi > 0 \text{ such that} \\ \|\xi(\theta_1) - \xi(\theta_2)\| \leqslant L_\xi\|\theta_1 - \theta_2\| \text{ for all } \theta_1, \theta_2 \in \mathbb{R}^d, \\ \text{(b) } \xi(\theta).\sigma.\tau = \sigma.\xi(\theta).\tau, \quad \forall\theta \in \mathbb{R}^d, \quad \forall \sigma, \tau \in \mathbb{S}_d, \\ \text{(c) There exists } \alpha > 0 \text{ such that } \ \xi(\theta).\sigma.\sigma \geqslant \alpha\|\sigma\|^2, \\ \quad \forall\theta \in \mathbb{R}^d, \forall\sigma \in \mathbb{S}_d, \\ \text{(d) } \xi(\theta) \text{ is Lebesgue measurable on } \Omega, \\ \text{(e) There exists } \beta > 0 \text{ such that } \ \|\xi(\theta)\| \leq \beta. \end{array}\right. \tag{15}$$

The *operator* $\mathcal{G} : \mathbb{S}_d \times \mathbb{S}_d \times \mathbb{R}^d \to \mathbb{S}_d$ satisfies

$$\left\{\begin{array}{l} \text{(a) There exists } L_\mathcal{G} > 0 \text{ such that} \\ \|\mathcal{G}(\sigma_1, \varepsilon_1, \theta_1) - \mathcal{G}(\sigma_2, \varepsilon_2, \theta_2)\| \leqslant L_\mathcal{G}\left(\|\sigma_1 - \sigma_2\| + \|\varepsilon_1 - \varepsilon_2\| + \|\theta_1 - \theta_2\|\right) \\ \text{for all } \sigma_1, \sigma_2 \in \mathbb{S}_d, \quad \varepsilon_1, \varepsilon_2 \in \mathbb{S}_d, \quad \theta_1, \theta_2 \in \mathbb{R}^d, \\ \text{(b) The mapping } \mathcal{G}(\sigma, \varepsilon, \theta) \text{ is Lebesgue measurable on } \Omega, \end{array}\right. \tag{16}$$

K is a symmetric and positively definite bounded tensor, i.e.,
the *tensor* $K : \Omega \times \mathbb{S}_d \to \mathbb{S}_d$ satisfies

$$\left\{\begin{array}{l} \text{(a) } K(x).q.p = q.K(x).p, \quad \forall q, p \in \mathbb{S}_d, \quad \text{a.e in } \Omega, \\ \text{(b) There exists } \lambda > 0 \text{ such that } \ K(x).q.q \geqslant \lambda\|q\|^2 \\ \ \text{for all } q \in \mathbb{S}_d, \quad \text{a.e in } \Omega, \\ \text{(c)} K_{ij} \in L^\infty(\Omega) \text{ for all } i, j \in 1, 2, 3. \end{array}\right. \tag{17}$$

$K^{-1}A$ is a symmetric and positively definite bounded tensor, i.e.,

$$\left\{\begin{array}{l} \text{(a) } K^{-1}A(x).q.p = q.K^{-1}A(x).p, \quad \forall q, p \in \mathbb{S}_d, \quad \text{a.e in } \Omega, \\ \text{(b) There exists } \delta > 0 \text{ such that } \ K^{-1}A(x).q.q \geqslant \delta\|q\|^2 \\ \ \text{for all } q \in \mathbb{S}_d \quad \text{a.e in } \Omega, \\ \text{(c) } \left(K^{-1}A\right)_{ij} \in L^\infty(\Omega) \text{ for all } i, j \in 1, 2, 3. \end{array}\right. \tag{18}$$

We also suppose that

$$f_0 \in C^1(0,T;H), \tag{19}$$
$$r \in L^2(0,T;L^2(\Omega)), \tag{20}$$
$$f_2 \in C^1(0,T;H^1_\Gamma), \tag{21}$$
$$\chi \in L^2(\Gamma_2), \tag{22}$$
$$Div\boldsymbol{\sigma}_0 + f_0\,(0) = 0 \text{ in } \Omega, \tag{23}$$
$$\boldsymbol{\sigma}_0.\nu = f_0\,(0) \text{ on } \Gamma_2, \tag{24}$$
$$u_0 \in H_1, \tag{25}$$
$$\boldsymbol{\sigma}_0 \in \mathcal{H}_1, \tag{26}$$
$$\theta_0 \in L^2\,(\Omega)\,. \tag{27}$$

By using standard arguments, we obtain the following variational formulation of the problem ((4)-(14)).

2.2 Problem $\mathcal{P}_V$

Find the displacement field $u : [0,T] \to \mathbb{R}^d$, the stress field $\boldsymbol{\sigma} : [0,T] \to \mathbb{S}_d$, the temperature function $\theta : [0,T] \to \mathbb{R}$, and the heat flux $q : [0,T] \to \mathbb{R}^d$ such that

$$u(t) = U_{ad}, \sigma(t) \in \sum_{ad}(t, w(t)), \quad \forall t \in [0,T], \tag{28}$$
$$\dot{\sigma}\,(t) = \xi(\theta\,(t)).\ \varepsilon(\dot{u}(t)) + \mathcal{G}\big(\sigma(t), \varepsilon(u(t)),\ \theta(t)\big), \tag{29}$$
$$u(0) = u_0, \quad \sigma(0) = \sigma_0, \tag{30}$$
$$(K\nabla\theta, \nabla\eta)_H + (\dot{\theta}, \eta)_H = (r,\eta) + (\chi, \gamma\eta)\,, \tag{31}$$
$$\theta(0) = \theta_0. \tag{32}$$

We notice that the variational formulation PV is formulated in terms of a displacement field, a stress field, a temperature and heat. The existence of the unique solution of the problem PV is stated and proved in the next section.

3 Existence and Uniqueness of a Solution

Now, we propose our existence and uniqueness result.

Theorem 3.1 *Assume that (*(15)-(27)*) hold. Then there exists a unique weak solution of the problem (*(28)-(32)*) such that*

$$\theta \in L^2(0,T;Q) \cap C(0,T;L^2(\Omega)), \tag{33}$$
$$u \in C^1(0,T;H_1), \tag{34}$$
$$\sigma \in C^1(0,T;\mathcal{H}_1). \tag{35}$$

The proof of Theorem 3.1 will be carried out in several steps. It is based on parabolic equations and a Cauchy-Lipschitz technique.

In the first step, we consider the following variational problem.

Problem PV$_\theta$

Find a temperature function $\theta : [0,T] \to \mathbb{R}$ such that

$$(K\nabla\theta, \nabla\eta)_H + (\dot{\theta}, \eta)_H = (r, \eta) + (\chi, \gamma\eta)\,, \tag{36}$$
$$\theta(0) = \theta_0. \tag{37}$$

The existence and uniqueness of the functions θ satisfying (33) can be obtained by using classical results concerning parabolic equations. For the problem $\mathbf{PV}_\theta$, we have the following lemma.

Lemma 3.1 $\mathbf{PV}_\theta$ *has a unique solution satisfying*

$$\theta \in L^2(0,T;Q) \cap C(0,T;L^2(\Omega)). \tag{38}$$

Proof Applying classical results concerning parabolic equations, we get the existence and uniqueness of the solution of ((36)-(37)) with the regularity

$$\theta \in L^2(0,T;Q) \cap C(0,T;L^2(\Omega)).$$

Now, the existence and uniqueness of the solution (u, σ) of the mechanical problem with the regularity(34), (35) can be proved by considering θ as a known function and the existence and uniqueness of the solution of the mechanical problem is proved by reducing the problem under consideration to an ordinary differential one in a Hilbert space.

In the second step, we consider the following variational problem.

Problem PV$_\mathbf{u}$

Find a displacement field $u : \Omega \times [0,T] \to \mathbb{R}^d$, and the stress $\sigma : \Omega \times [0,T] \to \mathbb{S}_d$ such that

$$u(t) = U_{ad}, \sigma(t) \in \sum_{ad}(t, w(t)), \quad \forall t \in [0,T]\,, \tag{39}$$
$$\dot{\sigma}\,(t) = \xi(\theta\,(t)).\ \varepsilon(\dot{u}(t)) + \mathcal{G}(\sigma(t), \varepsilon(u(t)),\ \theta(t)), \tag{40}$$
$$u(0) = u_0, \quad \sigma(0) = \sigma_0. \tag{41}$$

The existence and uniqueness of the functions (u, σ) satisfying ((35),(36)) is given by the following lemma.

Lemma 3.2 $\mathbf{PV}_\mathbf{u}$ *has a unique solution satisfying*

$$u \in C^1(0,T;H_1), \tag{42}$$
$$\sigma \in C^1(0,T;\mathcal{H}_1). \tag{43}$$

Proof. In order to prove Lemma 3.2, we need some preliminaries given by the following lemma, whose proof can be easily obtained.

Lemma 3.3 *Let* (15), $\theta \in C(0,T;L^2(\Omega))$ *hold, then for all* $t \in [0,T]$, *we have*

$$\begin{array}{rcl} \|\xi(\theta\,(t)).\sigma\|_{\mathcal{H}} & \leq & \beta\|\sigma\|_{\mathcal{H}}, \\ \langle\xi(\theta\,(t))\sigma, \sigma\rangle_{\mathcal{H}} & \geqslant & \alpha\|\sigma\|^2_{\mathcal{H}}, \\ \left\|\xi^{-1}(\theta\,(t)).\sigma\right\|_{\mathcal{H}} & \leq & \frac{1}{\alpha}\|\sigma\|_{\mathcal{H}}, \\ \left\langle\xi^{-1}(\theta\,(t))\sigma, \sigma\right\rangle_{\mathcal{H}} & \geqslant & \frac{\alpha}{\beta^2}\|\sigma\|^2_{\mathcal{H}}. \end{array}$$

Let now $X = V \times \mathcal{V}$. Using the properties of the trace maps, from (19) and (21), we obtain the existence of the function $\tilde{\sigma} \in W^{1,\infty}(0,T;\tilde{H})$ such that

$$\begin{array}{ll} \tilde{\sigma}\nu(t) = f_2\,(t) & \text{on } \Gamma_2 \times [0,T]\,, \\ Div\ \tilde{\sigma}\,(t) + f_0 = 0 & \text{in } \Omega \times [0,T]\,. \end{array}$$

Let now

$$\begin{array}{llll} a: & [0,T] \times X \times X & \to & \mathbb{R}, \\ F: & [0,T] \times X & \to & X \end{array}$$

be given by

$$a\,(t,x,y) = \langle \xi(\theta\,(t))\varepsilon\,(u)\,, \varepsilon\,(v)\rangle_{\mathcal{H}} + \left\langle \xi^{-1}(\theta\,(t))\sigma, \tau \right\rangle_{\mathcal{H}}\,, \tag{44}$$

$$\begin{aligned} \langle F\,(t,x)\,, y\rangle_X &= \left\langle \xi^{-1}(\theta\,(t))\mathcal{G}\,(\sigma + \tilde{\sigma}\,(t)\,, \varepsilon\,(u)\,, \theta\,(t))\,, \tau \right\rangle_{\mathcal{H}}\,, \\ &\quad - \langle \mathcal{G}\,(\sigma + \tilde{\sigma}\,(t)\,, \varepsilon\,(u))\,, \theta\,(t)\,, \varepsilon\,(v)\rangle_{\mathcal{H}}\,, \\ &\quad - \left\langle \dot{\tilde{\sigma}}\,(t)\,, \varepsilon\,(v) \right\rangle_{\mathcal{H}} - \left\langle \xi^{-1}(\theta\,(t))\dot{\tilde{\sigma}}\,(t)\,, \tau \right\rangle_{\mathcal{H}}\,, \qquad (45) \\ \text{for all } x &= (u,\sigma)\,,\ y = (v,\tau) \in X \text{ and } t \in [0,T]\,. \end{aligned}$$

Let us now denote

$$\sigma = \bar{\sigma} + \tilde{\sigma},\ x = (u, \bar{\sigma})\,, \tag{46}$$

$$\sigma_0 = \bar{\sigma}_0 + \tilde{\sigma}\,(0)\,,\ x_0 = (u_0, \bar{\sigma}_0)\,. \tag{47}$$

We have the following result

Lemma 3.4 *The pair $(u,\sigma) \in C^1(0,T; H_1 \times \mathcal{H}_1)$ is a solution of the problem P_u if and only if $x \in C^1(0,T;X)$ is a solution of the problem*

$$a\,(t, \dot{x}\,(t)\,, y) = \langle F(t,x), y\rangle_X\,, \tag{48}$$

$$x(0) = x_0, \tag{49}$$

where $X = V \times \mathcal{V}$, $x = (u, \bar{\sigma})$.

Proof. Using (46), (47), it is easy to see that $(u,\sigma) \in C^1(0,T; H_1 \times \mathcal{H}_1)$ is a solution of the viscoplastic problem if, and only if $x \in C^1(0,T;X)$ and

$$\dot{\bar{\sigma}} = \xi(\theta).\varepsilon(\dot{u}) + \mathcal{G}\,(\bar{\sigma} + \tilde{\sigma}, \varepsilon(u), \theta) - \dot{\tilde{\sigma}}, \tag{50}$$

$$u(0) = u_0, \quad \bar{\sigma}(0) = \bar{\sigma}_0. \tag{51}$$

Let us suppose (50)-(51) are fulfilled. Using the fact that $\boldsymbol{\varepsilon}(v)$ is the orthogonal complement of $\mathcal{V}$ in $\mathcal{H}$, we have (48).

Conversely, let (48) hold and let

$$z(t) = \dot{\bar{\sigma}}(t) - \xi(t)\varepsilon(\dot{u}) - \mathcal{G}(\bar{\sigma} + \tilde{\sigma}, \varepsilon(u), \theta) - \dot{\tilde{\sigma}}. \tag{52}$$

Taking $y = (v,0) \in X$ in (57) and using the orthogonality of $\varepsilon(v)$ and v, we get

$$\langle z\,(t)\,, \boldsymbol{\varepsilon}(v)\rangle_{\mathcal{H}} = 0. \tag{53}$$

Now, we take $y = (0, \tau) \in X$ in (48) and using the orthogonality of $\varepsilon(v)$ and v, we get

$$\left\langle \xi^{-1}(\theta(t))z(t), \tau \right\rangle_{\mathcal{H}} = 0. \tag{54}$$

Due to the orthogonality of $\boldsymbol{\varepsilon}(v)$ in $\mathcal{H}$ to v, from (53), we get $z(t) \in V$, thus we may put $\tau = z(t)$ in (54), and thus from (39), we deduce $z(t) = 0$. Hence, we proved that (50) is equivalent to (49).

The following lemma can be easily obtained.

Lemma 3.5 *For every $x \in X$ and $t \in [0,T]$, there exists a unique element $z \in X$ such that*

$$a(t, z, y) = \langle F(t, x), y \rangle_X, \tag{55}$$

where $X = V \times \mathcal{V}$, $x = (u, \bar{\sigma})$.

Proof. Let $x \in X$ and $t \in [0,T]$, using the properties of ξ, ξ^{-1} and Korn's equality, we get that $a(t, ., .)$ is bilinear continuous and coercive, hence the existence and uniqueness of z which satisfies (55) following from Lax-Miligram's Lemma.

The previous lemma allows us to consider the operator

$$A : \quad [0,T] \times X \quad \to \quad X$$

defined as $A(t, x) = z$, moreover, we have the following result.

Lemma 3.6 *The operator A is continuous and there exists $C > 0$ such that*

$$|A(t, x_1) - A(t, x_2)|_X \leq C |x_1 - x_2|_X, \ \forall x_1, x_2 \in X. \tag{56}$$

Proof. *Let us consider $t_1, t_2 \in [0,T]$; $\quad x_i = (u_i, \sigma_i) \in X$ and let $z_i = (w_i, \tau_i) \in X$ be defined by $z_i = A(t_i, x_i)$.*

Using (55), we have

$$a(t_1, z_1, z_1 - z_2) - a(t_2, z_2, z_1 - z_2) = \langle F(t_1, z_1) - F(t_2, z_2), z_1 - z_2 \rangle_X, \tag{57}$$

and from (39) and Korn's inequality, we get

$$\begin{aligned} a(t_1, z_1, z_{1-}z_2) \quad & -a(t_2, z_2, z_{1-}z_2) \\ & \geqslant C \|z_{1-}z_2\|_X^2 - \|[\xi(\theta(t_1)) - \xi(\theta(t_2))]\, \varepsilon(w_2)\|_H \|z_{1-}z_2\|_X \\ & \quad - \left\| \left[\xi^{-1}(\theta(t_1)) - \xi^{-1}(\theta(t_2))\right] \tau_2 \right\|_H \|z_{1-}z_2\|_X . \end{aligned} \tag{58}$$

In a similar way, from (36), (37), we get

$$\begin{aligned} \langle F(t_1, x_1) \quad & -F(t_2, x_2), z_{1-}z_2 \rangle_X \\ & \leq C(\|x_{1-}x_2\|_X + \|\tilde{\sigma}(t_1) - \tilde{\sigma}(t_2)\|_H \\ & \quad + \|\tilde{\sigma}(t_1) - \tilde{\sigma}(t_2)\|_H + \|\theta(t_1) - \theta(t_2)\|_{L^2(\Omega)} \\ & \quad + \left\| \left[\xi^{-1}(\theta(t_1)) - \xi^{-1}(\theta(t_2))\right] \right\|_H F(\sigma_2 + \tilde{\sigma}(t), \varepsilon(u), \theta(t_2)) \\ & \quad + \left\| \left[\xi^{-1}(\theta(t_1)) - \xi^{-1}(\theta(t_2))\right] \sigma(t_2) \right\|_H). \|z_{1-}z_2\|_X . \end{aligned} \tag{59}$$

So, from (57)-(58), it results

$$
\begin{aligned}
&\|z_1 - z_2\|_X \\
&\qquad \le \mathcal{C}\big(\|[\xi(\theta(t_1)) - \xi(\theta(t_2))]\,\varepsilon(w_2)\|_H \\
&\qquad\quad + \big\|\big[\,\xi^{-1}(\theta(t_1)) - \xi^{-1}(\theta(t_2))\big]\,\tau_2\big\|_H \\
&\qquad\quad + \|x_1 - x_2\|_X + \|\tilde\sigma(t_1) - \tilde\sigma(t_2)\|_H + \|\theta(t_1) - \theta(t_2)\|_{L^2(\Omega)} \\
&\qquad\quad + \big\|\big[\xi^{-1}(\theta(t_1)) - \xi^{-1}(\theta(t_2))\big]\big\|_H\, F(\sigma_2 + \tilde\sigma(t), \varepsilon(u), \theta(t_2)) \\
&\qquad\quad + \big\|\big[\xi^{-1}(\theta(t_1)) - \xi^{-1}(\theta(t_2))\big]\,\sigma(t_2)\big\|_H\,\big).\, \|z_1 - z_2\|_X\,. \qquad (60)
\end{aligned}
$$

Using the properties of ξ, ξ^{-1} and the regularity of $\tilde\sigma$, u, from (60), we get $z_1 \longrightarrow z_2$ in X when $t_1 \longrightarrow t_2$ in $[0, t]$, and $x_1 \longrightarrow x_2$ in X. Hence A is a continuous operator, moreover, taking $t_1 = t_2$ in (60), we get (56).

Now, we have all the ingredients needed to prove Theorem 3.1.

Proof of Theorem 3.1 Using the hypothesis on u_0, σ_0, we get that $x_0 \in X$, and by Lemma 3.5 and the classical Cauchy-Lipschitz theorem, we get that there exists a unique solution $x \in C^1(0, T; X)$ of the Cauchy problem

$$
\begin{aligned}
\dot x(t) &= A(t, x(t)), \\
x(0) &= x_0.
\end{aligned}
$$

Theorem **3.1** follows now from the definition of the operator A, and Lemma 3.3 .

4 The Continuous Dependence with respect to Parameter θ and Numerical Examples

In this section, we prove the continuous dependence of the solution (u, σ) upon the data θ. Moreover, we give two one-dimensional examples to illustrate the results.

4.1 The continuous dependence of the solution with respect parameter θ

We consider the case when ξ in (4) does not depend on θ and we replace (4) by ξ which is a symmetric and positively definite tensor.
We have the following result.

Theorem 4.1 *Let ξ be a symmetric and positively definite tensor,* (15), (18), (20)-(24) *hold, and let (u_i, σ_i) be the solutions of the problem* (28)-(32) *for $\theta = \theta_i, i = 1, 2$. Then there exists $C > 0$ such that*

$$
\|u_1 - u_2\|_{C^1(0,T;H_1)} + \|\sigma_1 - \sigma_2\|_{C^1(0,T;\mathcal{H}_1)} \le C\,\|\theta_1 - \theta_2\|_{C^0(0,T;Y)}\,. \qquad (61)
$$

Proof. Let $\tilde\sigma$ be a function which satisfies

$$
\begin{gathered}
\tilde\sigma \cdot \nu = f_2, \\
Div\tilde\sigma + f_0 = 0, \\
\bar\sigma_i = \sigma_i - \tilde\sigma, \quad x_i = (u_i, \sigma_i), \quad i = 1, 2. \qquad (62)
\end{gathered}
$$

From Theorem 3.1, we have

$$
\dot x_i(t) = A_i(t, x_i(t)), \qquad (63)
$$

$$
x_i(0) = x_0, \qquad (64)
$$

where x_0 is given by $x_0 = (u_0, \sigma_0)$ and the operators A_i are defined by Lemma 3.6 with replacing θ by θ_i in (44). In a similar way as in (60), we obtain

$$\|A(t, x_1(t)) - A(t, x_2(t))\|_X \le C(\|x_1(t) - x_2(t)\|_X + \|\theta_1(t) - \theta_2(t)\|_Y) \tag{65}$$

for all $t \in [0, T]$, hence from (63) and (64), using a standard technique, we get

$$(\|x_1(t) - x_2(t)\|_X) \le C \int_0^t \|\theta_1(s) - \theta_2(s)\|_X \, ds \tag{66}$$

$$(\|\dot{x_1}(t) - \dot{x_2}(t)\|_X) \le C(\|x_1(t) - x_2(t)\|_X + \|\theta_1(t) - \theta_2(t)\|_Y) \tag{67}$$

for all $t \in [0, T]$. Theorem 4.1 follows now from (62), (66) and (67).

4.2 One-dimensional Examples

In this section, we give two one-dimensional examples to illustrate the main results.

One-dimensional model

We consider a thermoviscoplastic body $\Omega =]0, 1[$ whose boundary is divided in three parts Γ_1, Γ_2 and Γ_3. We suppose that the body is fixed at $x = 0$ and is subject to the action of a body force of density $f_0(x, t) = 10$. On the part Γ_2, known tractions act on the body. We suppose then the volume heat $r = 0$ and the thermal boundary conditions are

$$\theta(0, t) = \theta_0, \quad \theta(1, t) = a,$$

where θ_0 and a are given.

We also use a thermoviscoplastic law, i.e.,

$$\dot{\sigma} = E(\theta)\dot{\varepsilon} - \sigma + E(\theta)\varepsilon. \tag{68}$$

Here $\varepsilon = \frac{\partial u}{\partial x}$, $\dot{\varepsilon} = \frac{\partial \varepsilon}{\partial t}$, $\dot{\sigma} = \frac{\partial \sigma}{\partial t}$ and $E(\theta)\dot{\varepsilon}$ is the modulus of elasticity. For this consideration, we have the following.

Example 1. Let us consider a thermoviscoplastic problem of the form (4)-(15) in the following context:

$\Omega =]0, 1[, \Gamma_1 = \{0\}, \Gamma_2 = \{1\}, \Gamma_3 = \emptyset, f_0(x, t) = 10, u(x, 0) = 0, u(0, t) = 0$ and $\sigma(1, t) = 0, \sigma(x, 0) = 10 - 10x, r = 0$.

In this case, the problem is the classical displacement-traction formulated as follows.

Find a displacement field $u : \Omega \times (0, T) \to \mathbb{R}^d$, a stress field $\sigma : \Omega \times (0, T) \to \mathbb{S}_d$, a temperature $\theta : \Omega \to \mathbb{R}$, and the heat flux function $q : \Omega \to \mathbb{R}^d$ such that

$$\frac{\partial q}{\partial x}(x,t) = 0, \tag{69}$$

$$q = \frac{\partial \theta}{\partial x}, \tag{70}$$

$$\theta(0,T) = \theta_0, \tag{71}$$

$$\theta(1,T) = a, \tag{72}$$

$$\frac{\partial \sigma}{\partial x}(x,t) + 10 = 0, \tag{73}$$

$$\dot{\sigma} = E(\theta)\dot{\varepsilon}(u(x,t)) - \sigma(x,t) + E(\theta)\varepsilon(u(x,t)), \tag{74}$$

$$u(0,t) = 0, \tag{75}$$

$$u(x,0) = 0, \tag{76}$$

$$\sigma(1,t) = 0, \tag{77}$$

$$\sigma(x,0) = 10 - 10x, \tag{78}$$

where u, σ, θ, and q are unknowns.

Example 2. In this case, we suppose that the body is in frictionless contact with a rigid foundation. Then problem (4)-(15) is the following Signorini contact problem:

$$\frac{\partial q}{\partial x}(x,t) = 0, \tag{79}$$

$$q = \frac{\partial \theta}{\partial x}, \tag{80}$$

$$\theta(0,T) = \theta_0, \tag{81}$$

$$\theta(1,T) = a, \tag{82}$$

$$\frac{\partial \sigma}{\partial x}(x,t) + 10 = 0, \tag{83}$$

$$\dot{\sigma} = E(\theta)\dot{\varepsilon}(u(x,t)) - \sigma(x,t) + E(\theta)\varepsilon(u(x,t)), \tag{84}$$

$$u(0,t) = 0, \tag{85}$$

$$u(x,0) = 0, \tag{86}$$

$$\sigma(x,0) = 10 - 10x, \tag{87}$$

$$u(1,t) \le \frac{1}{4}, \sigma(1,t) \le 0, \sigma(1,t)\left(u(1,t) - \frac{1}{4}\right) = 0, \tag{88}$$

where u, σ, θ, and q are unknowns.

In Section 2, we considered the Signorini contact problem with a zero gap. The results there can be extended straightforward to the situation with a nonzero initial gap g, here $g = \frac{1}{4}$.

Now, we present the exact solution for the example below. For the thermal problem, we can easily find the solution (θ, q). For the isotherm mechanical problem, we have the following.

For Example 1: From the equilibrium equation, we have

$$\sigma(x,t) = -10x + k(t). \tag{89}$$

Substituting for the equation law and boundary conditions, we have

$$\varepsilon(x,t) = C(t)e^{-t} + \frac{\sigma(x,t)}{E(\theta)}. \tag{90}$$

Using the initial conditions, we obtain

$$\varepsilon(u(x,t)) = \left(\frac{10}{E(\theta)}x - \frac{10}{E(\theta)}\right)e^{-t} + \frac{-10x + k(t)}{E(\theta)}, \tag{91}$$

$$u(x,t) = \left(\frac{5}{E(\theta)}x - \frac{10}{E(\theta)}\right)e^{-t} + \frac{-5x^2 + k(t)x}{E(\theta)}. \tag{92}$$

Using the boundary conditions of σ, we have $k(t) = 10$, the exact solution of the displacement traction problem is

$$\sigma(x,t) = -10x + 10, \tag{93}$$

$$u(x,t) = \frac{10}{E(\theta)}\left(\frac{x^2}{2} - x\right)\left(e^{-t} - 1\right). \tag{94}$$

For Example 2: Using the same technique as Example 1, we have

$$\sigma(x,t) = -10x + k(t), \tag{95}$$

$$u(x,t) = \left(\frac{5x^2}{E(\theta)} - \frac{10}{E(\theta)}\right)e^{-t} + \frac{-5x^2 + k(t)x}{E(\theta)}. \tag{96}$$

At $x = 1$, the body is in contact with the foundation, then $u(1,t) \leq \frac{1}{4}$.

- When $u(1,t) = \frac{1}{4}$, there is a contact, then we obtain

$$k(t) = \frac{5}{2}\left[\frac{E(\theta)}{10} + 2 + 2e^{-t}\right]$$

and $\sigma(1,t) < 0$ gives $k(t) < 10$ and $t > log\left[\frac{20}{20-E(\theta)}\right]$.

The exact solution of the Signorini problem is as follows.

- In the case when $t \in \left[0; log\left(\frac{20}{20-E(\theta)}\right)\right]$,

  there is no contact, we have $\sigma(1,t) = 0$, then $k(t) = 10$.

  The solution is

$$\begin{cases} \sigma(x,t) = -10x + 10, \\ u(x,t) = \frac{10}{E(\theta)}\left(\frac{x^2}{2} - x\right)\left(e^{-t} - 1\right). \end{cases} \tag{97}$$

- In the case when $t > log\left(\frac{20}{20-E(\theta)}\right)$,

  there is a contact and we have $u(1,t) = \frac{1}{4}$, $\sigma(1,t) < 0$.

  The solution is

$$\begin{cases} \sigma(x,t) = -10x - \frac{5}{2}\left(\frac{E(\theta)}{10} + 2 + 2e^{-t}\right), \\ u(x,t) = \frac{10}{E(\theta)}\left[\frac{x^2}{2}\left(e^{-t} - 1\right) + \frac{1}{4}\left(-2e^{-t} + E(\theta) + 2\right)\right]. \end{cases} \tag{98}$$

Remark. From these two one-dimensional examples, we deduce that the solution (u, σ) is dependent on $E(\theta)$.

5 Conclusion

This study addresses two uncoupled quasistatic problems in thermo-viscoplastic materials. A model is proposed where the mechanical properties of the problem are dependent on a parameter θ, which can be interpreted as the absolute temperature. The boundary conditions include displacement traction and the Signorini conditions. The existence of a unique solution to the problems is proven, and two examples in one-dimensional study are presented to describe the problem processes.

6 Acknowledgment

This work has been supported by: La Direction Générale de la Recherche Scientifique et du Développement Technologique (DGRSDT-MESRS), under project PRFU number C00L03UN190120230010. Algérie.

References

[1] K.T. Andrews, K.L. Kuttler and M. Shillor. On the dynamic behaviour of thermoviscoelastic body in frictional contact with a rigid obstacle. *Euro. Jnl. Appl. Math.* **8** (1997) 417–436.

[2] K.T.Andrews, A. Klarbring, M. Shillor and S. Wright. A dynamic contact problem with friction and wear. *Int. J. Engng. Sci.* **35** (1997) 1291–1309.

[3] V. Barbu. *Optimal Control of Variational Inequalities.* Research Notes in Mathematics, 100. Pitman (Advanced Publishing Program). Boston. 1984.

[4] I. Boukaroura and S. Djabi. A dynamic Tresca's frictional contact problem with damage for thermo elastic-viscoplastic bodies. *Studia Univ. Babes Bolayai Mathematica* **64** (2019) 433–449.

[5] I. Boukaroura and S. Djabi. Analysis of a quasistatic contact problem with wear and damage for thermo-viscoelastic materials. *Malaya Journal of Matematik* **6** (2018) 299–309.

[6] S. Djabi. A monotony method in quasistatic processes for viscoplastic materials with $\varepsilon = \varepsilon(\epsilon(\dot{u}), k)$. *Mathematical Reports* **2** (2000) 9–20.

[7] S. Djabi and M. Sofonea. A fixed point method in quasistatic rate-type viscoplasticity. *Appl. Math. and Comp Sci.* **3** (1993) 269–279.

[8] A. Djabi. A Frictional Contact Problem with Wear for Two Electro-Viscoelastic Bodies. *Nonlinear Dynamics and Systems Theory* **23** (2) (2023) 167—182

[9] A. Djabi and A. Merouani. A fixed point method for a class of nonlinear evolution systems modeling a mechanical phenomen. *Int. J. Open Problems Compt. Math*, **8** (1)(2015) 1–13.

[10] A. Djabi and A. Merouani. Bilateral contact problem with friction and wear for an electro elastic-viscoplastic materials with damage. *Taiwanese J. Math.* **19** (4) (2015) 1161–1182.

[11] A. Djabi, A. Merouani and A. Aissaoui. A frictional contact problem with wear involving elastic-viscoplastic materials with damage and thermal effects. *Electron. J. Qual. Theory Differ. Equ.* **27** (2015) 1–18.

[12] G. Duvaut and J. L. Lions. Les inéquations en mécanique et en physique (in French). [The inequalities in mechanics and physics]. *Springer*. Berlin. 1976.

[13] K.L. Kuttler. Dynamic friction contact problems for general normal and friction laws. *Nonlin. Anal.* **28** (1997) 559–575.

[14] S. Smata and N. Lebri. Contact Problem for Thermoviscoelastic Materials with Internal State Variable and Wear. *Nonlinear Dynamics and Systems Theory* **22** (5) (2022) 573-–585.

[15] M. Sofonea. On existence and behaviour of the solution of two uncoupled thermo-elastic-visco-plastic problems. *An. Univ. Bucharest* **38** (1989) 56–65.

Nonlinear Dynamics and Systems Theory, **23** (4) (2023) 381–388

Maximum Power Point Tracking Based on Remora Algorithm under PSC

Hamidia Fethia [1*], Abbadi Amel [1], Skender Mohamed Reda [1], Morsli Abdelkader [1], Bettache Farouk [1], Medjber Ahmed [2] and Tlemçani Abdelhalim [1]

[1] *LREA Laboratory, Yahia Feres University, Medea, Algeria.*
[2] *LMPM Laboratory, Yahia Feres University, Medea, Algeria.*

Received: May 26, 2023; Revised: September 22, 2023

Abstract: Full or partial shading conditions have a significant impact on power generation capacity and can lead to losses. It is necessary to get the maximum power that they can generate by reducing energy losses as much as possible; the power-voltage characteristic curve of PVG under the PSC (Partial Shading Condition) leads to multips power peak, the GMPP (Global Maximum Power Point) represents the peak with the higest value, the others are called LMPPs (Local Maximum Power Points). To extract the maximum power from a set of PV panels, an electronic controller (DC-DC converter) is incorporated between the PVG and the load, its main role is the continuous monitoring at all times of the point of MPP.
This paper proposes a bio-inspired metaheuristic algorithm named the Remora Optimization Algorithm (ROA), used to get the GMPP of the PV panel under the PSC. In this paper, to show the feasibility of the ROA, we propose two configurations, first, we have five PV panels connected in series as a source and resistance as a load, this configuration will be tested under three scenarios (without shading, under weak or strong shading), second, we will replace DC load by AC load (pumping system), this configuration will be tested under strong partial shading.

Keywords: *Remora algorithm; PV generator; global MPP; local MPP; DC load; AC load.*

Mathematics Subject Classification (2010): 70Kxx, 93C10, 93-XX.

* Corresponding author: mailto:fe_hamidia@yahoo.fr

1 Introduction

The continuously increasing power demand is met by both the conventional and renewable electric power generation sources [1]. Solar energy is the most abundant source of energy among renewable energies. Photovoltaic electricity comes from the direct transformation of part of the solar radiation into electrical energy. This energy conversion takes place through the so-called photovoltaic (PV) cell based on a physical phenomenon called the photovoltaic effect which consists of producing an electromotive force when the surface of this cell is exposed to light. The power delivered by a PVG strongly depends on the level of sunshine, the temperature of the cells, the shade and also the nature of the load supplied. The power characteristic curve of the PVG has a maximum power point (MPP) corresponding to a certain operating point of coordinates, VMPP for the voltage and IMPP for the current. Since the position of the MPP depends on the level of sunshine and the temperature of the cells, it is never constant over time. An MPPT (Maximum Power Point Tracker) converter must therefore be used to track these changes. Under the partial shading condition, several maximums appear in this P-V curve, a global maximum (GMPP) and one or more local maximum values (LMPPs). An MPPT converter (Boost converter) is a power conversion system equipped with an appropriate control algorithm to extract the maximum power that the PVG can provide.

The main disadvantage of the classical techniques, for example, the hill climbing algorithm, is that it remains trapped in the first local optimum encountered. Methods of this type do not present any form of diversification. An improvement of this algorithm consists in restarting several times, when a local optimum is found, from a new randomly generated solution. The classical technique P&O (Perturb and Observe) as the second example can not differentiate between these points and fail in tracking the global maximum point (GMPPT). Several researchers are currently working on bio-inspired techniques that belong to a group of soft computing techniques known as meta-heuristic algorithms for the best operation of the MPPT technique [2], [3],namely PSO (Particle Swarm Optimization), ACO (Ant Colony Optimization), ABC (Artificial Bee Colony), etc. The main objective of this paper is to propose one of very promising meta-heuristics named Remora, this technique is used to get this point (GMPPT) to show the effectiveness of the proposed method, and as cited bellow, the power delivered by a photovoltaic generator (PVG) strongly depends on the shade and also the nature of the load supplied. For this reason, this paper proposes five PV panels connected to DC load under three scenarios of Partial Shading Conditions (without shading, weak or strong shading). Then we will replace resistance (DC load) by a pumping system (AC load) by using the ROA with just one strong shading scenario.

2 MPPT Based on Remora Algorithm

2.1 Remora optimization principle

The ROA was recently proposed by Heming Jia et al. [4] in 2021. This algorithm is inspired by the intelligent behavior of the remora and random host replacement of the remora, see Figure 1c.

The remora is a fish that lives in warm waters. It is also known as a suckerfish (whalesucker, sharp-sucker and disc fish) because it gets into the habit of sticking itself using a natural suction cup to the skin of sharks in particular (as shown in Figure 1 a)). The remora feeds on the parasites and bacteria found there (as shown in Figure 1 b)). The sharks are thus preserved from various skin infections (their body is kept clean and safe from parasites – a service for which they are even ready to defend their remoras against predators). According to its behavior, the remora will follow algorithms for two hosts, the humpback whale and swordfish:

- The whale optimization algorithm (WOA),
- The swordfish optimization algorithm (SFA).

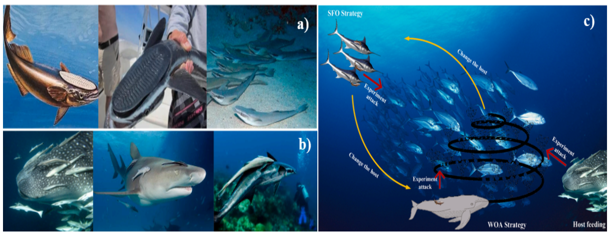

Figure 1: a) The individual remora, b) Remora parasitizes on different hosts, c) The different states of the remora [4].

2.1.1 Initialization

In the proposed ROA, it is assumed that the candidate solution is the remora. Initialize the population location and memory location X_{pre}, initialize the optimal solution X_{best} and corresponding optimal fitness $f(X_{best})$.

2.1.2 Free travel (Exploration)

- *SFO Strategy.*
The remora is stuck to the sworfish, the formula of its location update was improved and got the following equation:

$$X(t+1) = X_{best}(t) + rand.(\frac{X_{best} + X_{rand}}{2}) - X_{rand}. \tag{1}$$

- *Experience attack.*
To know whether it is necessary to change the host or not, the remora must continuously take small steps around the host, this behavior is modeled by the following equation:

$$X_{att} = X_i(t) + randn.(X_i(t) - X_{pre}), \tag{2}$$

X_{pre} represents the previous position, X_{att} represents the tentative position. If the cost function value obtained by the attempted solution is smaller than the current solution

$$f(X_i(t)) > f(X_{att}(t)), \tag{3}$$

the remora then chooses a different feeding method for local optimization shown in the next section. However, if it is not the case, see Eq.(4), the remora returns back to the host selection,

$$f(X_i(t)) < f(X_{att}(t)). \tag{4}$$

2.1.3 Eat thoughtfully (Exploitation)

- *WOA Strategy.*
To update the remora position in the reseach space for the WOA strategy, we use the following equations:

$$X_i(t+1) = D * \exp(\alpha) * cos(2\pi\alpha) + X_i(t). \tag{5}$$

$$D = |X_{best}(t) - X(i)|, \tag{6}$$

$$b = -(\frac{1 + Current_{iteration}}{Max_T}), \tag{7}$$

$$\alpha = rand * (b - 1) + 1, \tag{8}$$

D represents the distance between the best candidate and the remora, α is a random number in [-1, 1], and b is a linear decrease from (-1 to -2).
- *Host Feeding.*
The solution space can be minimized to the position space of the host. The movement of the remora on or around the host can be considered as small steps, which can be presented mathematically as follows:

$$X_i(t) = X_i(t) + A, \tag{9}$$

$$A = B * (X_i(t) - C * X_{best}, \tag{10}$$

$$B = 2 * V * rand - V, \tag{11}$$

$$V = 2 * (1 - \frac{1}{Max_{it}}). \tag{12}$$

2.2 Module

2.2.1 Proposed structure

The power chain of a PVG, where the load (a resistance or pumping system) is supplied by a generator through a static converter controlled by an MPPT, can be represented as shown in Figure 2. The MPPT command varies the duty cycle of the converter so that the power supplied by the PVG is the P_{MAX} available at its terminals. The MPPT algorithm can be more or less complicated to find the PPM, but in general, it is based on the variation of the duty cycle of the static converter until it is placed on the PPM. When we design a photovoltaic installation, we must ensure the electrical protection of this installation in order to increase its lifespan, in particular by avoiding destructive breakdowns linked to the association of the cells and their operation in the shading event. For this, two types of protection are conventionally used in current installations: protection in the case of the parallel connection of PV modules to avoid negative currents in the PVG (anti-return diode) and protection during the series connection of PV modules to avoid losing the entire chain (bypass diode) and avoid hot spots.

In this work, we propose, on one hand, DC load as a resistance and five panels as a source, this configuration is tested under three patterns, the first under zero shading (1000 W/m^2), the second under weak partial shading (1000-1000-500-1000-1000W/m^2) and the third under strong shading (400-1000-200-800-1000W/m^2).

On the other hand, we replace DC load by AC load. In this work, the pumping system (AC load) is containing the induction motor related to the centrifugal pump,

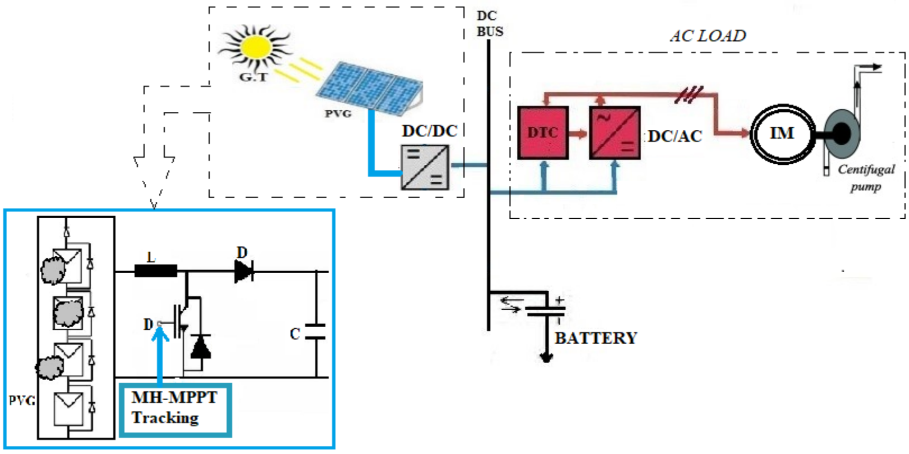

Figure 2: Proposed System with Boost Converter DC/DC.

the inverter (as shown in Figure 2) is controlled by direct torque control, this system is related to the battery. The excellent dynamic torque-control capabilities of traditional DTC are well-known in the literature for the permanent magnet synchronous motors, induction motor and for other motor types as well [5]. The first application of DTC to the asynchronous machine appeared in 1985 and was proposed by Takahachi and Depenbrock [6], [7]. The stator flux vector can be estimated using the measured current and voltage vectors [8], [9], [10]. We calculate the current and voltage in the axes $[\alpha, \beta]$ by using the Concordia transformation, for more details about this type of control, see [8], [9]. To get the needed value of DC voltage to feed the induction motor (514V), we use in this case twelve panels in series, these systems are tested under the PSC with strong shading (the first three panels under 900 W/m^2, the second three panels under 500 W/m^2, the third three panels under 200 W/m^2 and the fourth three panels are without shading).

2.2.2 Proposed ROA-MPPT

The maximum power point tracking by the ROA method is used to get the optimum power, the input of MPPT block is represented by the power (Vpv*Ipv) and the output by the duty cycle of DC-DC converter. Figure 3 represents the flowchart of the ROA used in this work with the initial position 0.1, 0.3, 0.5, 0.7, 0.9, the population number 50 and the maximum number of iterations 300.

3 Digital Simulation

The pumping system is built using MATLAB/SIMULINK. In this simulation, the induction machine parameters and PV panel parameters are listed in Tables of Reference [11].

4 Discussion of Results

In the first part, Figure 4 represents the Duty Cycle and PV Power responses (of the output of the DC-DC converter connected to the resistance load). It can be noticed

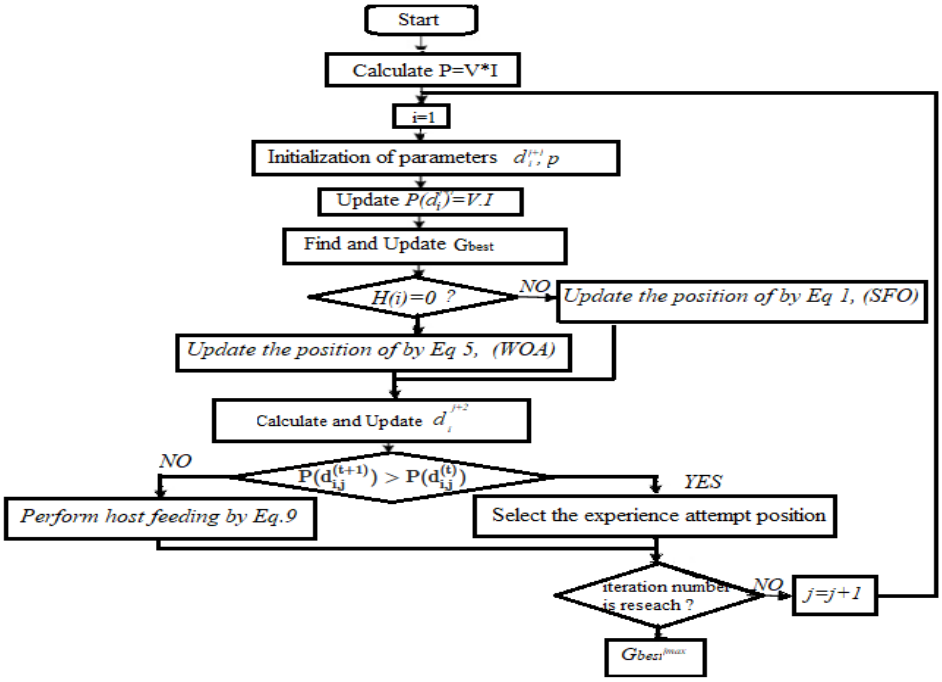

Figure 3: Flowchart of ROA.

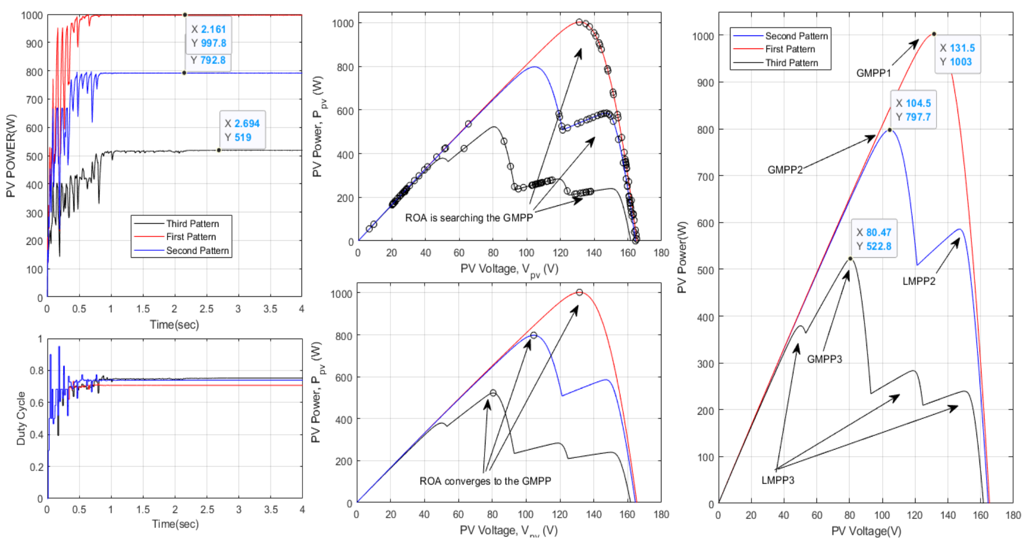

Figure 4: Duty Cycle and PV power responses using PV connected to the resistance load and based on the MPPT-ROA method under three scenarios of PSC(First: Without Shading, Second: Weak Shading, Third: Strong Shading).

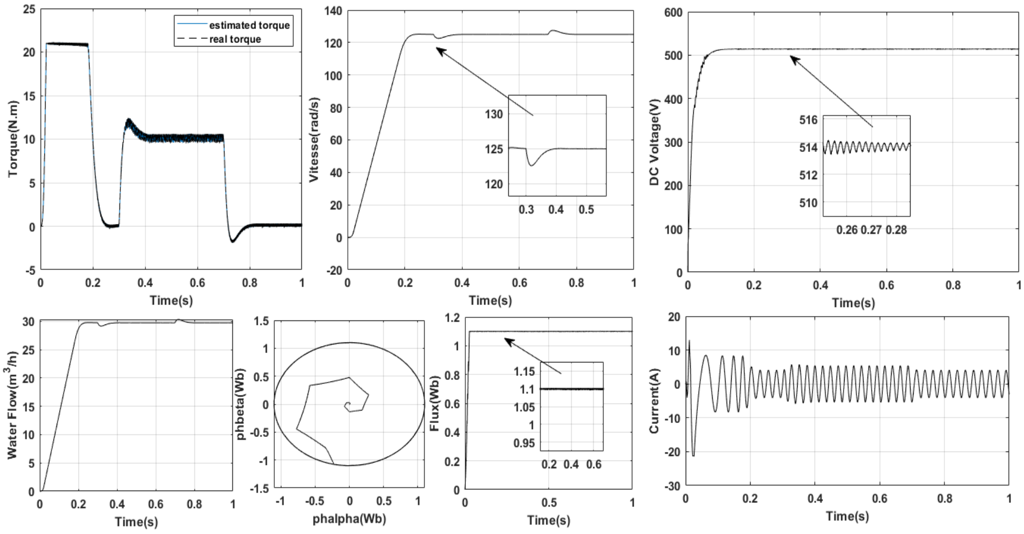

Figure 5: Current, Flow of water, Flux, Torque and Rotor Speed responses of a hybrid (PV-battery-IM-Pump) system based on the Remora method under the PSC.

that the proposed algorithm converges to the GMPP in three scenarios as shown in the same figure, the ROA (with 997.8W) converges to GMMP1 (1003W), the ROA (with 792.8W) converges to GMMP2 (797.7W) and the ROA (with 519W) converges to GMMP3 (522.8W).

In the second part, the pumping system is simulated with a constant load torque (10N.m) applied between 0.3sec and 0.7 sec under strong shading as cited above (at the end of the third paragraph of the proposed structure), and a simulation was run in a closed loop as shown in Figure 5, where it can be observed that the DC voltage, flux and rotor speed track their references (Vdc*=514V, Flux*=1.1Wb, w*=125 rad/ sec).

5 Conclusion

This paper has proposed the ROA to get MPPT under the partial shading condition, according to the results, the proposed method offers a better performance with both DC load and AC load and it can get nearly the GMPP of the proposed configuration cases, under the PSC or without shading regardless of the location of the global MPP.

References

[1] B. Malakondareddy, K.S. Senthil, G.N. Ammasai and I. Anand. An Effective Power Tracking Algorithm for Partially Shaded Solar PV Array Employing Micro Converters Feeding to DC Microgrid. *Periodica Polytechnica Electrical Engineering and Computer Science* **65** (1) (2021) 29–41.

[2] M. Dorigo and T. Stützle. The Ant Colony Optimization Metaheuristic: Algorithms, Applications, and Advances. *Handbook of Metaheuristics*, Chapter **9** (2009) 250–285.

[3] K. Karaboga and B. Basturk. Artificial Bee Colony (ABC) Optimization Algorithm for Solving Constrained Optimization Problems. *Foundations of Fuzzy Logic and Soft Computing* (2007) 789–798.

[4] J. Heming Jia, P. Xiaoxu and L. Chunbo. Remora optimization algorithm. *Expert Systems With Applications* **185** (2021), 115665, 1–25.

[5] V. Tibor, S. László and R. György. A Novel Modified DTC-SVM Method with Better Overload-capability for Permanent Magnet Synchronous Motor Servo Drives. *Periodica Polytechnica Electrical Engineering and Computer Science, Part 1* **62** (3) (2018) 65–73.

[6] I. Takahachi and T. Nogushi.T. A new quick-response and high-efficiency control strategy of an induction motor. *IEEE Trans. Ind. Appl.* **5** (1986) 820–827.

[7] M. Depenbrock. Direct self-control (DSC) of inverter fed induktion machine. *IEEE Power Electronics Specialists Conference* (1987) 632–641.

[8] F. Hamidia, A. Larabi, A. Tlemcani and M. S. Boucherit. AIDTC Techniques for Induction Motors. *Nonlinear Dynamics and Systems Theory* **13** (2) (2013) 147–156.

[9] F. Hamidia, A. Abbadi, A. Tlemcani and M. S. Boucherit. Dual Star Induction Motor supplied with double Photovoltaic Panels Based on Fuzzy Logic Type-2. *Nonlinear Dynamics and Systems Theory* **18** (4) (2018) 359–371.

[10] S. Bentouati, A. Tlemçani, M. S. Boucherit and L. Barazane. A DTC Neurofuzzy Speed Regulation Concept for a Permanent Magnet Synchronous Machine. *Nonlinear Dynamics and Systems Theory* **13** (4) (2013) 344–358.

[11] F. Hamidia and A. Abbadi. SOFC-PV System with Storage Battery Based on Cuckoo Search Algorithm. *Nonlinear Dynamics and Systems Theory* **22** (4) (2022) 367–378.

Nonlinear Dynamics and Systems Theory, **23** (4) (2023) 389–397

Motion Estimation of Third Finger Using Ensemble and Unscented Kalman Filter for Inverse Kinematic of Assistive Finger-Arm Robot

T. Herlambang [1*], H. Nurhadi [2], A. Suryowinoto [3], D. Rahmalia [4] and K. Oktafianto [5]

[1] *Department of Information Systems, Universitas Nahdlatul Ulama Surabaya, Indonesia.*
[2] *Department of Industrial Mechanical Engineering, Sepuluh Nopember Institute of Technology, Indonesia.*
[3] *Electrical Engineering Department, Adhi Tama Institute of Technology Surabaya, Indonesia.*
[4] *Department of Mathematics, University of Islam Darul Ulum Lamongan, Indonesia.*
[5] *Department of Mathematics, University of PGRI Ronggolawe, Indonesia.*

Received: October 20, 2022; Revised: October 16, 2023

Abstract: The Islamic Hospital (RSI) Jemursari and RSI A. Yani always attempts to achieve an optimal community health status by health maintenance, health improvement (promotive), disease prevention (preventive), healing (curative) and recovery (rehabilitative) approaches in a comprehensive, integrated, and sustainable way. Specialists in prosthetics and orthotics, as the health professionals who are members of the medical rehabilitation team unit in Indonesia, are responsible for carrying out medical rehabilitation activities. The goal of the medical rehabilitation is to achieve its maximum functional competence and to prevent recurrent attacks. For this, a biomedical technology, that is, an assistive finger-arm robot, is required to help the recovery. The assistive finger-arm robot is one solution to assist the recovery process of paresis patients, specifically for finger movement. One of the research and development efforts on the assistive finger-arm robot is finger motion estimation. Several reliable motion estimation methods frequently used are the Unscented Kalman Filter (UKF) and Ensemble Kalman Filter (EnKF) methods, which are very reliable for either forward and inverse kinematic models or nonlinear models. Therefore, both methods were used in this study. Before the estimation was carried out, we started with modeling the inverse kinematics of the finger-arm robot as a platform for emulating the real movement of the fingers, to be specific, the third finger only. In this case, the third finger size was taken from the Surabaya citizens from Indonesia. The simulation results show that both methods had a fairly small error of about 2.5% -4.23%.

Keywords: *finger-arm robot; UKF; EnKF; inverse kinematic models.*

Mathematics Subject Classification (2010): 93E10, 62F10.

* Corresponding author: mailto:teguh@unusa.ac.id

1 Introduction

University of Nahdlatul Ulama Surabaya (UNUSA) is under the Surabaya Islamic Hospital (RSI) Foundation running the Jemursari Islamic Hospital and the Wonokromo Islamic Hospital. To support RSI Jemursari and RSI A. Yani in Wonokromo in an effort to achieve optimal community health status by applying health maintenance, health improvement (promotive), disease prevention (preventive), healing (curative) and recovery (rehabilitative) approaches in a comprehensive, integrated, and sustainable way, it attempts to develop any relevant and effective devices [1].

Specialists in prosthetics and orthotics as professionals who are members of the medical rehabilitation team unit in Indonesia are responsible for carrying out medical rehabilitation activities [1]. The rehabilitation program is a form of integrated health services with medical, psychosocial, educational vocational approach aiming to achieve its maximum function and to prevent repeated attacks. This rehabilitation program provides services using a multidisciplinary approach involving neurologists, medical rehabilitation doctors, nurses, physiotherapists, occupational therapists, medical social workers, psychologists as well as clients and families. One of the medical rehabilitation activities is the recovery of paresis sufferers. Paresis is a condition characterized by weakness of body movement, or partial loss of body movement or movement disorders. Among them is weakness in the fingers of post-stroke patients. For that, we need a biomedical technology to help recovery after stroke [2].

One of such technologies is robotic finger-arm assistance [3]. An assistive finger-arm robot is one solution to assist the recovery process of paresis patients, especially the movement of the fingers. One of such efforts to develop the assistive finger-arm robot is estimation of finger motion [2]. Several reliable estimation methods frequently used are the Ensemble Kalman Filter (UKF) and Ensemble Kalman Filter (EnKF) methods, which are very reliable for either forward and inverse kinematic models or nonlinear models. In its application, prior to estimation, we start with modeling the inverse kinematics of the finger-arm robot as a platform for mimicing the real movement of the fingers, to be more specific, the third finger. In this case, for this study, the third finger size is taken from the citizens of Surabaya, Indonesia. The UKF and EnKF methods are also frequently used to estimate the motion and position of submarines [4–6] and surface ships [7, 8]. But the object of this study is finger motion estimation.

2 Finger Arm Motion Modelling

Specifically, the aim of the study in this paper was to estimate the motion of the fingers, especially the third finger of the left hand, using the EnKF and UKF methods by comparing the accuracy rates of these two motion estimation methods.

Here is the analysis of the finger-arm robot with 3 joints.

Figure 1 shows the 3-joint arm robot using the x and y coordinates in its working area. Just like the 2-joint arm robot, the 3-joint arm robot uses forward kinematics as an equation analysis [9].

The angle Ψ is the angle of the direction of the third part toward the X-axis, as in equation (1),

$$\Psi = (\theta_1 + \theta_2 + \theta_3). \tag{1}$$

Figure 2 is used to find the equation for the projections of link 1, link 2 and link 3 about the x-axis and y-axis, the projections can be analyzed and combined into an

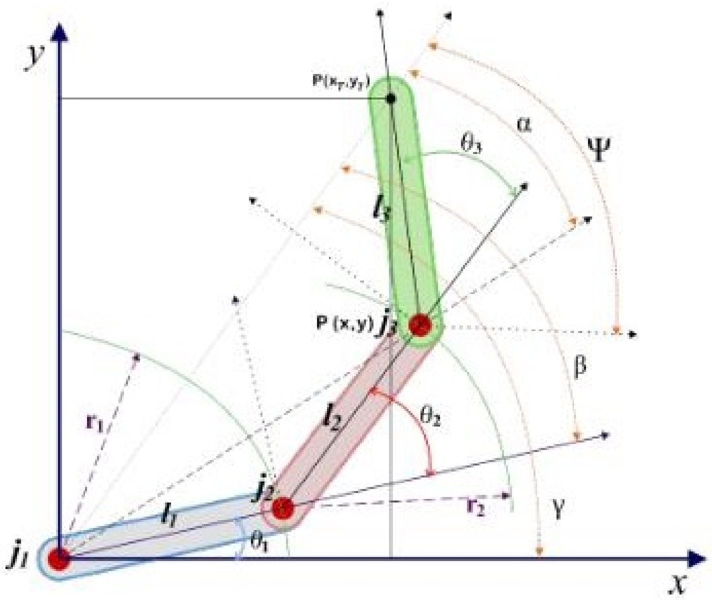

Figure 1: Configuration of the Finger-Arm Robot with 3 Joints.

equation.

For inverse kinematics, if the coordinates of $P(X_T, Y_T$ and $P(x, y)$ are known, then the angles θ_1, θ_2 and Ψ are as follows:

$$\begin{aligned} \theta_2 &= \cos^{-1}\left(\frac{x^2+y^2-l_1^2-l_2^2}{2l_1l_2}\right), \\ \theta_1 &= \tan^{-1}\left(\frac{y(l_1+l_2\cos\theta_2)-xl_2\sin\theta_2}{x(l_1+l_2\cos\theta_2)+yl_2\sin\theta_2}\right), \end{aligned} \tag{2}$$

$$\begin{aligned} \Psi &= \theta_1+\theta_2+\theta_3 \\ &= \sin^{-1}\left(\frac{l_1(\cos\theta_1-\sin\theta_1)+l_2(\cos(\theta_1+\theta_2)-\sin(\theta_1+\theta_2))}{2l_3}\right). \end{aligned} \tag{3}$$

Below is the picture of three joints of the finger of a Surabaya citizen.

3 Ensemble and Unscented Kalman Filter Algorithms

The Ensemble and Uscented Kalman Filter algorithms are summarized in Table 1.

4 Simulation Results

This study started with forward kinematics modeling to obtain the motion on the X and Y axes and, after that, to obtain an inverse kinematic model of a robotic finger prosthetic arm with 3 joint parts that match the structure of the human finger.

Figure 2: Image of the arm robot with a focus on its finger prosthetic arms.

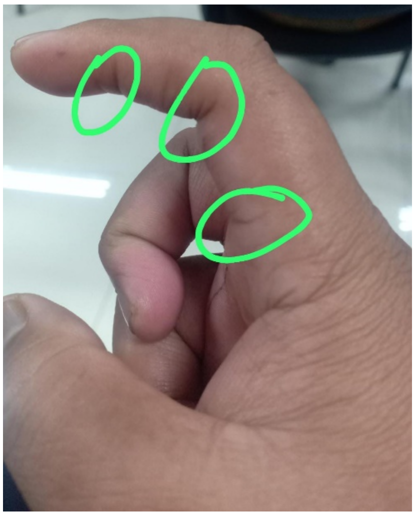

Figure 3: Picture of three joints of the finger of a Surabaya citizen.

In the numerical computation, the focus was on the movement of the third finger, the average length of which for Surabaya people, part of the Javanese tribe in Indonesia, is around 7.8 – 8.3 cm.

In this paper, the study used and compared the accuracy of the UKF and EnKF methods by comparing the four simulation results, that is, those by generating 500 and 600 ensembles and at 300 and 400 iterations. The third finger motion chosen in this simulation was the third finger motion in the form of a semicircular trajectory because

EnKF	**UKF**
System Model and Measurement Model	
$x_{k+1} = f(u_k, x_k) + w_k, w_k \sim N(0, Q_k)$ $z_k = Hx_k + v_k, v_k \sim N(0, R_k)$	$x_{k+1} = f(u_k, x_k) + w_k, w_k \sim N(0, Q_k)$ $z_k = Hx_k + v_k, v_k \sim N(0, R_k)$
Initialization	
Generate N *ensemble* in accordance with initial estimate $\overline{x}_0$ $x_{0,i} = [x_{0,1}\ x_{0,2}\ x_{0,3}\ \dots\ x_{0,Ne}]$ Determine initial value : $\widehat{x}_0 = \frac{1}{N_e}\sum\limits_{i=1}^{N} X_{0,i}$	$\widehat{x}_0 = E[x_0]$ $P_{x_0} = E[(x_0 - \widehat{x}_0)(x_0 - \widehat{x}_0)^T]$ $\widehat{x}_0^a = E[x^a] = E[\widehat{x}_0^T\ 0\ 0]^T$
Prediction Stage	
$\widehat{x}_{k,i}^- = f(\widehat{x}_{k-1,i}, u_{k-1,i}) + w_{k,i}$ with $w_{k,i} \sim N(0, Q_k)$ Estimate : $\widehat{x}_k^- = \frac{1}{N_e}\sum\limits_{i=1}^{N} \widehat{x}_{k,i}^-$ Covariance error : $P_k^- = \frac{1}{N_e-1}\sum\limits_{i=1}^{N}(\widehat{x}_{k,i}^- - \widehat{x}_k^-)(\widehat{x}_{k,i}^- - \widehat{x}_k^-)^T$	$X_{k\|k-1}^- = f(X_{k\|k-1}^x, X_{k\|k-1}^v)$ Estimate : $\widehat{x}_k^- = \sum\limits_{i=0}^{2L} W_i^{(m)} X_{i,k\|k-1}^x$ Covariance error : $P_{x_k}^- = \sum\limits_{i=0}^{2L} W_i^{(c)}(X_{i,k\|k-1}^x - \widehat{x}_k^-)(X_{i,k\|k-1}^x - \widehat{x}_k^-)^T$
Correction Stage	
$z_{k,i} = z_k + v_{k,i}$ with $v_{k,i} \sim N(0, R_k)$ Kalman gain : $K_k = P_k^- H^T(HP_k^- H^T + R_k)^{-1}$ Estimate : $\widehat{x}_{k,i} = \widehat{x}_{k,i}^- + K_k(z_{k,i} - H\widehat{x}_{k,i}^-)$ $\widehat{x}_k = \frac{1}{N_e}\sum\limits_{i=1}^{N} \widehat{x}_{k,i}$ Covariance error : $P_k = [I - K_k H]P_k^-$	$P_{\bar{z}_k,\bar{z}_k} = \sum\limits_{i=0}^{2L} W_i^{(c)}(Z_{i,k\|k-1} - \widehat{z}_k^-)(Z_{i,k\|k-1} - \widehat{z}_k^-)^T$ Kalman gain : $P_{x_k,\bar{z}_k} P_{\bar{z}_k,\bar{z}_k}^{-1}$ Estimate : $\widehat{x}_k = \widehat{x}_k^- + K_k(Z_k - \widehat{Z}_k^-)$ Covariance error : $P_{x_k} = P_{x_k}^- - K_k P_{\bar{z}_k} K_k^T$

Table 1: EnKF and UKF Algorithms [10–13].

within that range, all finger joints could move optimally. With a semi-circular motion with a diameter of about 7.8 cm, the physical exercise on the third finger could be done to the maximum. The simulation results can be seen in Figures 4–7.

Figures 4 and 5 represent the simulation results of the estimated motion of the third finger resembling a semi-circle by generating 500 and 600 ensembles with 300 iterations, while Figures 6 and 7 used 400 iterations in the simulations.

Figure 4 shows the results of the simulations by the UKF and EnKF methods, using 300 iterations and generating 500 Ensembles for the EnKF method, resulted in a motion resembling a semi-circle with a diameter of $\sqrt{7.3^2 + 1.8^2} = \sqrt{53.29 + 3.24} = \sqrt{56.53} = 7.158$ cm, so overall, for the diameter of about $7.8 - 8.3$ cm, and using 500 ensembles, it had an error of around 3.6%, in other words, it gained an accu-

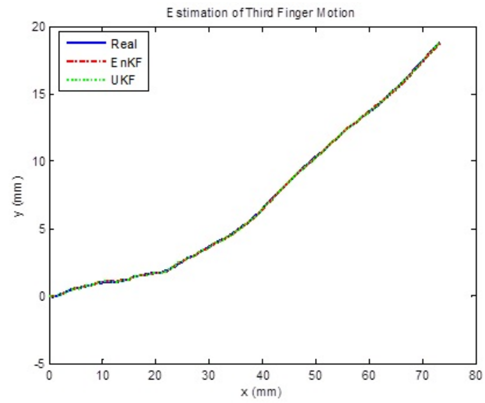

Figure 4: Estimation of Third Finger Motion in XY Plane using UKF and EnKF with 300 iterations and 500 Ensembles

racy of about 96.7%, while the UKF method produced a motion with a diameter of $\sqrt{7.25^2 + 1.82^2} = \sqrt{52.5625 + 3.3124} = \sqrt{55.8749} = 7.47$ resulting in an error of about 4.23%, in other words, it gained an accuracy of about 95.77%.

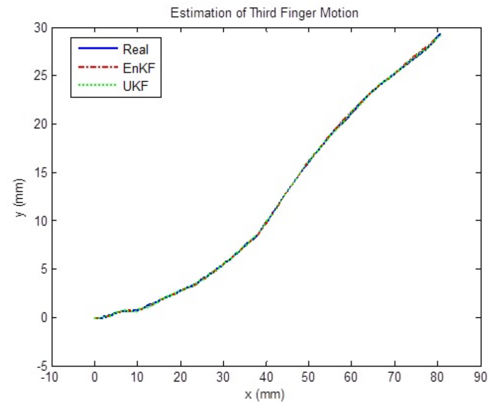

Figure 5: Estimation of Third Finger Motion in XY Plane using UKF and EnKF with 300 iterations and 600 Ensembles.

Figure 5 shows the results of the simulations by the UKF and EnKF methods, using 300 iterations and generating 500 ensembles, the EnKF method resulted in a motion resembling a semi-circle with a diameter of $\sqrt{8^2 + 2.9^2} = \sqrt{64 + 8,41} = \sqrt{72.41} = 8.509$ cm, so overall, for the diameter of about $7.8 - 8.3$ cm, and using 600 ensembles, it had an error of about 2.51%, in other words, it gained an accuracy of about 97.49%. Meanwhile, the UKF method produced a motion with a diameter of $\sqrt{8.1^2 + 2.92^2} = \sqrt{65.61 + 8.5264} = \sqrt{74.1364} = 8.61$, resulting in an error of about $3,73\%$, in other words, it gained an accuracy of about 96.27%.

According to Table 2, it is clear that the Ensemble Kalman Filter was more accurate than the UKF for both 500 and 600 ensembles. However, the UKF method had a faster

	EnKF with 500 Ensembles	UKF	EnKF with 600 Ensembles	UKF
XY Motion	96.7%	95.77 %	97.49%	96,27%
Simulation Time	10.85 s	10. 66 s	13.31 s	13,1 s

Table 2: Accuracy rate of motion estimation of third finger using UKF and EnKF methods with 300 iterations.

simulation time because it did not generate a number of ensembles. Overall, in terms of the level of accuracy above 95%, both methods were effective and can be used to effectively estimate the motion of the assistive finger-arm robot.

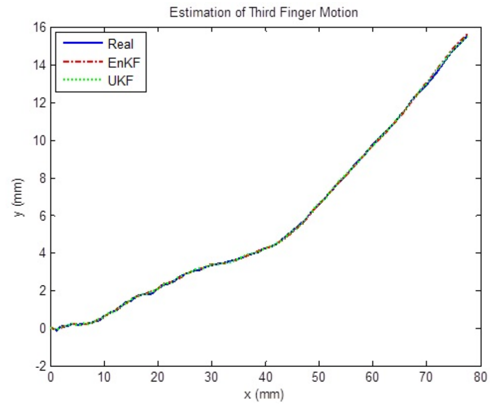

Figure 6: Estimation of Third Finger Motion in XY Plane using UKF and EnKF with 400 iterations and 500 Ensembles.

Figure 6 shows the results of the simulations by the UKF and EnKF methods, using 400 iterations and generating 500 ensembles, the EnKF method produced a motion resembling a semi-circle with a diameter of $\sqrt{7.8^2 + 1.5^2} = \sqrt{60.84 + 2.25} = \sqrt{63.09} = 7.94$ cm, so overall, for the diameter of about $7.8cm - 8.3$ cm, the range of 7.94 cm is included in the average length range of the third finger of Surabaya residents, in other words, there is no error or one has 100% accuracy. Meanwhile, the UKF method produced a motion with a diameter of $\sqrt{7.82^2 + 1.53^2} = \sqrt{61.1524 + 2.3409} = \sqrt{63.4993} = 7.968$, which is included within the average length range of the third finger of Surabaya people.

Figure 7 shows the results of the simulations by the UKF and EnKF methods, using 400 iterations and generating 600 ensembles, the EnKF method produced a motion resembling a semi-circle with a diameter of $\sqrt{7.8^2 + 2.4^2} = \sqrt{60.84 + 5.76} = \sqrt{66.6} = 8.16$ cm, so overall, for the diameter of about $7.8 - 8.3$ cm, the range of 8.16 cm is included within the range of the average length of the third finger of Surabaya people, in other words there is no error or one has 100% accuracy. Meanwhile, the UKF method produced a motion with a diameter of $\sqrt{7.77^2 + 2.36^2} = \sqrt{60.3729 + 5.5696} = \sqrt{65.9425} = 8.12$ cm, so overall, for the diameter of about $7.8 - 8.3$ cm, the range of 8.12 cm is included within the range of the average length of the third finger of Surabaya people, in other words, there is no error or one has 100% accuracy.

According to Table 3, it is clear that using the Ensemble Kalman Filter and Unscented

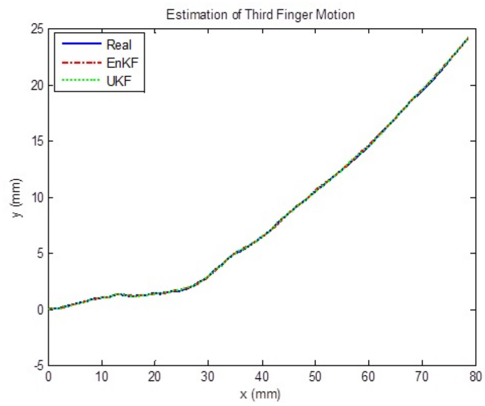

Figure 7: Estimation of Third Finger Motion in XY Plane using UKF and EnKF with 400 iterations and 600 Ensembles.

	EnKF with 500 Ensembles	UKF	EnKF with 600 Ensembles	UKF
XY Motion	100%	100 %	100%	100%
Simulation Time	15.45 s	15.18 s	17.62 s	17,33 s

Table 3: Accuracy rate of third finger motion estimation using UKF and EnKF with 400 iterations.

Kalman Filter produced the same accuracy of 100%. However, the UKF method had a faster simulation time because it did not generate a number of ensembles. Overall, in terms of the level of accuracy above 95%, both methods were effective and applicable to estimate the motion of the assistive finger-arm robot.

5 Conclusion

Based on the simulation results and the analysis above, it was found out that the EnKF and UKF methods were able to effectively estimate the third finger motion, especially for the finger size of the Javanese people in Indonesia, with an accuracy of around 95% – 100%. The error generated by the EnKF method in the simulation using 300 iterations was about 2.51% – 3.6%, while the UKF method produced an error of 3.7% – 4.2%. However, the simulation results using 400 iterations by the two methods, EnKF and UKF, had the same 100% accuracy rate. Overall, in terms of the level of accuracy above 95%, the two methods were effective and applicable to estimate the motion of the assistive finger-arm robot.

Acknowledgment

High appreciation to the Kemdikbudristek for the very fund support for the research conducted in the year of 2023 with contract number 077/ E5/PG.02.00.PL/2023, 035/SP2H/PT-L/LL7/2023 and 1034/UNUSA-LPPM/Adm-I/VI/2023.

References

[1] O. S. Purwanti and A. Maliya. Rehabilitasi Klien Pasca Stroke. *Berita Ilmu Keperawatan* **1** (1) (2008) 43–46.

[2] T. Herlambang, H. Nurhadi, A. Muhith, D. Rahmalia and P. B. Tomosouw. Estimation of Third Finger Motion Using Ensemble Kalman Filter. *BAREKENG: Jurnal Ilmu Matematika Dan Terapan* **16** (3) (2022).

[3] T. Herlambang, A. Muhith, D. Rahmalia and H. Nurhadi. Motion Optimization using Modified Kalman Filter for Inverse-Kinematics based Multi DOF Arm Robot. *International Journal of Control and Automation* **13** (2s) (2020) 6–71.

[4] S. Subchan, T. Herlambang and H. Nurhadi. UNUSAITS AUV Navigation and Guidance System with Nonlinear Modeling Motion Using Ensemble Kalman Filter. In: *Proc. International Conference on Advanced Mechatronics, Intelligent Manufacture, and Industrial Automation (ICAMIMIA)* Malang, Indonesia, 2019.

[5] T. Herlambang, S. Subchan and H. Nurhadi. Navigation and Guidance Control System of UNUSAITS AUV Based on Dynamical System Using Ensemble Kalman Filter Square Root. In: *Proc. The Third Internatonal Conference on Combinatorics, Graph Teory and Network Topology* Jember, Indonesia, 2019.

[6] T. Herlambang, D. Rahmalia, H. Nurhadi, D. Adzkiya and S. Subchan. Optimization of Linear Quadratic Regulator with Tracking Applied to Autonomous Underwater Vehicle (AUV) Using Cuckoo Search. *Nonlinear Dynamics and Systems Theory* **20** (3) (2021) 282–298.

[7] H. Nurhadi, T. Herlambang and D. Adzkiya. Trajectory Estimation of Autonomous Surface Vehicle Using Square Root Ensemble Kalman Filter. In: *Proc. International Conference on Advanced Mechatronics, Intelligent Manufacture, and Industrial Automation (ICAMIMIA)* Malang, Indonesia, 2019.

[8] H. Nurhadi, T. Herlambang and D. Adzkiya. Position Estimation of Touristant ASV Using Ensemble Kalman Filter. In: *Proc.International Conference on Mechanical Engineering* Indonesia, 2019.

[9] I. Sugiharto. Pemodelan dan Simulasi Dinamika Lengan Robot 3-DOF Menggunakan Perangkat Lunak Open Source. *Jurnal Teknik Elektro* **8** (2) (2008).

[10] A. Muhith, T. Herlambang, D. Rahmalia, Irhamah and D. F. Karya. Estimation of Thrombocyte Concentrate (TC) in PMI Gresik using unscented and square root Ensemble Kalman Filter. In: *Proc. The* 5^{th} *International Conference of Combinatorics, Graph Theory, and Network Topology (ICCGANT)* Jember, Indonesia, 2021.

[11] M. Y. Anshori and T. Herlambang. Profitability Estimation of XYZ Company Using H-Infinity and Ensemble Kalman Filter. In: *Proc. The* 5^{th} *International Conference of Combinatorics, Graph Theory, and Network Topology (ICCGANT)* Jember, Indonesia, 2021.

[12] T. Herlambang, A. Muhith, Irhamah, M. Y. Anshori, D. Rahmalia and D. F. Karya. Implementation of H-infinity and Ensemble Kalman Filter for Whole Blood (WB) Estimation in PMI Bojonegoro. In: *Proc. Proceedings of the 6th National Conference on Mathematics and Mathematics Education* AIP Conference Proceedings, 2022.

[13] D. F. Karya, M. Y. Anshori, R.Rizqina, P. Katias, A. Muhith and T. Herlambang. Estimation of Crude Oil Price Using Unscented Kalman Filter. In: *Proc. The* 5^{th} *International Conference of Combinatorics, Graph Theory, and Network Topology (ICCGANT)* Jember, Indonesia, 2019.

Nonlinear Dynamics and Systems Theory, **23** (4) (2023) 398–409

Stability and Hopf Bifurcation of a Generalized Differential-Algebraic Biological Economic System with the Hybrid Functional Response and Predator Harvesting

M. C. Benkara Mostefa [1*] and N. E. Hamri [2]

[1] *Departement of Mathematics, University of Mentouri, Constantine 1, Algeria.*
[2] *Mathematics and their Interactions Laboratory (Melilab), University Center of Abdelhafid Boussouf, Mila, Algeria.*

Received: May 8, 2023; Revised: September 6, 2023

Abstract: This paper examines the dynamics of a bio-economic predator-prey system that employs harvesting and the hybrid response function. The system includes an algebraic equation because of the economic revenue. We give a thorough mathematical study of the suggested model to highlight some of the significant results. The boundedness and positivity of model's solutions are examined. The coexistence equilibrium of the bio-economic system has been extensively studied, and the behavior of the model around it has been explained using the qualitative theory of dynamical systems (such as local stability and the Hopf bifurcation). The data gained offer a useful framework for understanding the role of economic revenue v. We establish that a positive equilibrium point is locally asymptotically stable when the profit v falls below a particular critical value v^*. Our research shows it to be true. According to our research, economic revenue can stabilize the system, which is the most important of all spaces.

Keywords: *algebraic differential equations; equilibrium point; Hopf bifurcation; predator-prey system; stability.*

Mathematics Subject Classification (2010): 70K42, 70K50, 93A10, 93A30.

* Corresponding author: mailto:che.benkara@gmail.com

1 Introduction

For humanity's long-term welfare, there is a great deal of interest in comprehending and developing bio-economic models for biodiversity. To preserve the long-term viability and prosperity of the ecosystem, researchers are attempting to generate some possibly beneficial effects.

Numerous studies have focused on understanding these processes. The dynamical behavior of a specific predator-prey ecosystem was explored using a number of differential equations and an algebraic equation [12, 17]. They made important discoveries, including limit cycle, singularity-driven bifurcation, control, and interior equilibrium stability. However, in all of the models examined, only the prey population is harvested. The relationship between the predator and the prey was investigated using a variety of functional responses, including Holling-type I, Holling-type II [10, 11], Holling-type III [13], and Beddington-DeAngelis [19], under the presumption that the isolated predator species had natural mortality.

As far as we know, a dynamical investigation of a predator-prey model with a hybrid functional response has never been done. Since this model exhibits stability and the Hopf bifurcation, we explore it and describe it in this paper [13, 15]. Additionally, we are interested in learning some theoretical guidelines for administering and regulating renewable resources.

We organized the existing information in the manner described below to achieve the predetermined goals: we started our investigation by going through the model-building idea and its biological importance. We sequentially prove the pomposity and boundedness of the model. Following a thorough discussion of the system's stability and the Hopf bifurcation analysis, the existence of a positive equilibrium is then investigated. We conclude by presenting numerical simulation tests that support the theoretical findings.

2 The Model

The study of population dynamics with harvesting has emerged as a fascinating subject in mathematical bio-economics due to the significance of the effective management of renewable resources. When Gordon [7] established a standard property resource economic theory in 1954, he made the following economic proposition. This theory examined the impact of harvest effort on the ecosystem from an ecological perspective.

$$NetEconomicRevenue(NER) = TotalRevenue(TR) - TotalCost(TC). \tag{1}$$

Studying the predator-prey paradigm with the hybrid functional response is both intriguing and crucial:

$$\begin{cases} \frac{dX}{d\tau} = (a_1 - b_1 X - \frac{m_1 Y}{\alpha_1 X + \beta_1 Y + \gamma_1})X, \\ \frac{dY}{d\tau} = (a_2 - \frac{m_2 Y}{X + K_1})Y \end{cases} \tag{2}$$

with the initial values $X(0) > 0$ and $Y(0) > 0$. The constants a_1, a_2, b_1, b_2, m_1, m_2, α_1, β_1, γ_1 and K_1 are the parameters of the model and are assumed to be nonnegative with β_1 non trivial (if $\beta_1 = 0$, then the model (2) is the same as that in [14]).

These parameters are defined as follows: a_1 (resp.,a_2) describes the growth rate of the prey (resp., of the predator), b_1 measures the strength of competition among the individuals of the prey's species, m_1 is the maximum value which per capita reduction rate of the prey can attain, γ_1 (resp., K_1) measures the extent to which environment provides protection to the prey (resp., to the predator), and m_2 has a similar meaning to m_1. The functional response in (2) was introduced by Beddington [2] and DeAngelis et al. [6].

When introducing the following scaling (see [14]): $t = a_1\tau$, $x(t) = (b_1/a_1)X(\tau)$, and $y(t) = (m_2b_1/a_1a_2)Y(\tau)$, the hybrid functional response model (2) should take the following nondimensional form:

$$\begin{cases} \frac{dx}{dt} = x(1-x) - \frac{axy}{\alpha x+\beta y+\gamma}, \\ \frac{dy}{dt} = b(1 - \frac{y}{x+k})y \end{cases} \tag{3}$$

where $a = (a_1/a_2)(m_1/m_2)$, $b = a_2/a_1$, $\alpha = \alpha_1$, $\beta = \beta_1(a_2/m_2$, $\gamma = \gamma_1(b_1/a_1)$, and $k = K_1(b_1/a_1)$. The model (3) that interests us is introduced in [14].

It is known that the harvest effort is an important factor to construct a useful bioeconomic mathematical model, for this reason, taking (1) into account, we extend the system (3) by considering the following algebraic equation which describes the economic profit v of the harvest effort on the predator:

$$E(t)(py(t) - c) = v, \tag{4}$$

where $0 \leq E(t) \leq E_{max}$ and $y(t) \geq 0$ represent the harvest effort and the density of the predator, respectively. p represents the unit price of the harvested population and c is the cost of harvest effort, the total revenue and total cost are

$$TR = pE(t)y(t), \quad TC = cE(t).$$

Based on (3) and (4), a singular differential-algebraic model that consists of two differential equations and an algebraic equation can be established as follows:

$$\begin{cases} \frac{dx}{dt} = x(1-x) - \frac{axy}{\alpha x+\beta y+\gamma}, \\ \frac{dy}{dt} = b(1 - \frac{y}{x+k})y - Ey, \\ 0 = E(py-c) - v \end{cases} \tag{5}$$

which is a semi-explicit differential-algebraic equation of the form

$$\begin{cases} \dot{z} = \frac{dz}{dt} = f(v, X), \\ \quad\; 0 = g(v, X), \end{cases} \tag{6}$$

where we denote $X = (x, y, E)^T$, with $z = (x, y)^T$ being the differential variable, E being the algebraic variable, v is the bifurcation parameter, f and g are the smooth functions given by

$$f(v, X) = \begin{pmatrix} f_1(v, X) \\ f_2(v, X) \end{pmatrix} = \begin{pmatrix} x((1-x) - \frac{ay}{\alpha x+\beta y+\gamma}) \\ y(b(1 - \frac{y}{x+k}) - E) \end{pmatrix},$$
$$g(v, X) = E(py - c) - v.$$

3 Mathematical Analysis

We are just concerned with this model's dynamics, positive octant $\mathbb{R}^3_+$ for biological reasons. Thus, we consider the biologically meaningful initial condition

$$x(0) = x_0 \geq 0, \; y(0) = y_0 \geq 0, \; E(0) = E_0 = \frac{v}{py_0 - c}, \; py_0 - c > 0. \tag{7}$$

3.1 Existence and uniqueness

Proposition 3.1 *The system (5) with the initial conditions (7) has a unique maximal solution* $(x(t), y(t), E(t))$ *in an open subset* U *of* $\Omega = \{(x, y, E)^T \in \mathbb{R}^3_+ /\ py - c > 0\}$ *defined on some maximal interval* $[0, T[$.

Proof. Let $(x, y, E)^T \in U$, then from the algebraic equation $g(x, y, E, v) = 0$, we get $E = \frac{v}{px-c}$, substituting in the first differential equation of (5). The differential-algebraic equation is transformed to the following ordinary differential equation that has the same solution with respect to the differential variables $z = (x, y)^T$:

$$\begin{cases} \frac{dx}{dt} = x(1-x) - \frac{axy}{\alpha x+\beta y+\gamma}, \\ \frac{dy}{dt} = b(1-\frac{y}{x+k})y - \frac{vy}{py-c}, \end{cases} \tag{8}$$

its vectorial form is $\dot{z} = \frac{dz}{dt} = F(z)$, where

$$F(z) = \begin{pmatrix} x((1-x) - \frac{ay}{\alpha x+\beta y+\gamma}) \\ y(b(1-\frac{y}{x+k}) - \frac{v}{py-c}) \end{pmatrix}.$$

Clearly, $F \in C^1(U^{'})$, where $U^{'}$ is an open subset of $\Omega^{'} = \{(x, y,)^T \in \mathbb{R}^2_+ /\ py - c > 0\}$. Thus, by applying Cauchy-Lipschitz's theorem for ordinary differential equations [9], we deduce the local existence and uniqueness of the maximal solution $(x, y)^T$ to (8) for any $(x_0, y_0) \in U^{'}$, then the local existence and uniqueness of solution for (5) is straightforward.

3.2 Positivity and boundedness

Regarding the positivity of solution for the system (5), we introduce the following proposition.

Proposition 3.2 *Any smooth solution of (5), defined on the maximal interval* $[0, T[$, *with positive initial condition (7), remains positive for all* $t \in [0, T[$.

Proof. From the system (8), it follows that $x = 0$ implies $\frac{dx}{dt} = 0$ and $y = 0$ implies $\frac{dy}{dt} = 0$, thus $x = 0$ and $y = 0$ are invariant sets showing that $x(t) \geq 0$ and $y(t) \geq 0$ whenever $x(0) > 0$ and $y(0) > 0$.

From the second equation of (8), we deduce that for all $t \in [0, T[$,

$$py(t) - c \neq 0. \tag{9}$$

Suppose that there exists $t^* \in [0, T[$ such that $E(t^*) < 0$, it follows that $px(t^*) - c < 0$, then by applying the intermediate value theorem to the continuous function $py(t) - c$ on the interval $[0, t^*]$, we deduce the existence of $\tilde{t} \in]0, t^*[$ such that $py(\tilde{t}) - c = 0$, which contradicts (9), thus, $E(t) \geq 0$ for all $t \in [0, T[$.

Clearly, when the prey biomass x approaches to the critical value $y_c = \frac{c}{p}$, the finishing effort E will being unbounded is not realistic.

To answer the boundedness of the solution for system (5), we impose a realistic ecological contraint in the context that the economic policy requires a minimum level $y_{min} > 0$ for the resource given by

$$y(t) \geq y_{min} > \frac{c}{p}, \quad \forall t \geq 0. \tag{10}$$

This constraint will affect the fishing effort E that will be constrained by a fixed production capacity. We denote this limit capacity by E_{max}, then

$$0 < E(t) \leq E_{max} = \frac{v}{py_{min} - c}, \quad \forall t \geq 0. \tag{11}$$

Next, we will show that, under some assumptions, the solutions of system (5), which start in $\mathbb{R}^3_+$, are ultimately bounded. First, let us give the following comparison result.

Definition 3.1 A solution $\phi(t, t_0, x_0, y_0, E_0)$ of system (5) is said to be ultimately bounded with respect to $\mathbb{R}^3_+$ if there exists a compact region $A \subset \mathbb{R}^3_+$ and a finite time T $(T = T(t_0, x_0, y_0, E_0)$ such that, for any $(t_0, x_0, y_0, E_0) \in \mathbb{R} \times \mathbb{R}^3_+$,

$$\phi(t, t_0, x_0, y_0, E_0) \in A, \quad \forall t \geq T. \tag{12}$$

Proposition 3.3 *All solutions of the system (5) subject to the initial conditions (7) and constraint (11) are bounded in $\mathbb{R}^3_+$ with an ultimate bound.*

Proof. (1) We have for all $t \geq 0$, $0 \leq x(t) \leq 1$ and $0 \leq x + y \leq L_1$, see [14]

$$L_1 = \frac{1}{4b}(5b + (1+b)^2(1+k).$$

Then

$$(x(t), y(t), E(t)) \in A = \{(x, y, E) \in \mathbb{R}^3_+ : \ 0 \leq x \leq 1, \ 0 \leq x + y \leq L_1, \ 0 \leq E \leq E_{max}\}.$$

(2) We have to prove that, for $(x(0), y(0), E(0)) \in \mathbb{R}^3_+$, $(x(t), y(t), E(t)) \in A$ when $t \to +\infty$. We will show that $\overline{lim}_{t\to+\infty} x(t) \leq 1$, $\overline{lim}_{t\to+\infty}(x(t) + y(t)) \leq L_1$, and $\overline{lim}_{t\to+\infty} E(t) \leq E_{max}$, see [14]. Then we conclude that system (5) is dissipative in $\mathbb{R}^3_+$.

4 Existence and Positivity Equilibrium Points

In this section, we aim to inspect the existence of the positive equilibrium points and to study their stability.
An equilibrium point of the system (5) is a solution of the following equations:

$$\begin{cases} f_1(v, X) = 0, \\ f_2(v, X) = 0, \\ g(v, X) = 0. \end{cases} \tag{13}$$

By the analysis of the roots for (13), it follows that

(i) If $v = 0$, then there exist at least three boundary equilibrium points

$$X_{e1} = (0, 0, 0), \ X_{e2} = (1, 0, 0), \ X_{e3} = (0, 0, k),$$

and if $k(\alpha - \beta) \leq \gamma$, the system (5) has a unique equilibrium $P^*(x^*, y^*, 0)$, where x^* is the root of the equation

$$a(a(x + k) = (1 - x)((\alpha + \beta)x + \beta k + \gamma) \tag{14}$$

or, equivalently, the quadratic equation

$$(\alpha+\beta)x^2+(\beta k+\gamma+a-\alpha-\beta)x+(a-\beta)k-\gamma=0 \tag{15}$$

satisfying $0<x^*\leq 1$, and

$$y^*=x^*+k. \tag{16}$$

For the proof see [14].

(ii) If $v>0$, the interior equilibrium points $P^*(x^*,y^*,E^*)$ are defined by the system

$$\begin{cases} 1-x-\frac{ay}{\alpha x+\beta y+\gamma}=0, \\ b(1-\frac{y}{x+k})=\frac{v}{py-c} \end{cases} \tag{17}$$

or, equivalently, the system

$$\begin{cases} 1-x-\frac{ay}{\alpha x+\beta y+\gamma}=0, \\ x=\frac{by(py-c)}{b(py-c)-v}-k \end{cases} \tag{18}$$

satisfying $0<x^*\leq 1$, and y^* is a solution of the fourth degree equation

$$y^4+By^3+Cy^2+Dy+E=0, \tag{19}$$

where A,B,C,D,E are given by

$$A=b^2p^2(\alpha+\beta),$$

$$B=bp[bp(a+\beta(k-1)+\gamma-\alpha)-2\alpha bc-\beta(bc+v)]/A,$$

$$C=b[2\alpha bpck+pv(\alpha k-\gamma-2a)-2bpc(a+\gamma)+(\alpha+\beta)bc^2+$$

$$+\beta cv+p(1-k)(2bc(\alpha+\beta)+pb(\alpha k-\gamma))]/A,$$

$$D=(bv+v)[(k-1)(bp(2\alpha k-\gamma)+bc(\alpha k-\gamma)+\beta v)+a(bc+v)^2]/A,$$

$$E=(cb+v)[(1-k)(bp(\gamma-2\alpha k)-bc(\alpha+\beta-\beta v)+b(ac-\alpha k)+B\gamma+av]/A.$$

The equation (19) is equivalent by the change of variable $y=Y-\frac{B}{4}$ of the equation

$$Y^4+PY^2+QY+R=0, \tag{20}$$

where P,Q,R are given by

$$P=-\frac{3B^2}{8}+C,$$

$$Q=(\frac{B}{2})^3-\frac{BC}{2}+D,$$

$$R=-3(\frac{B}{4})^4-\frac{B^2C}{16}-\frac{BD}{4}+E.$$

We use Ferrari's method to solve the equation (19). If $Q=0$ if and only if $B^3-4BC+8D=0$, the equation reduces to a bisquare equation which is easy to solve.
We assume that the equation does not reduce to a bisquare equation ($8Q=B^3-4BC+8D\neq 0$), the equation (20) is rewrite as

$$(Y^2+\frac{B}{2})^2=(\frac{B^2}{4}-C)Y^2-DY-E,$$

or

$$(Y^2+\frac{B}{2}+\lambda)^2=(\frac{B^2}{4}-C+2\lambda)Y^2+(B\lambda-D)Y+\lambda^2-E.$$

The second member is a square if and only if

$$(B\lambda-D)^2=4(\frac{B^2}{4}-C+2\lambda)(\lambda^2-E),$$

or

$$8\lambda^3-4C\lambda^2+(2BD-8E)\lambda+B^2E+4CE-D^2=0.$$

Let λ_0 be a solution of this cubic solvent and let μ_0 be the square root of $2\lambda_0-c+\frac{B^2}{4}$ which is necessarily nonzero according to the hypothesis $Q\neq 0$. The equation is then written as

$$(Y^2+\frac{B}{2}+\lambda)^2=(\mu_0 Y+\frac{B\lambda_0-D}{2\mu_0})^2.$$

Therefore, it is equivalent to

$$Y^2+(\mu_0+\frac{B}{2})Y+\lambda_0+\frac{B\lambda_0-D}{2\mu_0}=0 \tag{21}$$

or

$$Y^2+(-\mu_0+\frac{B}{2})Y+\lambda_0-\frac{B\lambda_0-D}{2\mu_0}=0. \tag{22}$$

For (21), the discriminant is

$$\Delta_+=-2\lambda_0-C+2\frac{D-B\lambda_0}{\mu_0}+B\mu_0+\frac{B^2}{2},$$

$$y_{e,0}=\frac{-\mu_0+\sqrt{\Delta_+}}{2}-\frac{B}{4}\quad and\quad y_{e,1}=\frac{-\mu_0-\sqrt{\Delta_+}}{2}-\frac{B}{4}.$$

(22) is solved in the same way as (21) by replacing everywhere μ_0 by $-\mu_0$,

$$\Delta_-=-2\lambda_0-C-2\frac{D-B\lambda_0}{\mu_0}-B\mu_0+\frac{B^2}{2},$$

$$y_{e,2}=\frac{\mu_0+\sqrt{\Delta_-}}{2}-\frac{B}{4}\quad and\quad y_{e,3}=\frac{\mu_0-\sqrt{\Delta_-}}{2}-\frac{B}{4}.$$

5 Dynamic Analysis near the Coexistence Equilibria

In this section, we study the stability of the interior equilibrium X_e and analyse the bifurcation through it using the bifurcation theory and normal form theory.

5.1 Local stability analysis

For the analysis of the local stability of X_e, we let $X=Q\bar{X}$, here

$$\bar{X}=(x,y,\bar{E})^T,\quad Q=\begin{pmatrix}1&0&0\\0&1&0\\0&-\frac{E_e p}{px_e-c}&1\end{pmatrix}.$$

Then we get

$$D_X g(X_e)Q = (0, 0, py_e - c),$$

and

$$\bar{E} = E + \frac{E_e py}{py_e - c}.$$

Then the system can be expressed as follows:

$$\begin{cases} \frac{dx}{dt} = x(1 - x - \frac{ay}{\alpha x+\beta y+\gamma}), \\ \frac{dy}{dt} = y(b(1 - \frac{y}{x+k}) - \bar{E} + \frac{E_e py}{py_e - c}), \\ 0 = (\bar{E} - \frac{E_e py}{py_e - c})(py - c) - v. \end{cases} \tag{23}$$

We denote also

$$f(v, \bar{X}) \begin{pmatrix} f_1(v, \bar{X}) \\ f_2(v, \bar{X}) \end{pmatrix} = \begin{pmatrix} x(1 - x - \frac{ay}{\alpha x+\beta y+\gamma}) \\ y(b(1 - \frac{y}{x+k}) - \bar{E} + \frac{E_e py}{py_e - c}) \end{pmatrix},$$

$$g(v, \bar{X}) = (\bar{E} - \frac{E_e py}{py_e - c})(py - c) - v, \quad \bar{X} = (x, y, \bar{E})^T,$$

and

$$D_X g(\bar{X}_e)Q = (0, 0, py_e - c).$$

For system (23), we consider the following local parametrization:

$$\bar{X} = \phi(v, Y) = \bar{X}_e + U_0 Y + v_0 h(v, Y), \quad g(v, \phi(v, Y)) = 0.$$

Here, $Y = (y_1, y_2)$, $U_0 = \begin{pmatrix} 1 & 0 \\ 0 & 1 \\ 0 & 0 \end{pmatrix}$, $V_0 = \begin{pmatrix} 0 \\ 0 \\ 1 \end{pmatrix}$, and $h : \mathbb{R}^2 \longrightarrow \mathbb{R}$ is a smooth mapping. More information about the local parametrization can be found in [4,8]. Then we can deduce that the parametric system of (23) takes the form

$$\begin{cases} \dot{y_1} = \frac{dy_1}{dt} = f_1(v, \phi(v, Y)), \\ \dot{y_2} = \frac{dy_2}{dt} = f_2(v, \phi(v, Y)). \end{cases} \tag{24}$$

Consequently, the Jacobian matrix $A(v)$ of the parametric system (24) at $Y = 0$ takes the form

$$\begin{aligned} A(v) &= \begin{pmatrix} D_{y_1} f_1(v, \phi(v, Y)) & D_{y_2} f_1(v, \phi(v, Y)) \\ D_{y_1} f_2(v, \phi(v, Y)) & D_{y_2} f_2(v, \phi(v, Y)) \end{pmatrix}, \\ &= \begin{pmatrix} D_{\bar{X}} f_1(v, \bar{X}_e) \\ D_{\bar{X}} f_2(v, \bar{X}_e) \end{pmatrix} \begin{pmatrix} D_{\bar{X}} g(v, \bar{X}_e) \\ U_0^T \end{pmatrix}^{-1} \begin{pmatrix} 0 \\ I_2 \end{pmatrix}, \\ &= \begin{pmatrix} D_x f_1(v, \bar{X}_e(v)) & D_y f_1(v, \bar{X}_e(v)) \\ D_x f_2(v, \bar{X}_e(v)) & D_y f_2(v, \bar{X}_e(v)) \end{pmatrix}, \\ &= \begin{pmatrix} x_e(-1 + \frac{a\alpha y_e}{(\alpha x_e+\beta y_e+\gamma)^2}) & -\frac{a x_e(\alpha x_e+\gamma)}{(\alpha x_e+\beta y_e+\gamma)^2} \\ \frac{b y_e^2}{(x_e+k)^2} & y_e(\frac{-b}{x_e+k} + \frac{pE_e}{py_e - c}) \end{pmatrix}. \end{aligned}$$

Therefore, the characteristic equation of the matrix $A(v)$ can be expressed as

$$\lambda^2 + T_1\lambda + T_2 = 0, \tag{25}$$

where

$$T_1 = x_e(1 - \frac{a\alpha y_e}{(\alpha x_e + \beta y_e + \gamma)^2}) + y_e(\frac{b}{x_e + k} - \frac{pE_e}{py_e - c}),$$

$$T_2 = x_e y_e(1 - \frac{a\alpha y_e}{(\alpha x_e + \beta y_e + \gamma)^2})(\frac{-b}{x_e + k} + \frac{pE_e}{py_e - c}) + \frac{aby_e^2 x_e(\alpha x_e + \gamma)}{(x_e + k)^2(\alpha x_e + \beta y_e + \gamma)^2}.$$

Remark 5.1 *The positive equilibrium point $\bar{X}_e$ of the system (5) corresponds to the equilibrium point $Y = 0$ of system (24).*

Corollary 5.1 *For the positive equilibrium point $\bar{X}_e$ of the system (23), we have*
(i) If $T_1^2(v) \geq 4T_2(v)$ and $T_2(v) > 0$, then when $T_1(v) > 0$, $\bar{X}_e$ is a locally asymptotically stable node. When $T_1(v) < 0$, $\bar{X}_e$ is an unstable node.
(ii) If $T_2(v) < 0$, then $\bar{X}_e$ is an unstable saddle point.
(iii) If $T_1^2(v) < 4T_2(v)$, then when $T_1(v) > 0$, $\bar{X}_e$ is a locally asymptotically focus. When $T_1(v) < 0$, $\bar{X}_e$ is an unstable focus.

5.2 Hopf bifurcation analysis

The Hopf bifurcation is a very interesting type of bifurcation of systems. It refers to the local birth or death of a periodic solution from an equilibrium point as a parameter crosses a critical value named a bifurcation value.

We discuss the Hopf bifurcation in the system (23) from the equilibrium point $\bar{X}_e$ by considering the economic profit v as a bifurcation value.
If $T_1^2(v) < 4T_2(v)$, then the equation (25) has a pair of conjugate complex roots

$$\lambda_{1,2} = -\frac{1}{2}T_1(v) \pm i\sqrt{T_2(v) - \frac{T_1^2(v)}{4}} = \eta(v) \pm i\theta(v).$$

Let $2\eta(v) = T_1(v) = 0$, we get the bifurcation value v^* that satisfies

$$v^* = \frac{(py_e - c)^2}{p}(\frac{x_e}{y_e}(1 - \frac{a\alpha y_e}{(\alpha x_e + \beta y_e + \gamma)^2}) + \frac{b}{x_e + k})$$

if

$$\frac{a\alpha y_e}{(\alpha x_e + \beta y_e + \gamma)^2} = 1.$$

Moreover,

$$\eta(v^*) = 0, \quad \theta^* = \theta(v^*) = \frac{y_e}{(x_e + k)(\alpha x_e + \beta y_e + \gamma)}\sqrt{abx_e(\alpha x_e + \gamma)},$$

$$v^* = \frac{b(px_e - c)^2}{p(x_e + k)},$$

which implies that if

$$\eta'(v^*) = \frac{1}{2}\frac{d}{dv}(x_e(1 - \frac{a\alpha y_e}{(\alpha x_e + \beta y_e + \gamma)^2}) + y_e(\frac{b}{x_e + k} - \frac{pv_e}{(py_e - c)^2})_{v=v^*} =$$

$$= -\frac{py_e}{2(py_e - c)^2} \neq 0,$$

then the Hopf bifurcation occurs at the value v^*. The signal of the number σ is given by

$$16\sigma = \frac{1}{\theta^*}(a_{11}^1(a_{11}^2 - a_{12}^1) + a_{22}^2(a_{12}^2 - a_{22}^1) + (a_{11}^2 a_{12}^2 - a_{12}^1 a_{22}^1)) + (a_{111}^1 + a_{122}^1 + a_{112}^2 a_{222}^2),$$

where
$a_{11}^1 = \tau_1 f_{1y_1y_1}$, $a_{12}^1 = \tau_2 f_{1y_1y_2}$, $a_{22}^1 = \frac{\tau_2^2}{\tau_1} f_{1y_2y_2}$, $a_{111}^1 = \tau_1^2 f_{1y_1y_1y_1}$, $a_{112}^1 = \tau_1\tau_2 f_{1y_1y_1y_2}$,
$a_{122}^1 = \tau_2^2 f_{1y_1y_2y_2}$, $a_{222}^1 = \frac{\tau_2^3}{\tau_1} f_{1y_2y_2y_2}$.
$a_{11}^2 = \frac{\tau_1^2}{\tau_2} f_{2y_1y_1}$, $a_{12}^2 = \tau_1 f_{2y_1y_2}$, $a_{22}^2 = \tau_2 f_{2y_2y_2}$, $a_{111}^2 = \frac{\tau_1^3}{\tau_2} f_{2y_1y_1y_1}$, $a_{112}^2 = \tau_1^2 f_{2y_1y_1y_2}$,
$a_{122}^2 = \tau_1\tau_2 f_{2y_1y_2y_2}$, $a_{222}^2 = \tau_2^2 f_{2y_2y_2y_2}$,
which determines the direction of the Hopf bifurcation through the interior equilibrium $X_e(v)$ of the system (2.5), as stated in the following theorem.

Theorem 5.1 *For the system (5), there exist a positive constant $0 < \varepsilon \ll 1$ and two small neighborhoods of the positive equilibrium point $X_e(v)$: O_1 and O_2, where $O_1 \subset O_2$.*

Case $1:$ *If $\sigma > 0$, then*

1. *When $v^* < v < v^* + \varepsilon$, $X_e(v)$ rejects all the points in O_2, so it is unstable.*
2. *When $v^* - \varepsilon < v < v^*$, sytem (5) has at least a periodic solution located in $\bar{O}_1$ (the cloture of O_1), one of them rejects all the points in $\bar{O}_1 \setminus X_e(v)$, at the same time another periodic solution (may be the same one) rejects all points in $O_2 \setminus \bar{O}_1$, and $X_e(v)$ is locally asympototic stable.*

Case $2:$ *If $\sigma < 0$, then*

1. *When $v^* - \varepsilon < v < v^*$, $X_e(v)$ attracts all the points in O_2, and $X_e(v)$is locally asymptotic stable.*
2. *When $v^* < v < v^* - \varepsilon$, system (5) has at least a periodic solution located in $\bar{O}_1$, one of them attracts all the points in $\bar{O}_1 \setminus X_e(v)$, at the same time another periodic solution (may be the same one) attracts all points in $O_2 \setminus \bar{O}_1$, and $X_e(v)$ is unstable.*

For the proof see [19], where we use
$f_{1y_1}(v^*, \bar{X}_e) = 0$, $f_{2y_2}(v^*, \bar{X}_e) = 0$, $f_{1y_2}(v^*, \bar{X}_e) =, \quad -\frac{ax_e(\alpha x_e+\gamma)}{(\alpha x_e+\beta y_e+\gamma)^2}$,
$f_{2y_1}(v^*, \bar{X}_e) = \frac{by_e^2}{(x_e+k)^2}$, $f_{1y_1y_1}(v^*, \bar{X}_e) = -2 + 2\frac{a\alpha^2 y_e(\beta y_e+\gamma)}{(\alpha x_e+\beta y_e+\gamma)^3}$,
$f_{1y_1y_2}(v^*, \bar{X}_e) = f_{1y_2y_1}(v^*, \bar{X}_e) = \frac{-a\gamma(\alpha x_e+\beta y_e+\gamma)-2a\alpha\beta x_e y_e}{(\alpha x_e+\beta y_e+\gamma)^3}$,
$f_{1y_2y_2}(v^*, \bar{X}_e)=\frac{2a\beta x_e(\alpha x_e+\gamma)}{(\alpha x_e+\beta y_e+\gamma)^3}$, $f_{2y_1y_1}(v^*, \bar{X}_e)=\frac{-2by_e^2}{(x_e+k)^3}$,
$f_{2y_1y_2}(v^*, \bar{X}_e)=f_{2y_2y_1}(v^*, \bar{X}_e)=\frac{2by_e}{(x_e+k)^2}$, $f_{2y_2y_2}(v^*, \bar{X}_e)=-2\frac{by_e}{(x_e+k)(py_e-c)}$,
$f_{1y_1y_1y_1}(v^*, \bar{X}_e)=\frac{-4a\alpha^2 y_e(\beta y_e+\gamma)+2a\alpha^3 x_e y_e}{(\alpha x_e+\beta y_e+\gamma)^4}$,
$f_{1y_1y_1y_2}(v^*, \bar{X}_e)=f_{1y_1y_2y_1}(v^*, \bar{X}_e)=f_{1y_2y_1y_1}(v^*, \bar{X}_e)= \frac{2a\alpha(-\beta y_e+\gamma)(\alpha x_e+\beta y_e+\gamma)+6a\alpha^2\beta x_e y_e}{(\alpha x_e+\beta y_e+\gamma)^4}$,
$f_{1y_1y_2y_2}(v^*, \bar{X}_e) = f_{1y_2y_2y_1}(v^*, \bar{X}_e) =$
$= f_{1y_2y_1y_2}(v^*, \bar{X}_e)=\frac{2a\beta(2\alpha x_e+\gamma)(\alpha x_e+\beta y_e+\gamma)-6a\alpha\beta x_e(\alpha x_e+\gamma)}{(\alpha x_e+\beta y_e+\gamma)^4}$,
$f_{1y_2y_2y_2}(v^*, \bar{X}_e)=\frac{-6\alpha\beta^2 x_e(\alpha x_e+\gamma)}{(\alpha x_e+\beta y_e+\gamma)^4}$, $\quad f_{2y_1y_1y_1}(v^*, \bar{X}_e)=\frac{6by_e^2}{(x_e+k)^4}$,

$f_{2y_1y_1y_2}(v^*,\bar{X}_e)=f_{2y_1y_2y_1}(v^*,\bar{X}_e)=f_{2y_2y_1y_1}(v^*,\bar{X}_e)=\frac{-4by_e}{(x_e+k)^3}$,
$f_{2y_1y_2y_2}(v^*,\bar{X}_e)=f_{2y_2y_2y_1}(v^*,\bar{X}_e)=f_{2y_2y_1y_2}(v^*,\bar{X}_e)=\frac{2b}{(x_e+k)^2}$,
$f_{2y_2y_2y_2}(v^*,\bar{X}_e)=\frac{6p^2cE_e}{(py_e-c)^3}$.
and
$\tau_1=\frac{\sqrt{ax_e(\alpha x_e+\gamma)}}{\alpha x_e+\beta y_e+\gamma}$, $\tau_2=-\frac{y_e\sqrt{b}}{x_e+k}$.

6 Conclusion

This paper examines the stability and the Hopf bifurcation of a differential-algebraic biological economic system with a hybrid functional response. A dynamical investigation of a predator-prey model with a hybrid functional response equiped with an algebraic equation has never been done. We consider the system's dynamic behavior when only the prey is vulnerable to harvesting. Only the positive equilibrium points are of interest from a biological standpoint. By examining their associated characteristic equation and applying the new normal form theorem, the local stability of the inner equilibrium is determined. When the economic revenue v is changed, the inner equilibrium's stability property changes. Additionally, a one-parameter bifurcation analysis of the economic revenue is performed. When the system bifurcates, the properties of periodic solutions in the system are obtained by computing the parameter σ. The qualitative analysis, that is, the foundation of the revised model will be completed by future research. Additionally, it will include the numerical simulations used to support the outcomes.

References

[1] R. Arditi and L. R Ginzburg. Coupling in predator-prey dynamics ratio-dependence. *Journal of Theoretical Biology* **139** (1989) 311–326.

[2] J. R. Beddington. Mutual interference between parasites or predator and its effect on searching efficiency. *Journal of Animal Ecology* **44** (1975) 331–340.

[3] R. S. Cantrell and C. Cosner. On the dynamics of predator-prey models with the Beddington-DeAngelis functional response. *Journal of Mathematical Analysis and Applications* **257** (1) (2001) 206–222.

[4] B. S. Chen, X.Ẋ. Liao and Y. Q. Liu. Normal forms and bifurcations for the differential-algebraic systems. *Acta Math. Appl. Sinica.* **23** (2000) 429–443.

[5] C. W. Clark. *Mathematical bio-economics: The Optimal Management of Renewable Resources, 2^{nd} edition.* John Wiley and Sons, New York, 1990.

[6] D. L. DeAngelis, R. A Goldestein and R.V. O'Neil. A model for trophic inter-action. *Ecology* **56** (1975) 881–892.

[7] H. S. Gordon. The economic theory of common property resource: The fishery. *Journal of Political Economy* **62** (1954) 124–142.

[8] J. Guckenheimer and P. Holmes. *Nonlinear Oscillations, Dynamical system, and Bifurcations of Vector Fields.* Springer-Verlag, New York, 1983.

[9] J. Hale. *Theory of Functional Differential Equations, 2^{nd} edition.* Applied Mathematical Sciences, Vol. 3, Springer-Verlag, New York-Heidelberg, 1977.

[10] C. S. Holling. The components of predation as revealed by a study of small mammal predation of the European pine sawfly. *Canadian Entomology* **91** (1959a) 293–320.

[11] C. S Holling. The functional response of predators to prey density and its role in mimicry and population regulation. *Memoirs of the Entomological Society of Canada* **97** (1965) 5–60.

[12] T. K. Kar and K. Chakraborty. Effort dynamics in a prey-predator model with harvesting. *Int. J. Inf. Syst. Sci.* **6** (2010) 318–332.

[13] N. Kerioui and M. S. Abdelouahab. Stability and Hopf Bifurcation of the Coexistence Equilibrium for a Differential-Algebraic Biological Economical System with Predator Harvesting. *Electronic Research Archive* **29** (1) (2021) 1641–1660.

[14] W. Khellaf and N. E. Hamri. Boundedness and Global Stability for a Predator-Prey System with the Beddington-DeAngelis Functional Response. *Differential Equations and Nonlinear Mechanics* **2010** (2010) 1–24.

[15] M. Labid and N. Hamri. Chaos Synchronization between Fractional-Order Lesser Date Moth Chaotic System and Integer-Order Chaotic System via Active Control. *Nonlinear Dyn. Syst. Theory* **22** (4) (2022) 407–413.

[16] W. Liu, C.J. Fu and B. Chen. Hopf bifurcation for a predator-prey biological economic system with Holling type II functional response. *J. Franklin Inst* **348** (2011) 1114–1127.

[17] C. Liu, Q. zhang, Y. Zhang and X. D. Duan. Bifurcation and control in differential-algebraic harvested prey-predator model with stage structure for predator. *Internat. J. Bifur. Chaos Appl. Sci. Engrg.* **18** (2008) 3159–3168.

[18] A. F Nindjin, M.A. Aziz-Alaoui, and M. Cadivel, Analysis of a predator-prey model with modified leslie-gower and Holling-type II schemes with time delay, *Nonlinear Analysis: Real World Applications*, **7** (5) (2006) 1104–1118.

[19] W. Zhu, J. Huang and W. Liu. The stability and Hopf bifurcation of the differential-algebraic biological economic system with single harvesting. In: *2015 Sixth International Conference on Intelligent Control and information Processing (ICICIP)*. Wuhan, China, November 26–28, 2015, P. 92–97.

Nonlinear Dynamics and Systems Theory, **23** (4) (2023) 410–421

Synchronization of the Restricted Charged Three-Body Problem

Krishan Pal *

.

Department of Mathematics, Maharaja Agrasen College, University of Delhi, Vasundhara Enclave-110096, New Delhi, India.

Received: December 26, 2021;   Revised: September 26, 2023

Abstract: This paper deals with the chaos and synchronization behavior of two identical nonlinear dynamical systems of the restricted charged three-body problem. An active control technique is introduced to achieve synchronization between the drive and response systems. Also, an error dynamical system of the drive and response systems has been investigated using active control inputs. Secondly, the Lyapunov theorem on stability and the Routh-Hurwitz criteria have been taken into account for the study of stability of the error dynamical system. Further, a six degree coefficient matrix of the error dynamical system has been investigated. We have concluded by the Lyapunov stability criteria, the error dynamical system is stable. Numerical simulation is taken into account to check the effectiveness of the proposed active control technique.

Keywords: *restricted charged three-body problem; synchronization; Lyapunov stability; Routh-Hurwitz criteria*

Mathematics Subject Classification (2010): 34H10, 37N35, 93C10, 93C15, 93C95.

1 Introduction

The basic theory of chaos and synchronization has a very powerful application in the real world. There are various dynamical systems which have real life applications. There is an opportunity of doing well research and obtaining some new information about real life from the study of the solar dynamical system. There are many forces acting between the celestial bodies of a solar dynamical system. There exist many perturbations such as radiation pressure, oblateness, the Coriolis and centrifugal forces and drag force between the solar system bodies. These perturbations can make new contributions in the study

* Corresponding author: mailto:kpal1987@gmail.com

of chaos and synchronization of solar system bodies. The basic idea of synchronization between two dynamical systems is one of the important phenomena occurring in nature.

The synchronization of chaotic systems have been studied by many authors and researchers. They have introduced the basic concept and analytical approach to study the chaotic behavior of dynamical systems. Also, they have incorporated some techniques of controlling chaos and studying synchronization in the chaotic systems. Synchronization has been studied by many authors for different physical systems, namely, chaotic systems, the fractional L*ü* system, coupled chaotic systems, between two different chaotic systems via nonlinear feedback control, two Lorenz systems using active control and the Rossler and Chen chaotic dynamical systems [1-6].

In continuation of research on synchronization, chaos synchronization, anti-synchronization, hybrid synchronization, synchronization of the finance chaotic system, synchronization of fractional-order systems, projective synchronization and function projective dual synchronization of chaotic systems, adaptive synchronization, sliding mode control synchronization and adaptive sliding mode control synchronization have been studied by many authors [7-13]. Moreover, the restricted charged three-body problem, low-thrust restricted three-body problem, chaos synchronization in the restricted three-body problem have been studied by many authors [14-18]. In addition, synchronization of fractional-order 3D chaotic system analysis has been incorporated in [19].

In this paper, we have studied the synchronization behavior of two identical systems of the restricted charged three-body problem using the active control technique. This paper is arranged as follows. Section 1 discussed the introductory part of the paper. In Section 2, we have derived the equations of motion of the restricted charged three-body problem. In Section 3, we have used the active control technique for synchronization. In Section 4, we have discussed the numerical simulation for synchronization. Finally, in Section 5, we have concluded the results obtained.

2 Equations of Motion

Let two charged bodies $M_1 = (m_1, q_1)$ and $M_2 = (m_2, q_2)$ with masses m_1 and $m_2\,(m_1 > m_2)$ and charges q_1, q_2 be moving with angular velocity ω in circular orbits about their center of mass O taken as an origin, and let the third charged infinitesimal body M of mass m_3 be moving in the plane of motion of m_1 and m_2 (see Fig. 1). The motion of the third charged infinitesimal body is affected by the motion of m_1 and m_2 but does not affect them. We shall determine the equations of motion of the charged infinitesimal body of mass m_3 in synodic and dimensionless variables. The angular velocity of the primaries is given by the relation $\omega = \sqrt{\frac{G(m_1+m_2)}{l^3}}$, where l is the distance between the primaries, and G is the gravitational constant. We scale the units by taking the sum of the masses and the distance between the primaries both equal to unity. Therefore $m_1 = 1-\mu$, $m_2 = \mu\,(0 < \mu \leq 0.5)$ and $\mu = \frac{m_2}{m_1+m_2}$ with $m_1 + m_2 = 1$. Also, the scale of the time is chosen so that the gravitational constant is unity. For the classical case, $q_1 = q_2 = 0$, only the range $0 \leq \mu \leq 0.5$ is of interest since the range $0 < \mu \leq 1$ is the reflection of the previous one with respect to the y-axis. Let us assume that $0 < \mu \leq 0.5$, continuing, we may define $\frac{q_1}{q_1+q_2} = q_1 = 1-\mu$, $\frac{q_2}{q_1+q_2} = q_2 = \mu$, where $q_1 + q_2 = 1$. The equations of motion of the charged infinitesimal body in the dimensionless co-ordinate system according to [14] can be written as

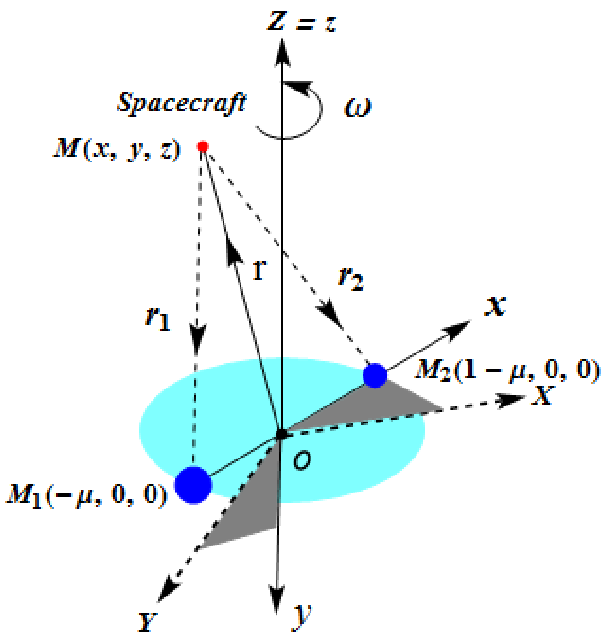

Figure 1: Configuration of the restricted charged three-body problem.

$$\left.\begin{aligned} \ddot{x} - 2\,\dot{y} &= x - \frac{q-\mu}{r_1^3}(x+\mu) \\ &\quad - \frac{\mu - q}{r_2^3}(x+\mu-1), \\ \ddot{y} + 2\,\dot{x} &= y - \frac{q-\mu}{r_1^3}\,y - \frac{\mu-q}{r_2^3}\,y, \\ \ddot{z} &= -\frac{q-\mu}{r_1^3}\,z - \frac{\mu-q}{r_2^3}\,z, \end{aligned}\right\} \tag{1}$$

where

$$r_1 = \sqrt{(x+\mu)^2 + y^2 + z^2}$$

and

$$r_2 = \sqrt{(x+\mu-1)^2 + y^2 + z^2}.$$

3 Synchronization of the Restricted Charged Three-Body Problem

In this section, we have introduced an active control method to study the synchronization behavior of two identical systems of the restricted charged three-body problem. We have introduced a dynamical system of the restricted charged three-body problem of the solar system bodies. We have formulated the master and slave systems of the solar system bodies with the help of the restricted charged three-body problem. The master system

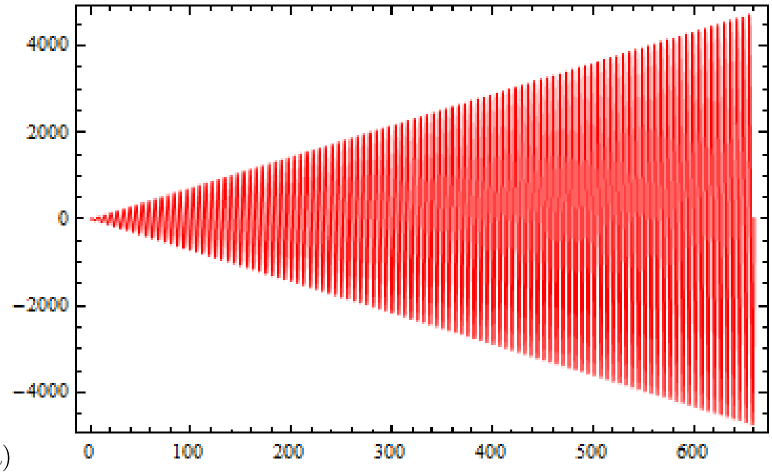

(a)

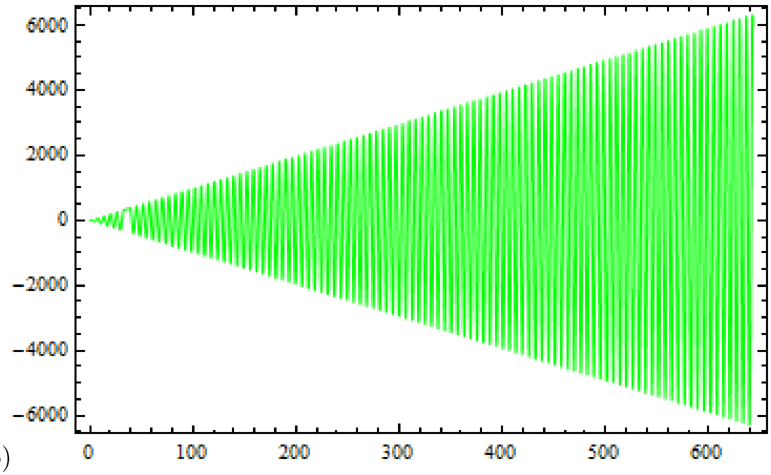

(b)

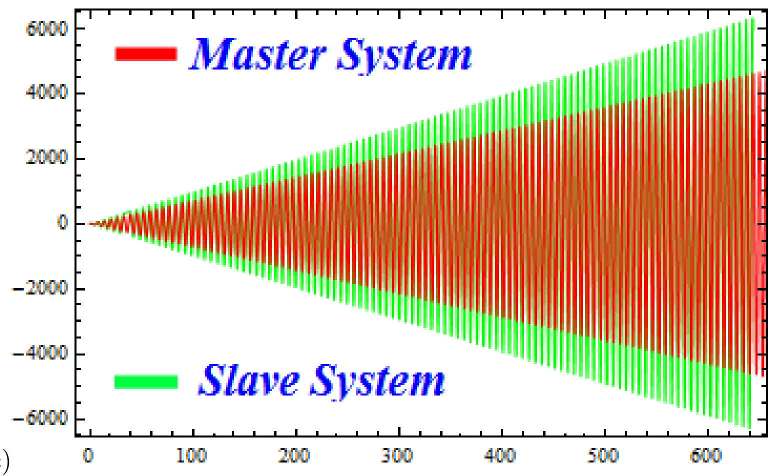

(c)

Figure 2: Time series graphs of the master and slave systems for $\mu = 0.05$, $q = 0.15$, (a) For the master system of $x_1(t)$, (b) For the slave system of $y_1(t)$, (c) Combined graphs of the master and slave systems of $x_1(t)$ and $y_1(t)$.

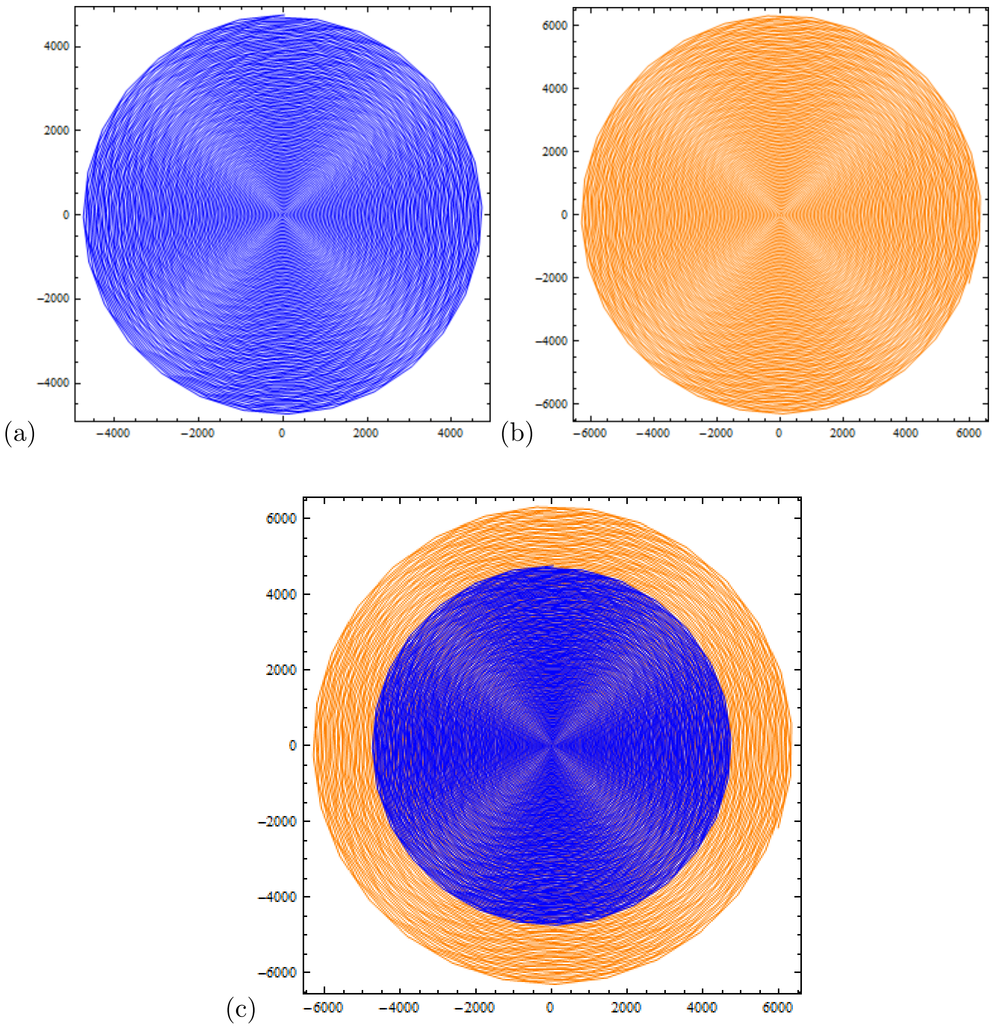

Figure 3: Phase portrait graphs of the master and slave systems for $\mu = 0.05$, $q = 0.15$, (a) For the master system of $(x_1(t), x_2(t))$, (b) For the slave system of $(y_1(t), y_2(t))$, and (c) Combined graphs of the master and slave systems of $(x_1(t), x_2(t))$ and $(y_1(t), y_2(t))$.

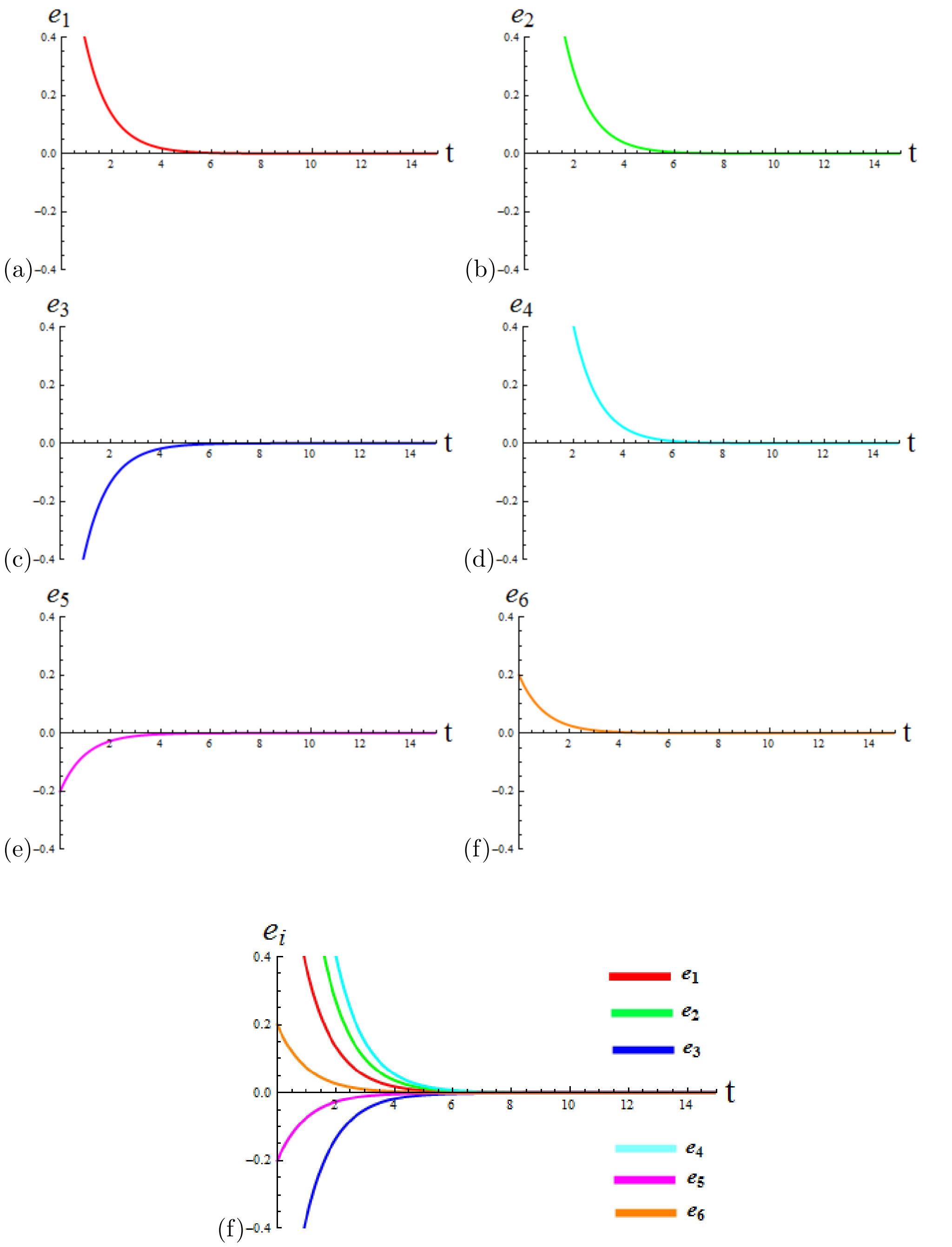

Figure 4: The convergence of the error dynamical system, (a) for $e_1(t)$, (b) for $e_2(t)$, (c) for $e_3(t)$, (d) for $e_4(t)$, (e) for $e_5(t)$, (f) for $e_6(t)$, and (g) the combined convergence of errors $e_1(t)$, $e_2(t)$, $e_3(t)$, $e_4(t)$, $e_5(t)$, $e_6(t)$.

for the restricted charged three-body problem is defined by $\dot{x} = f(x, y, z)$ and the slave system $\dot{y} = g(x, y, z)$, where $x(t), y(t)$ and $z(t)$ are the phase space (state variables), and $\dot{x} = f(x, y, z)$, $\dot{y} = g(x, y, z)$, and $\dot{z} = h(x, y, z)$ are the corresponding nonlinear functions. We want to study the synchronization behavior of the master and slave systems for the restricted charged three-body problem.

Synchronization is defined as a process in which two or more systems interact with each other. We can obtain a combined effect of the dynamical properties using the synchronization phenomenon. Mathematically, we can define the synchronization by the expression $|x(t)-y(t)| \to 0$ as $t \to 0$. When the above expression holds, then the systems of six equations are said to be completely synchronized. According to the control theory of synchronization, a dynamical system depends on the design of control laws for the slave system using the known information of the master system so as to ensure that the controlled receiver synchronizes with the master system. Therefore, the slave chaotic system completely investigates the dynamics of the master system with respect to time. The model of the restricted charged three-body problem defined by Eq. (1) can be written as a system of six first-order differential equations. We have introduced six variables such as $x_1 = x$, $x_2 = \dot{x}$, $x_3 = y$, $x_4 = \dot{y}$, $x_5 = z$ and $x_6 = \dot{z}$. Therefore, the master system of the Eq.(1) is defined as

$$\left.\begin{aligned}
\dot{x_1} &= x_2, \\
\dot{x_2} &= x_1 + 2\,x_4 - \left(\frac{q-\mu}{r_1^3}(x_1+\mu) + \frac{\mu-q}{r_2^3}(x_1+\mu-1)\right), \\
\dot{x_3} &= x_4, \\
\dot{x_4} &= x_3 - 2\,x_2 - \left(\frac{q-\mu}{r_1^3} + \frac{\mu-q}{r_2^3}\right) x_3, \\
\dot{x_5} &= x_6, \\
\dot{x_6} &= -\left(\frac{q-\mu}{r_1^3} + \frac{\mu-q}{r_2^3}\right) x_5,
\end{aligned}\right\} \tag{2}$$

where $r_1^2 = (x_1+\mu)^2 + x_3^2 + x_5^2$ and $r_2^2 = (x_1+\mu-1)^2 + x_3^2 + x_5^2$. We can write the identical slave system of six first-order differential equations corresponding to Eq.(2) as

$$\left.\begin{aligned}
\dot{y_1} &= y_2 + u_1(t), \\
\dot{y_2} &= y_1 + 2\,y_4 - \frac{q-\mu}{d_1^3}(y_1+\mu) - \frac{\mu-q}{d_2^3}(y_1+\mu-1) + u_2(t), \\
\dot{y_3} &= y_4 + u_3(t), \\
\dot{y_4} &= y_3 - 2\,y_2 - \left(\frac{q-\mu}{d_1^3} + \frac{\mu-q}{d_2^3}\right) y_3 + u_4(t), \\
\dot{y_5} &= y_6 + u_5(t), \\
\dot{y_6} &= -\left(\frac{q-\mu}{d_1^3} + \frac{\mu-q}{d_2^3}\right) y_5 + u_6(t)
\end{aligned}\right\} \tag{3}$$

with $d_1^2 = (y_1+\mu)^2 + y_3^2 + y_5^2$ and $d_2^2 = (y_1+\mu-1)^2 + y_3^2 + y_5^2$, where $u_i(t) = 1, 2, 3, 4, 5, 6$ are called the control functions. We can define the error functions in such a way that in the synchronization state

$$\lim_{t\to\infty} e_i(t) \to 0, i = 1, 2, 3, 4, 5, 6,$$

$$
\begin{aligned}
e_1 &= y_1 - x_1,\\
e_2 &= y_2 - x_2,\\
e_3 &= y_3 - x_3,\\
e_4 &= y_4 - x_4,\\
e_5 &= y_5 - x_5,\\
e_6 &= y_6 - x_6.
\end{aligned}
$$

We can transform the above error dynamical system in the derivative form of the input variables. After taking the derivative of the above error dynamical system, a new form can be written as

$$
\left.
\begin{aligned}
\dot{e_1} &= \dot{y_1} - \dot{x}_1,\\
\dot{e_2} &= \dot{y_2} - \dot{x}_2,\\
\dot{e_3} &= \dot{y_3} - \dot{x}_3,\\
\dot{e_4} &= \dot{y_4} - \dot{x}_4,\\
\dot{e_5} &= \dot{y_5} - \dot{x}_5,\\
\dot{e_6} &= \dot{y_6} - \dot{x}_6.
\end{aligned}
\right\}
\tag{4}
$$

In the error dynamical system of Eqs. (4), the dot over e_i, x_i, y_i, $i = 1, 2, 3, 4, 5, 6$ indicates the differentiation with respect to time. After using Eqs. (2), (3) and (4), the above error dynamical system can be transformed into a new form and can be written as

$$
\left.
\begin{aligned}
\dot{e_1}(t) &= e_2(t) + u_1(t),\\
\dot{e_2}(t) &= e_1(t) + 2\, e_4(t) - e_1(t) \left(\frac{q-\mu}{r_1^3} + \frac{\mu - q}{r_2^3} \right) + u_2(t),\\
\dot{e_3}(t) &= e_4(t) + u_3(t),\\
\dot{e_4}(t) &= e_3(t) - 2\, e_2(t) - e_3(t) \left(\frac{q-\mu}{r_1^3} + \frac{\mu - q}{r_2^3} \right) + u_4(t),\\
\dot{e_5}(t) &= e_6(t) + u_5(t),\\
\dot{e_6}(t) &= -\, e_5(t) \left(\frac{q-\mu}{r_1^3} + \frac{\mu - q}{r_2^3} \right) + u_6(t).
\end{aligned}
\right\}
\tag{5}
$$

In Eq.(5), we have introduced the input variables to study the behavior of a dynamical system. The error dynamical system defined by Eq. (5) to be controlled must be a linear system with control inputs. Hence, we have incorporated the control functions after eliminating the non-linear terms in $e_1(t)$, $e_2(t)$, $e_3(t)$, $e_4(t)$, $e_5(t)$ and $e_6(t)$ of equation (5) as given below

$$
\left.
\begin{aligned}
u_1(t) &= v_1(t),\\
u_2(t) &= e_1(t) \left(\frac{q-\mu}{r_1^3} + \frac{\mu - q}{r_2^3} \right) + v_2(t),\\
u_3(t) &= v_3(t),\\
u_4(t) &= e_3(t) \left(\frac{q-\mu}{r_1^3} + \frac{\mu - q}{r_2^3} \right) + v_4(t),\\
u_5(t) &= v_5(t),\\
u_6(t) &= e_5(t) \left(\frac{q-\mu}{r_1^3} + \frac{\mu - q}{r_2^3} \right) + v_6(t).
\end{aligned}
\right\}
\tag{6}
$$

The control inputs have been introduced to study the behavior of a dynamical system. We can take one or more input variables to control a dynamical system, which depend on our choice. We want to control an output of a dynamical system. We can obtain the desired output of a dynamical system using these control inputs. There are two control inputs which are used in Eqs. (5) and (6). Using Eqs. (5) and (6), we can write the linear error dynamical system as given below

$$\left.\begin{aligned} \dot{e_1}(t) &= e_2(t) + v_1(t), \\ \dot{e_2}(t) &= e_1(t) + 2\,e_4(t) + v_2(t), \\ \dot{e_3}(t) &= e_4(t) + v_3(t), \\ \dot{e_4}(t) &= e_3(t) - 2\,e_2(t) + v_4(t), \\ \dot{e_5}(t) &= e_6(t) + v_5(t), \\ \dot{e_6}(t) &= v_6(t). \end{aligned}\right\} \tag{7}$$

Equation (7) represents the error dynamical system with new control inputs. The formulated Eq. (7) is the error dynamics, which can be interpreted as a control problem where the system to be controlled is a linear system with control inputs $v_1(t)$, $v_2(t)$, $v_3(t)$, $v_4(t)$, $v_5(t)$ and $v_6(t)$. We have introduced some new active control variables $v_1(t)$, $v_2(t)$, $v_3(t)$, $v_4(t)$, $v_5(t)$ and $v_6(t)$ which are given by the relation

$$\left.\begin{pmatrix} v_1(t) \\ v_2(t) \\ v_3(t) \\ v_4(t) \\ v_5(t) \\ v_6(t) \end{pmatrix} = M \begin{pmatrix} e_1(t) \\ e_2(t) \\ e_3(t) \\ e_4(t) \\ e_5(t) \\ e_6(t) \end{pmatrix}\right\}. \tag{8}$$

In Eq. (8), M is a 6×6 constant matrix to be determined. The error dynamical system (7) can be re-written as given below

$$\left.\begin{pmatrix} \dot{e_1}(t) \\ \dot{e_2}(t) \\ \dot{e_3}(t) \\ \dot{e_4}(t) \\ \dot{e_4}(t) \\ \dot{e_6}(t) \end{pmatrix} = N \begin{pmatrix} e_1(t) \\ e_2(t) \\ e_3(t) \\ e_4(t) \\ e_5(t) \\ e_6(t) \end{pmatrix}\right\}. \tag{9}$$

In equation (9), N is a 6×6 coefficient matrix. According to the Lyapunov stability theory and Routh-Hurwitz criteria, the eigenvalues of the coefficient matrix of the error system must be real or complex with negative real parts. We can choose the elements of the matrix arbitrarily, there are several ways to choose in order to satisfy the Lyapunov and Routh-Hurwitz criteria. Therefore, the matrix corresponding to Eq. (7) can be defined as

$$M = \begin{pmatrix} -1 & -1 & 0 & 0 & 0 & 0 \\ -1 & -1 & 0 & -2 & 0 & 0 \\ 0 & 0 & -1 & -1 & 0 & 0 \\ 0 & 2 & -1 & -1 & 0 & 0 \\ 0 & 0 & 0 & 0 & -1 & -1 \\ 0 & 0 & 0 & 0 & 0 & -1 \end{pmatrix}$$

and the matrix corresponding to Eq. (9) given by

$$N = \begin{pmatrix} -1 & 0 & 0 & 0 & 0 & 0 \\ 0 & -1 & 0 & 0 & 0 & 0 \\ 0 & 0 & -1 & 0 & 0 & 0 \\ 0 & 0 & 0 & -1 & 0 & 0 \\ 0 & 0 & 0 & 0 & -1 & 0 \\ 0 & 0 & 0 & 0 & 0 & -1 \end{pmatrix} \tag{10}$$

becomes a matrix with the eigenvalues having negative real parts. After using Eqs. (9) and (10), we have obtained an expression which is given below

$$\left.\begin{aligned} \dot{e_1}(t) &= -e_1(t) \\ \dot{e_2}(t) &= -e_2(t) \\ \dot{e_3}(t) &= -e_3(t) \\ \dot{e_4}(t) &= -e_4(t) \\ \dot{e_5}(t) &= -e_5(t) \\ \dot{e_6}(t) &= -e_6(t). \end{aligned}\right\} \tag{11}$$

The system of Eqs.(11) indicates an equation of the error dynamical system of the restricted charged three-body problem. We shall study the stability of the above error dynamical system given by Eq.(11). In order to study the stability of the error dynamical system, we shall determine the solution of Eq.(11) using the Lyapunov stability criteria. It is concluded by the Lyapunov stability theory, the above error dynamical system is stable.

4 Analysis of Numerical Simulation

We have introduced two parameters, namely, the mass ratio μ and the charge q of the second primary. We shall discuss the effects of these two parameters μ and q. We have taken the numerical values of the given parameters and the initial conditions for studying simulation. For the parameters included in the system under investigation $\mu = 0.05$, $q = 0.15$ and with the initial conditions for the master and slave systems $[x_1(0), x_2(0), x_3(0), x_4(0), x_5(0), x_6(0)] = [3.5, -4.75, -2.5, 3.35, 0.85, 0.75]$ and $[y_1(0), y_2(0), y_3(0), y_4(0), y_5(0), y_6(0)] = [4.5, -2.75, -3.5, 6.35, 0.65, 0.95]$, respectively. We have simulated the system under consideration using mathematica. The phase portraits and time series analysis of the master and slave systems show the irregular behavior of the dynamical system (see Figures 2 and 3). And for $[e_1(0), e_2(0), e_3(0), e_4(0), e_5(0), e_6(0)] = [1, 2, -1, 3, -0.2, 0.2]$, the convergence diagrams of errors are the proof of achieving synchronization between the master and slave systems (see Figure 4).

5 Conclusion

In this paper, we have studied the synchronization behavior of two identical nonlinear systems of the restricted charged three-body problem using different initial conditions through active control technique depending on the Lyapunov stability theory and the

Routh-Hurwitz criteria. We have observed that the master and slave systems of the restricted charged three-body problem are completely synchronized. Also, we have observed that the error propagation between the master and slave systems of the restricted charged three-body problem is tending to zero. The obtained results were certified by numerical simulations using the latest version 12.0 of Wolfram Mathematica®. In this paper, the present work is applicable for the study of some perturbations on the artificial satellite in space. This paper is applicable in various astrophysical systems. There are three examples such as Sun-Earth-Satellite system, Sun-Jupiter-Satellite system and Earth-Moon-Satellite system.

Acknowledgment

The author is thankful to the Center for Fundamental Research in Space dynamics and Celestial mechanics (CFRSC), New Delhi, Delhi, India, for providing every research facilities.

References

[1] L. M. Pecora and T. L. Carroll. Synchronization in chaotic systems. *Phys. Rev. Lett.* **64** (1990) 821–824.

[2] S. Boccaletti, J. Kurths, G. Osipov, D. L. Valladares and C. S. Zhou. The synchronization of chaotic systems. *Physics Reports.* **366** (1–2) (2002) 1–101.

[3] W. H. Deng and C. P. Li. Chaos synchronization of the fractional Lü system. *Physica A.* **353** (2005) 61–72.

[4] H. H. Chen, G. J. Sheu, Y. L. Lin and C. S. Chen. Chaos synchronization between two different chaotic systems via nonlinear feedback control. *Nonlinear Analysis: Theory, Methods and Applications.* **70** (12) (2009) 4393–4401.

[5] E. W. Bai and K. E. Lonngren. Synchronization of two Lorenz systems using active control. *Chaos, Solitons & Fractals.* **8** (1) (1997) 51–58.

[6] H. N. Agiza and M. T. Yassen. Synchronization of Rossler and Chen chaotic dynamical systems using active control. *Physics Letters A.* **278** (4) (2001) 191–197.

[7] S. Kaouache, N. E. Hamri, A. S. Hacinliyan, E. Kandiran, B. Deruni and A. C. Keles. Increased order generalized combination synchronization of non-identical dimensional fractional-order systems introducing different observable variable functions. *Nonlinear Dynamics & Systems Theory.* **20** (3) (2020) 307–315.

[8] W. Laouira and N. Hamri. New Design of Stability Study for Linear and Nonlinear Feedback Control of Chaotic Systems. *Nonlinear Dynamics and Systems Theory.* **22** (4) (2022) 414–423.

[9] F. Hannachi. Adaptive sliding mode control synchronization of a novel, highly chaotic $3-D$ system with two exponential nonlinearities. *Nonlinear Dynamics and Systems Theory.* **20** (1) (2020) 38–50.

[10] M. Labid and N. Hamri. Chaos Synchronization between Fractional-Order Lesser Date Moth Chaotic System and Integer-Order Chaotic System via Active Control. *Nonlinear Dynamics and Systems Theory.* **22** (4) (2022) 407–413.

[11] M. Labid and N. Hamri. Chaos Anti-Synchronization between Fractional-Order Lesser Date Moth Chaotic System and Integer-Order Chaotic System by Nonlinear Control. *Nonlinear Dynamics and Systems Theory.* **23** (2) (2023) 207–213.

[12] M. Mellah, A. Ouannas, A. A. Khennaoui and G. Grassi. Fractional Discrete Neural Networks with Different Dimensions: Coexistence of Complete Synchronization, Antiphase Synchronization and Full State Hybrid Projective Synchronization. *Nonlinear Dynamics and Systems Theory.* **21** (4) (2021) 410–419.

[13] A. A. Othman, M. S. M. Noorani and M. Mossa Al-Sawalha. Function projective dual synchronization of chaotic systems with uncertain parameters. *Nonlinear Dynamics and Systems Theory.* **17** (2) (2017) 193–204.

[14] D. D. Dionysios and D. A. Vaiopoulos. On the restricted circular three charged-body problem. *Astrophysics and Space Science.* **135** (1987) 253–260 .

[15] M. Shahzad and A. Khan. Synchronization in a circular restricted three body problem under the effect of radiation. *Chaos and Complex Systems*, (2012) 59–68.

[16] M. S. Suraj, A. Mittal, K. Pal. Stability of the artificial equilibrium points in the low-thrust restricted three-body problem when the bigger primary is a source of radiation. *Nonlinear Dynamics and Systems Theory.* **20** (3) (2020) 333–344.

[17] M. S. Suraj, A. Mittal and K. Pal. Stability of the artificial equilibrium points in the low-thrust restricted three-body problem when the smaller primary is an oblate spheroid. *Nonlinear Dynamics and Systems Theory.* **20** (4) (2020a) 439–450.

[18] J. A. Arredondo and J. J. Cardenas. About the Restricted Three-Body Problem with the Schwarszchild-de Sitter Potential. *Nonlinear Dynamics and Systems Theory.* **21** (2) (2021) 126–137.

[19] D. Hamri and F. Hannachi. A New fractional-order 3D chaotic system analysis and synchronization. *Nonlinear Dynamics and Systems Theory.* **21** (4) (2021) 381–392 .

Nonlinear Dynamics and Systems Theory, **23** (4) (2023) 422–433

Modelling and MultiSim Simulation of a New Hyperchaos System with No Equilibrium Point

A. Sambas [1,2], S. Vaidyanathan [3], S. F. Al-Azzawi [4], M. K. M. Nawawi [5,6*], M. A. Mohamed [1], Z. A. Zakaria [1], S. S. Abas [1] and M. Mamat [1]

[1] *Faculty of Informatics and Computing, Universiti Sultan Zainal Abidin, Besut Campus, 22200, Terengganu, MALAYSIA.*
[2] *Department of Mechanical Engineering, Universitas Muhammadiyah Tasikmalaya, Tasikmalaya, 46196, INDONESIA.*
[3] *Center for Control Systems, Vel Tech University, Avaddi, 60062, Chenai, INDIA.*
[4] *Department of Mathematics, College of Computer Science and Mathematics, University of Mosul, Mosul 41002, IRAQ.*
[5] *Institute of Strategic Industrial Decision Modeling, School of Quantitative Sciences, Universiti Utara Malaysia, 06010, UUM Sintok, Kedah, MALAYSIA.*
[6] *School of Quantitative Sciences, Universiti Utara Malaysia, 06010, UUM Sintok, Kedah, MALAYSIA.*

Received: April 16, 2023; Revised: October 2, 2023

Abstract: Crypto-devices and encryption applications make good use of nonlinear dynamical systems with hyperchaotic attractors due to their inherent complexity. Using four quadratic nonlinearities, a new 12-term hyperchaos system with hidden attractor is proposed in this research paper. It is established that the new hyperchaos system has no balance point and a hidden attractor exists for the system. Coexisting attractors and multistability are also proven to exist for the new system. The Kaplan-Yorke fractal dimension is determined for the new hyperchaos system with hidden attractor. MultiSim circuit design and simulation are carried out for the validation and real-world applications of the new hyperchaos system with hidden attractor. Finally, the chaos control results based on feedback control are also derived for the new 4D hyperchaotic system with no equilibrium point.

Keywords: *hidden attractor; hyperchaotic systems; MultiSim design; chaos control.*

Mathematics Subject Classification (2010): 34A34, 34D06, 34H10, 70Q05, 93B52.

* Corresponding author: mailto:mdkamal@uum.edu.my

1 Introduction

Chaos applications of dynamical models arise in various engineering domains such as nonlinear oscillatory systems [1, 2], biological models [3, 4], circuit devices [5, 6], ANN models [7,8], chemical models [9,10], finance models [11,12], robotics [13,14], mechanical systems [15, 16] etc.

Dynamical systems with positive Lyapunov index numbers are addressed as hyperchaotic systems [17] which possess diverse engineering applications such as secure devices [18,19], crypto-devices [20,21], memristor devices [22–24], neural networks [25,26], etc. The hyperchaotic attractor extends in two or more directions concurrently as compared to a chaotic attractor with a singularly positive Lyapunov exponent. It implies that the hyperchaotic attractor performs significantly better in many real-world applications such as secure communication and encryption because it has a topological structure that is highly complex.

Hyperchaotic models are broadly divided as hyperchaos systems exhibiting self-excited or hidden attractors. The hyperchaos models with no balance point belong to the class of systems exhibiting hidden attractors [27, 28]. Li et al. [29] proposed an optical image encryption scheme based on the fractional Fourier transform and five-dimensional host-induced nonlinearity fractional-order laser hyperchaotic system. Erkan et al. [30] studied a novel two-dimensional (2D) chaotic system depending on the Schaffer function and the recursive 2D discrete model of the Schaffer function has superior chaotic behavior. Yu et al. [31] introduced two-dimensional logistic-adjusted-sine map (2D-LASM) and four-dimensional quadratic autonomous hyperchaotic system (4D-QAHS). Also, the experimental results demonstrate that the encryption approach is secure, with an average information entropy of 7.9972. Hosny et al. [32] proposed a novel utilization of fractional-order chaotic systems in color image encryption using the 4D hyperchaotic Chen system of fractional-order combined with the Fibonacci Q-matrix. Pavithran et al. [33] proposed a novel encryption process based on Deoxyribonucleic Acid (DNA) cryptography, a hyperchaotic system and a Moore machine. Alkhayyat et al. [34] studied a novel four-dimensional continuous-time dynamical system with the features of hyperchaotic phenomenon, dissipativity, rich dynamics, unstable equilibrium point, multistability and cryptographic S-box application.

In this work, we report a new 4-D nonlinear dynamical system with a hyperchaotic attractor. We show that the proposed nonlinear dynamical system has no balance point and it displays a hidden hyperchaotic attractor. We illustrate the qualitative properties of the proposed nonlinear dynamical system with a hyperchaotic attractor via MATLAB signal plots, balance points, multi-stability, coexisting hyperchaotic attractors, etc. The proposed nonlinear dynamical system with a hyperchaotic attractor has good applications in cryptosystems [35, 36] and secure communications [37].

For practical implementation of the hyperchaos systems, designs carried out via electronic circuits [38–40] or FPGA [41, 42] are immensely useful. In this research work, we exhibit MultiSim circuit design of the proposed new hyperchaos system in the four-dimensional space with no balance point.

This paper is organised as follows. Section 2 describes the dynamics and basic properties of the new 4D hyperchaotic system. Electronic circuit using MultiSim (Version 14.0) of the new 4D hyperchaotic system is given in Section 3. Section 4 presents control results using feedback control for the new 4D hyperchaotic system. Section 5 contains the conclusions of this work.

2 A Four-Dimensional Hyperchaos Systems with No Balance Point

A novel four-dimensional dynamical system is described in this work as follows:

$$\begin{cases} \dot{\xi} = \alpha(\eta - \xi) - \eta\zeta + \omega, \\ \dot{\eta} = -\gamma\xi\zeta + \beta\eta - \varepsilon\zeta^2 + \omega, \\ \dot{\zeta} = \xi\eta - \vartheta, \\ \dot{\omega} = -\xi - \eta. \end{cases} \tag{1}$$

The four-dimensional vector $K = (\xi, \eta, \zeta, \omega)$ designates the state of the system (1). It is remarked that there are four quadratic nonlinearities (in the first, second and third differential equations). It will be established using the Lyapunov Index (LI) values spectrum analysis in MATLAB that there is hyperchaos in the system (1) when the parameters assume the values

$$\alpha = 18,\ \beta = 6,\ \gamma = 14,\ \vartheta = 10,\ \varepsilon = 0.2. \tag{2}$$

For the time-series analysis of the state K of the system (1), we assume the initial state as

$$\xi(0) = 0.2,\ \eta(0),\ \zeta(0) = 0.4,\ \omega(0) = 0.2. \tag{3}$$

Using Wolf's procedure [43], the Lyapunov Index (LI) values of the 4-D model (1) are numerically found in seconds (see Figure 1) as follows:

$$\mu_1 = 2.8033,\ \mu_2 = 0.0535,\ \mu_3 = 0,\ \mu_4 = -14.8266. \tag{4}$$

The existence of two positive LI values (*viz.* μ_1, μ_2) summarily signifies that the model (1) has hyperchaos nature. As the total of all LI values in the LI spectrum is seen to be negative, the model (1) has also dissipative motion of all its trajectories converging to the hyperchaotic attractor. The Kaplan-Yorke dimension of the hyperchaotic system (1) is computed as follows:

$$D_{KY} = 3 + \frac{\mu_1 + \mu_2 + \mu_3}{\mu_4} = 3.1927. \tag{5}$$

Figures 1 and 2 show the LI values and signal plots of the model (1) simulated in MATLAB for the parameter set $(\alpha, \beta, \gamma, \vartheta, \varepsilon) = (18, 6, 14, 10, 0.2)$. The MATLAB plots show the high complexity of the hyperchaos system (1).

Multistability means two or more attractors coexist together with different initial conditions and has been found in many nonlinear systems. Let the parameters be fixed as $\alpha = 18,\ \beta = 6,\ \gamma = 14,\ \vartheta = 10,\ \varepsilon = 0.2$ and we suppose that the initial states of the system (1) are picked as $K_0 = (0.2, 0.4, 0.4, 0.2)$ and $\Lambda_0 = (-0.8, 0.8, -0.8, 0.8)$. Figure 3 shows the multistability of the hyperchaotic system (1) with two coexisting hyperchaotic attractors emanating from K_0 (blue color) and Λ_0 (red color), respectively.

3 Multisim Simulation of the Novel Hyperchaos System with Hidden Attractor

This study will consider the analog circuit implementation of the new double-scroll hyperchaos system described in (1). Figure 4 shows a four channels electronic circuit scheme

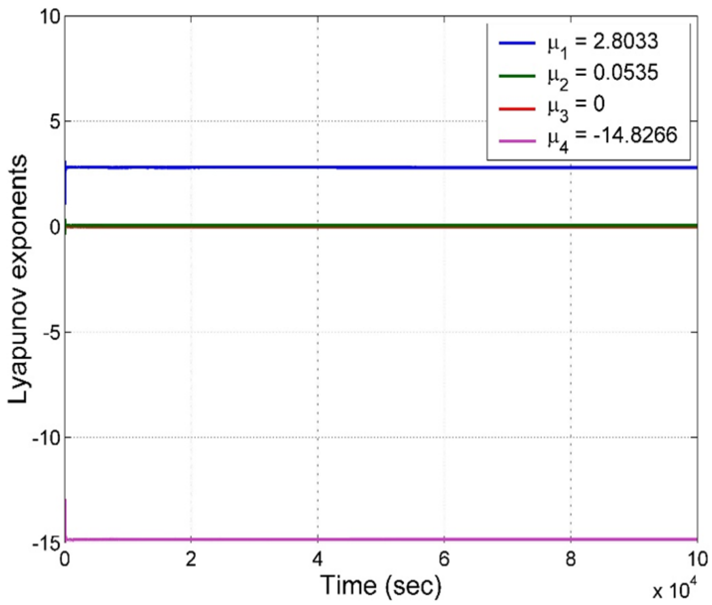

Figure 1: Lyapunov index values spectrum for the new hyperchaos system (1).

with variables ξ, η, ζ, ω from the system (1). For circuit implementation, we rescale the state variables of the new chaotic system (1) as follows: $\xi = \frac{1}{2}\xi, \eta = \frac{1}{2}\eta, \zeta = \frac{1}{2}\zeta$ and $\omega = \frac{1}{2}\omega$. In the new coordinates $(\xi, \eta, \zeta, \omega)$, the chaotic system (1) becomes

$$\begin{cases} \dot{\xi} = \alpha(\eta - \xi) - 2\eta\zeta + \omega, \\ \dot{\eta} = -2\gamma\xi\zeta + \beta\eta - 2\varepsilon\zeta^2 + \omega, \\ \dot{\zeta} = 2\xi\eta - \frac{1}{2}\vartheta, \\ \dot{\omega} = -\xi - \eta. \end{cases} \tag{6}$$

By applying Kirchhoff's laws to the designed electronic circuit, its nonlinear equations can be derived in the following form:

$$\begin{cases} \dot{\xi} = \dfrac{1}{C_1R_1}\eta - \dfrac{1}{C_1R_2}\xi - \dfrac{1}{10C_1R_3}\eta\zeta + \dfrac{1}{C_1R_4}\omega, \\[2ex] \dot{\eta} = -\dfrac{1}{10C_2R_5}\xi\zeta + \dfrac{1}{C_2R_6}\eta - \dfrac{1}{10C_2R_7}\zeta^2 + \dfrac{1}{C_2R_8}\omega, \\[2ex] \dot{\zeta} = \dfrac{1}{10C_3R_9}\xi\eta - \dfrac{1}{C_3R_{10}}V_1, \\[2ex] \dot{\omega} = -\dfrac{1}{C_4R_{11}}\xi - \dfrac{1}{C_4R_{12}}\eta. \end{cases}$$

Here, ξ, η, ζ, ω are the voltages across the capacitors C_1, C_2, C_3 and C_4, respectively.

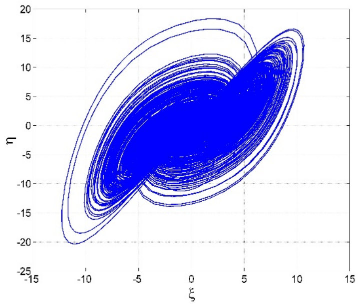

(a)

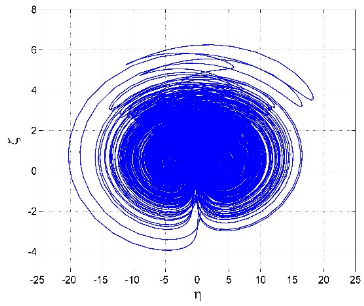

(b)

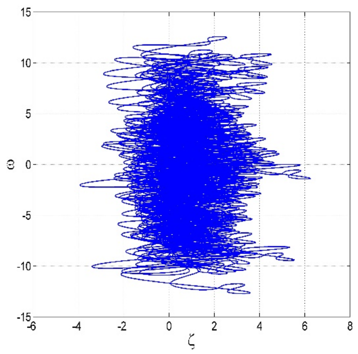

(c)

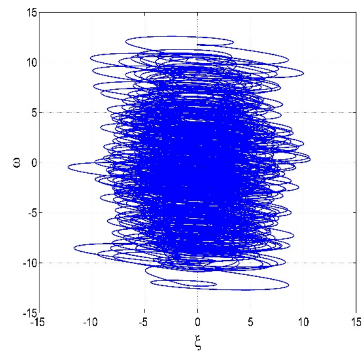

(d)

Figure 2: Signal plots of the new hyperchaos system (1) simulated in MATLAB.

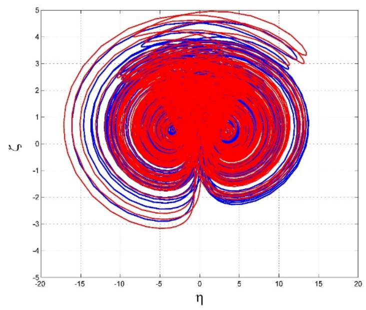

(a)

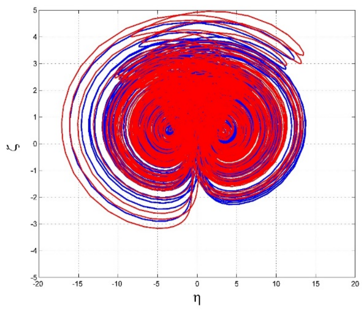

(b)

Figure 3: Phase portraits of the coexisting hyperchaotic attractors (1) for the initial states $K_0 = (0.2, 0.4, 0.4, 0.2)$ and $\Lambda_0 = (-0.8, 0.8, -0.8, 0.8,)$.

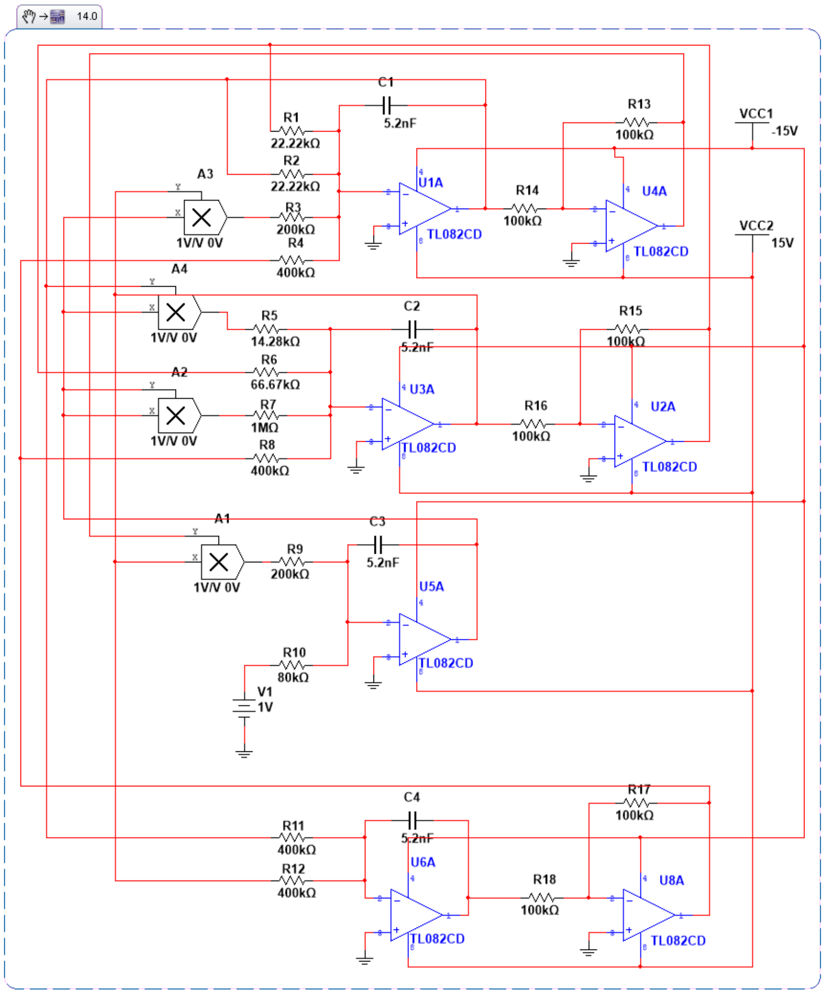

Figure 4: Circuit design for the new hyperchaotic two-scroll system.

We choose the values of the circuital elements as $R_1 = R_2 = 22.22$ k$\Omega, R_3 = R_9 = 200$ k$\Omega, R_4 = R_8 = R_{11} = R_{12} = 400$ k$\Omega, R_5 = 14.28$ k$\Omega, R_6 = 66.67$ k$\Omega, R_7 = 1$ M$\Omega, R_{10} = 80$ k$\Omega, R_{13} = R_{14} = R_{15} = R_{16} = R_{17} = R_{18} = 100$ k$\Omega, C_1 = C_2 = C_3 = C_4 = 5.2$ nF. The corresponding phase portraits on the oscilloscope are shown in Figure 5. The agreement between the Multisim results (Figure 5) and the MATLAB plots (Figure 2) shows the feasibility of the proposed hyperchaotic system.

4 Chaos Control

The system (1) is modified by introducing feedback controllers $U = [u_1, u_2, u_3,\ u_4]^T$ and is expressed as

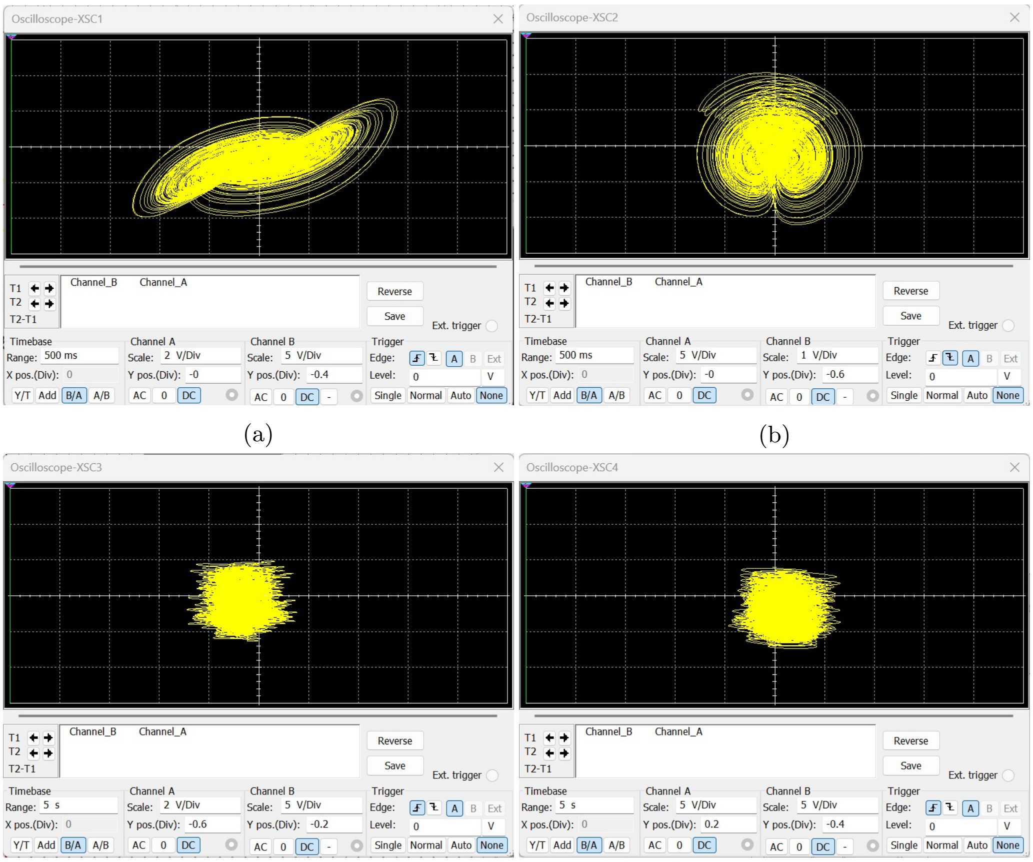

(a) (b) (c) (d)

Figure 5: MultiSIM chaotic attractors of the new hyperchaotic two-scroll system (a) ξ–η plane, $(b)\eta$–ζ plane, $(c)\zeta-\omega$ plane and $(d)\xi$–ω plane.

$$\begin{cases} \dot{\xi} = \alpha(\eta - \xi) - \eta\zeta + \omega + u_1, \\ \dot{\eta} = -\gamma\xi\zeta + \beta\eta - \varepsilon\zeta^2 + \omega + u_2, \\ \dot{\zeta} = \xi\eta - \vartheta + u_3, \\ \dot{\omega} = -\xi - \eta + u_4. \end{cases} \tag{7}$$

Consider the nonlinear control strategy [44, 45] and assume the parameters $\alpha, \beta, \gamma, \vartheta$ and ε are unknown, while $u_i,\ i = 1, 2, 3, 4$, is a feedback controller to be designed.

Theorem 1. *If the controller designed in (8) is implemented using a nonlinear control strategy, the system (1) will be suppressed.*

$$\begin{cases} u_1 = 0, \\ u_2 = -\alpha\xi - 2\beta\eta, \\ u_3 = \gamma\xi\eta + (\varepsilon\eta - 1)\zeta + \vartheta, \\ u_4 = -\omega. \end{cases} \tag{8}$$

Proof. Substituting the controllers (8) into the system (7), we have

$$\begin{cases} \dot{\xi} = \alpha(\eta - \xi) - \eta\zeta + \omega, \\ \dot{\eta} = -\gamma\xi\zeta + \beta\eta - \varepsilon\zeta^2 + \omega - \alpha\xi, \\ \dot{\zeta} = \zeta\eta + \gamma\xi\eta + (\varepsilon\eta - 1)\zeta, \\ \dot{\omega} = -\xi - \eta - \omega. \end{cases} \tag{9}$$

Construct the Lyapunov candidate function as

$$v = \tfrac{1}{2}[\ \xi^2 + \ \eta^2 + \zeta^2 + \omega^2]$$

and

$$\begin{gathered} \dot{v} = \ \xi\dot{\xi} + \eta\dot{\eta} + \zeta\dot{\zeta} + \omega\dot{\omega}, \\ \dot{v} = \ \xi(\alpha\,(\eta - \xi) - \eta\zeta + \omega) \\ +\eta(-\gamma\xi\zeta - \beta\eta - \varepsilon\zeta^2 + \omega - \alpha\xi) \\ +\zeta\,(\xi\eta + \gamma\xi\eta + (\varepsilon\eta - 1)\,\zeta) \\ +\omega(-\xi - \eta - \omega), \\ \Rightarrow \dot{v} = \ -\alpha\xi^2 - \beta\eta^2 - \zeta^2 - \omega^2. \end{gathered}$$

By using a theoretical method (the Lyapunov stability theorem), the system (1) was suppressed, and the accuracy of the analytical results was validated by the numerical simulations via Figure 6.

5 Conclusions

The main novelty of this work is the modelling of a new 4-D hyperchaos system with no balance point. We remark that the proposed hyperchaos system displays a hidden attractor as it has no balance point. In this research paper, invoking the use of four quadratic nonlinearities, a new nonlinear dynamical system with a hidden hyperchaotic attractor was proposed and illustrated with MATLAB signal plots. For nonlinear dynamical systems with chaotic or hyperchaotic attractors, multistability is a special property

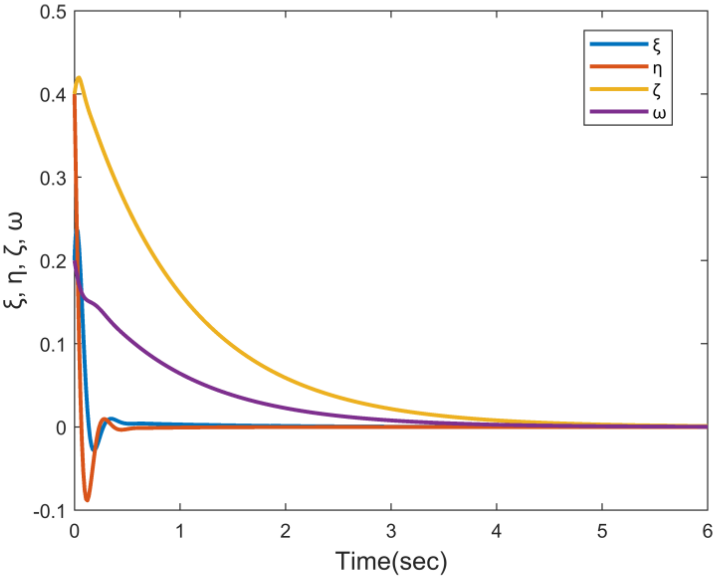

Figure 6: Convergence of attractors to zero by controller (8).

which refers to the existence of chaotic or hyperchaotic attractors for the fixed set of parameters but different choices of initial states. In this research work, we showed the existence of multistability with coexisting hyperchaotic attractors for the proposed hyperchaos system. MultiSim circuit simulation of the new hyperchaos system was designed for the validation of the new hyperchaos system with a hidden attractor, which has many practical applications in secure communication devices. Finally, the chaos control results based on feedback control are also derived for the new 4D hyperchaotic system with no equilibrium point.

References

[1] M. Labid and N. Hamri. Chaos Synchronization between Fractional-Order Lesser Date Moth Chaotic System and Integer-Order Chaotic System via Active Control. *Nonlinear Dynamics and Systems Theory* **22**(4) (2022) 407–413.

[2] H. Yousfi, A. Gasri and A. Ouannas. Stabilization of Chaotic h-Difference Systems with Fractional Order. *Nonlinear Dynamics and Systems Theory* **2** (4) (2023) 468–472.

[3] S. Kumar, A. Kumar, B. Samet, J. F. Gómez-Aguilar and M. S. Osman. A chaos study of tumor and effector cells in fractional tumor-immune model for cancer treatment. *Chaos, Solitons & Fractals* **141** (2020) 110321.

[4] S. S. Sajjadi, D. Baleanu, A. Jajarmi and H. M. Pirouz. A new adaptive synchronization and hyperchaos control of a biological snap oscillator. *Chaos, Solitons & Fractals* **138** (2020) 109919.

[5] A. Sambas, S. Vaidyanathan, X. Zhang, I. Koyuncu, T. Bonny, M. Tuna, M. ALcin, S. Zhang, I. M. Sulaiman, A. M. Awwal and P. Kumam. A novel 3D chaotic system with line equilibrium: multistability, integral sliding mode control, electronic circuit, FPGA implementation and its image encryption. *IEEE Access* **10** (2022) 68057–68074.

[6] A. Sambas, S. Vaidyanathan, E. Tlelo-Cuautle, B. Abd-El-Atty, A. A. Abd El-Latif, O. Guillén-Fernández and G. Gundara. A 3-D multi-stable system with a peanut-shaped equilibrium curve: Circuit design, FPGA realization, and an application to image encryption. *IEEE Access* **8** (2020) 137116–137132.

[7] C. Xiu, R. Zhou and Y. Liu. New chaotic memristive cellular neural network and its application in secure communication system. *Chaos, Solitons and Fractals* **141** (2016) 110316.

[8] S. Vaidyanathan. Hybrid chaos synchronization of 3-cells cellular neural network attractors via adaptive control method. *International Journal of PharmTech Research* **8** (8) (2015) 61–73.

[9] A. J. Adéchinan, Y. J. F. Kpomahou, L. A. Hinvi and C. H. Miwadinou. Chaos, coexisting attractors and chaos control in a nonlinear dissipative chemical oscillator. *Chinese Journal of Physics* **77** (2022) 2684–2697.

[10] H. Chaudhary, A. Khan and M. Sajid. An investigation on microscopic chaos controlling of identical chemical reactor system via adaptive controlled hybrid projective synchronization. *The European Physical Journal Special Topics* **231** (3) (2022)453–463.

[11] B. A. Idowu, S. Vaidyanathan, A. Sambas, O. I. Olusola, and O. S. Onma. A new chaotic finance system: Its analysis, control, synchronization and circuit design. *Nonlinear Dynamical Systems with Self-Excited and Hidden Attractors* (133) (2018) 271–295.

[12] W. A. Wali. Application of particle swarm optimization with ANFIS model for double scroll chaotic system. *International Journal of Electrical and Computer Engineering* **11** (1) (2021) 328–335.

[13] S. Bazzi and D. Sternad. Human control of complex objects: towards more dexterous robots. *Advanced Robotics* **34** (17) (2020) 1137–1155.

[14] L. Moysis, E. Petavratzis, M. Marwan, C. Volos, H. Nistazakis and S. Ahmad. "Analysis, synchronization, and robotic application of a modified hyperjerk chaotic system.*Complexity* **2020** (2020) 2826850.

[15] M. Marwan, V. Dos Santos, M. Z. Abidin and A. Xiong. Coexisting attractor in a gyrostat chaotic system via basin of attraction and synchronization of two nonidentical mechanical systems.*Mathematics* **10**, (11) (2022) 1914.

[16] S. Bentouati, A. Tlemçani, N. Henini, and H. Nouri. Adaptive Sliding Mode Control Based on Fuzzy Systems Applied to the Permanent Magnet Synchronous Machine. *Nonlinear Dynamics and Systems Theory* **21** (5) (2021) 457–470.

[17] M. Zhou, and C. Wang. A novel image encryption scheme based on conservative hyperchaotic system and closed-loop diffusion between blocks. *Signal Processing* **171** (2020) 107484.

[18] C. Zhong and M. S. Pan. Encryption algorithm based on scrambling substitution of new hyperchaotic Chen system. Chin. J. Liquid Crystals Displays, *Chin. J. Liquid Crystals Displays* **35** (1) (2020) 91–97.

[19] N. Nguyen, G. Kaddoum, F. Pareschi, R. Rovatti and G. Setti. A fully CMOS true random number generator based on hidden attractor hyperchaotic system. *Nonlinear Dynamics* **102** (4) (2020) 2887–2904.

[20] L. Ding and Q. Ding, Q. A novel image encryption scheme based on 2D fractional chaotic map, dwt and 4d hyper-chaos. *Electronics* **9** (8)(2020)1280.

[21] A. Shakiba. A novel randomized bit-level two-dimensional hyperchaotic image encryption algorithm. *Multimedia Tools and Applications* **79** (43) (2020) 32575–32605.

[22] F. Setoudeh and A. K. Sedigh. Nonlinear analysis and minimum L2-norm control in memcapacitor-based hyperchaotic system via online particle swarm optimization. *Chaos, Solitons & Fractals* **151** (2021) 111214.

[23] C. Xiu, J. Fang and X. Ma. Design and circuit implementations of multimemristive hyperchaotic system. *Chaos, Solitons & Fractals* **161** (2022) 112409.

[24] S. Vaidyanathan, V. T. Pham and C. Volos. Adaptive control, synchronization and circuit simulation of a memristor-based hyperchaotic system with hidden attractors. In Advances in Memristors, Memristive Devices and Systems. *Springer, Cham* **701** (2017) 101–130.

[25] P. S. Swathy and K. Thamilmaran. Hyperchaos in SC-CNN based modified canonical Chua's circuit. *Nonlinear Dynamics* **78** (4) (2014) 2639–2650.

[26] H. Lin, C. Wang and Y. Tan. Hidden extreme multistability with hyperchaos and transient chaos in a Hopfield neural network affected by electromagnetic radiation. *Nonlinear Dynamics* **99** (3) (2020) 2369–2386.

[27] N.Wang, G. Zhang, N. V. Kuznetsov and H. Bao. Hidden attractors and multistability in a modified Chua's circuit. *Communications in Nonlinear Science and Numerical Simulation* **92** (2021) 105494.

[28] L. Yang, Q. Yang and G. Chen. Hidden attractors, singularly degenerate heteroclinic orbits, multistability and physical realization of a new 6D hyperchaotic system. *Communications in Nonlinear Science and Numerical Simulation* **90** (2020) 105362.

[29] X. Li, J. Mou, Y. Cao and S. Banerjee. An optical image encryption algorithm based on a fractional-order laser hyperchaotic system. *International Journal of Bifurcation and Chaos* **32** (3)(2022) 2250035.

[30] U. Erkan, A. Toktas and Q. Lai. 2D hyperchaotic system based on Schaffer function for image encryption. *Expert Systems with Applications* **213** (2023) 119076.

[31] J. Yu, W. Xie, Z. Zhong and H. Wang. Image encryption algorithm based on hyperchaotic system and a new DNA sequence operation. *Chaos, Solitons & Fractals* **162** (2022) 112456.

[32] K. M. Hosny, S. T. Kamal and M. M. Darwish. Novel encryption for color images using fractional-order hyperchaotic system. *Journal of Ambient Intelligence and Humanized Computing* **13** (2) (2022)973–988.

[33] P. Pavithran, S. Mathew, S. Namasudra, and G. Srivastava. A novel cryptosystem based on DNA cryptography, hyperchaotic systems and a randomly generated Moore machine for cyber physical systems. *Computer Communications* **188** (2022) 1–12.

[34] A. Alkhayyat, M. Ahmad, N. Tsafack, M. Tanveer, D. Jiang and A. A. Abd El-Latif. A novel 4D hyperchaotic system assisted josephus permutation for secure substitution-box generation. *Journal of Signal Processing Systems* **94** (3)(2022) 315–328.

[35] J. Wu, Y. Shen and G. Xu. Integrating Fresnel diffraction, multi-phase retrieval, and hyperchaos mapping for color image encryption. *Applied Optics* **62** (4) (2023) 844-860.

[36] D. Xu, G. Li, W. Xu and C. Wei. Design of artificial intelligence image encryption algorithm based on hyperchaos. *Ain Shams Engineering Journal* **14** (3) (2023) 101891.

[37] Q. Lai and Y. Liu. A cross-channel color image encryption algorithm using two-dimensional hyperchaotic map. *Expert Systems with Applications* **223** (2023) 119923.

[38] S. Vaidyanathan, I. M. Moroz, A. Sambas and W. S. M. Sanjaya. A New 4-D Hyperchaotic Two-Wing System with a Unique Saddle-Point Equilibrium at the Origin, its Bifurcation Analysis and Circuit Simulation. In: *Journal of Physics: Conference Series* **1477** (2) (2020) 022016.

[39] W. Zhou, G. Wang, H. H. C. Iu, Y. Shen, and Y. Liang. Complex dynamics of a nonvolatile memcapacitor-aided hyperchaotic oscillator. *Nonlinear Dynamics* **100** (4) (2020) 3937–3957.

[40] A. Sambas, M. Mamat, S. Vaidyanathan, M. A. Mohamed, and W. S. M. Sanjaya. A new 4-D chaotic system with hidden attractor and its circuit implementation. *International Journal of Engineering & Technology* **7** (3) (2018) 1245–1250.

[41] S. Vaidyanathan, E. Tlelo-Cuautle, A. Sambas, L. G. Dolvis and O. Guillén-Fernández. FPGA design and circuit implementation of a new four-dimensional multistable hyperchaotic system with coexisting attractors. *International Journal of Computer Applications in Technology* **64** (3) (2020) 223–234.

[42] A. Sambas, S. Vaidyanathan, T. Bonny, S. Zhang, Y. Hidayat, G. Gundara and M. Mamat. Mathematical model and FPGA realization of a multi-stable chaotic dynamical system with a closed butterfly-like curve of equilibrium points.*Applied Sciences* **11** (2)(2021) 788.

[43] A. Wolf, J. B. Swift, H. L. Swinney and J. A. Vastano. Determining Lyapunov exponents from a time series.*Physica D: nonlinear phenomena* **16** (3) (1985) 285–317.

[44] S. F. AL-Azzawi and A. S. Al-Obeidi. Chaos synchronization in a new 6D hyperchaotic system with self-excited attractors and seventeen terms.*Asian-European Journal of Mathematics* **14** (05) (2021) 2150085.

[45] A. S. Al-Obeidi and S. F. Al-Azzawi. A novel six-dimensional hyperchaotic system with self-excited attractors and its chaos synchronisation.*International Journal of Computing Science and Mathematics* **15** (1) (2022) 72–84.

Nonlinear Dynamics and Systems Theory, **23** (4) (2023) 434–446

Properties of Solutions and Stability of a Diffusive Wage-Employment System

S. Sutrima * and R. Setiyowati

Department of Mathematics, Sebelas Maret University, Ir. Sutami, no.36 A Kentingan, 57126, Surakarta, Indonesia.

Received: June 9, 2023; Revised: August 5, 2023

Abstract: This paper focuses on the analysis of the properties of solutions and stability of a diffusive wage-employment system. The system is of a diffusive predator-prey type. By choosing appropriate parameters, the global existence, positivity, uniform boundedness and decay estimates of solutions of the system can be characterized. The stability of the system can be also justified.

Keywords: *wage-employment system; global existence; positivity; predator-prey; stability.*

Mathematics Subject Classification (2010): 35A01, 35A02, 35B0.

1 Introduction

Goodwin [1] has constructed a model of the dynamic relationship between wage and employment. The model incorporates three behaviors of economic systems (the market is in a stable equilibrium, the growth is cyclical and its equilibrium is affected by past changes, the economic relations resemble white noise and the economic motion is random [2]). Goodwin's model is analogous to the Lotka-Volterra predator-prey model, the wage and the employment correspond to the predator and the prey, respectively. The model forms a cyclical pattern. When the employment is at high level, the bargaining power of the employed workers drives up the wages, and so shrinks profits. But when the profits diminish, fewer workers are hired and the employment will decrease leading to the increment of the profits. The more profits, the more workers are hired leading to the increment of the employment.

* Corresponding author: mailto:sutrima@mipa.uns.ac.id

Let σ be the capital intensity showing how many years of income have to be tied up to produce a unit of income. The reciprocal value $1/\sigma$ measures the capital productivity, which determines the amount of national income generated by each unit of the invested capital. Goodwin assumes that the labor supply and the labor productivity are exponential processes, which means that the growth rates of both are constants. Let α and β denote the percentage per year of the rise of the labor productivity and the labor supply, respectively.

The change of the real wage (workers' share) depends on the real employment. The rates of both are positively correlated. The employment fluctuates between fairly narrow limits in real life, so the interdependence in a small neighborhood of the equilibrium is permitted to linearize by the linear Phillips curve. Let ρ and γ be the slope and the intercept of the linearization, respectively. Goodwin's real wage - real employment cycle is modeled by [3, 4]

$$\begin{aligned} \dot{u} &= -\eta_1 u + \theta_1 uv, \\ \dot{v} &= \eta_2 v - \theta_2 uv, \end{aligned} \tag{1}$$

where u and v are the rate of real wage and the rate of real employment, respectively, $\eta_1 = \alpha + \gamma$, $\theta_1 = \rho$, $\eta_2 = \frac{1}{\sigma} - (\alpha + \beta)$ and $\theta_2 = \frac{1}{\sigma}$.

In the absence of wages u, the employment rate v in (1) grows exponentially without boundaries. In reality, the employment cannot increase without limits and decreases in productivity since additional workers will not be just as productive as the employed workers. To enhance the more realistic model, a logistic saturation is considered in the second equation in (1) at $u = 0$ by

$$\dot{v} = \eta_2 \left(1 - \frac{v}{K}\right) v.$$

Since the employment cannot surpass total population, the model requires $K = 1$.

The second problem with Goodwin's original model is the reaction of wages to employment since any changes in wages as a result of changes in employment cannot be instantaneous as they are assumed to be. Wage contracts planed ahead do not affect the changes of demand of labor in future, causing a delay in the reaction of wages to employment. This delay can be inserted in the first equation in (1) by

$$w(t) = (h * v)(t) := \int_0^t h(t-s)v(s)\, ds,$$

where h is a nonnegative integrable weight function such that $\int_0^\infty h(s)\, ds = 1$. One of the comfortable weight functions in the economic model is

$$h(t) = ae^{-at}, \quad a > 0. \tag{2}$$

On the other hand, the analysis of stability of equilibriums of the various types of the Lotka-Volterra model has been done. Moreover, many applications including forecasting have also been widely used even in finance and economics, see [5–9] and references therein. This paper focuses on studying the geographical expansion of the wage-employment interaction, as a generalization of (1) obeying the diffusive Lotka-Volterra system

$$\begin{aligned} u_t &= \delta_1 \Delta u - \eta_1 u + \theta_1 u(h * v), \\ v_t &= \delta_2 \Delta v + \eta_2 (1 - v)v - \theta_2 uv, \end{aligned} \tag{3}$$

subject to the initial conditions

$$u(x,0) = u_0(x), \quad v(x,0) = v_0(x), \quad x \in \Omega, \tag{4}$$

where Δ is the Laplace operator, Ω is the bounded domain in $\mathbb{R}^n$, and δ_1, δ_2 are positive constants of the movement rates of wages and employment, respectively, and h is the weight function in (2). Some results on the dynamics, stability, bifurcation of solutions for the systems of reaction-diffusion systems were established in [10–14] not including the system (3)-(4). Recently, by quasi-semigroup and quasi-group approaches, time-dependent diffusion problems are also being done, see [15, 16].

This paper focuses on the global existence, positivity, and uniform boundedness of the solutions of the wage-employment system (3)-(4). Moreover, the stability of the equilibrium points of the systems is also analyzed.

2 Existence of Positive Solution

In what follows, we denote by X the space of bounded and uniformly continuous functions on $\Omega \subset \mathbb{R}$ endowed with the supremum norm. It is well-known that the linear operators $\delta_1\Delta$ and $\delta_2\Delta$ generate the semigroups of contractions T_1 and T_2 on the Banach space X given by

$$[T_i(t)w](x) = \frac{1}{\sqrt{4\pi\delta_i t}} \int_{-\infty}^{\infty} e^{-\frac{|x-s|^2}{4\delta_i t}} w(s)\, ds, \quad T_i(0) = I, \tag{5}$$

respectively, where I is the identity operator on X and $i = 1, 2$. Further, $u(t) = T_1(t)u_0$ and $v(t) = T_2(t)v_0$ are the unique solutions of

$$\begin{aligned} u_t &= \delta_1 \Delta u, \\ v_t &= \delta_2 \Delta v, \end{aligned} \tag{6}$$

subject to the initial conditions (4), respectively.

We also assume that the initial conditions u_0 and v_0 in (4) are the nonnegative elements of X. Following the scheme in [17], we shall show the existence of a global solution to the problem (3)–(4).

Theorem 2.1 *Let $u_0, v_0 \in X$ and $\eta_2 \geq 0$. There exists a unique global classical nonnegative solution (u, v) to the problem* (3)-(4).

Proof. Local existence and uniqueness follow from the solutions to (6) and the Duhamel principle; there exists a $\tau_0 > 0$ such that the problem (3)-(4) has a unique local mild solution $(u, v) \in C([0, \tau_0], X) \times C([0, \tau_0], X)$, i.e.,

$$\begin{aligned} u(t) &= T_1(t)u_0 + \int_0^t T_1(t-s)f(s)\, ds, \quad t \in [0, \tau_0], \\ v(t) &= T_2(t)v_0 + \int_0^t T_2(t-s)g(s)\, ds, \quad t \in [0, \tau_0], \end{aligned}$$

where $f(t) = -\eta_1 u(t) + \theta_1 u(t)(h * v)(t)$ and $g(t) = \eta_2(1 - v(t))v(t) - \theta_2 u(t)v(t)$ for all $t \in [0, \tau_0]$. Since $f, g \in C^\infty((0, \tau_0], X)$, the Lebesgue theory concludes that $u(t), v(t) \in C^\infty(\Omega, \mathbb{R})$ for all $t \in (0, \tau_{\max}]$, where $\tau_{\max} := \tau_0$ is the maximal time of existence of the solution (u, v).

Next, we prove the nonnegativity of the solutions. Let $\lambda_v = \sup\{\|(h*v)(t)\|; 0 \le t \le \tau\}$, where $0 < \tau < \tau_{max}$ and $\lambda_0 = -\eta_1 + \theta_1\lambda_v$. The substitution $u = e^{\lambda_0 t}\varphi$ to the first equation of (3) gives

$$\varphi_t - \delta_1\varphi_{xx} + (\eta_1 - \theta_1(h*v) + \lambda_0)\varphi \equiv 0, \quad x \in \Omega, \quad 0 < t \le \tau,$$

where $\varphi(x,0) = u_0(x)$. Since $v \in C([0,\tau], X)$ and $\eta_1 - \theta_1(h*v) + \lambda_0 \ge 0$, the maximum principle (Theorem 9 on page 43) in [18] implies that φ is nonnegative, which in turn gives the nonnegativity of u.

The substitution $v = e^{\lambda_0 x}\phi(t) + \psi(t)$ to the second equation of (3) yields two Bernoulli's equations in t,

$$\begin{aligned}\phi'(t) + (\theta_2 u - \lambda_0^2 - \eta_2)\phi(t) &= -\eta_2 e^{\lambda_0 x}\phi^2(t), \quad x \in \Omega, \quad 0 < t \le \tau,\\ \psi'(t) + (\theta_2 u + 2\eta_2 e^{\lambda_0 x}\phi(t) - \eta_2)\psi(t) &= -\eta_2\psi^2(t), \quad x \in \Omega, \quad 0 < t \le \tau.\end{aligned}$$

A direct computation to these equations on $\Omega \times (0,\tau]$ gives a solution

$$v(x,t) = \begin{cases} e^{-\theta_2 ut}(e^{\lambda_0^2 t + \lambda_0 x} + 1), & \eta_2 = 0,\\ \dfrac{e^{-P(t)}}{\eta_2 \int e^{-P(t)}dt} + \dfrac{e^{-Q(t)}}{\eta_2 \int e^{-Q(t)}dt}, & \eta_2 > 0,\end{cases} \tag{7}$$

where

$$P(t) = \int (\theta_2 u - \lambda_0^2 - \eta_2)dt, \quad Q(t) = \int (\theta_2 u + 2w(t) - \eta_2)dt, \quad w(t) = \frac{e^{-P(t)}}{\int e^{-P(t)}dt}.$$

The condition $\eta_2 \ge 0$ implies the nonnegativity of v in (7). Thus, we just proved the existence of a priori bounds for the solution u, v on $[0, \tau_{max})$. From this, we shall prove the global solution of (u, v).

The solution of the problem (3)-(4) can be represented by

$$u(t) = e^{-\eta_1 t}T_1(t)u_0 + \int_0^t e^{-\eta_1(t-s)}T_1(t-s)\theta_1 u(s)(h*v)(s)\,ds, \tag{8}$$

$$v(t) = e^{\eta_2 t}T_2(t)v_0 - \int_0^t e^{\eta_2(t-s)}T_2(t-s)[\eta_2 v^2(s) + \theta_2 u(s)v(s)]\,ds. \tag{9}$$

The contraction of T_2, the nonnegativity of u and v, and (9) give

$$\|v(t)\| \le e^{\eta_2 t}\|v_0\| \quad \text{for all} \quad t \ge 0. \tag{10}$$

Since $\|h*v\| \le \|v\|$, from (8) and (10), we have

$$\|u(t)\| \le \|u_0\| + \theta_1\|v_0\| \int_0^t e^{\eta_2 s}\|u(s)\|\,ds, \quad \text{for all} \quad t \ge 0.$$

Finally, Gronwall's inequality implies

$$\|u(t)\| \le \|u_0\| e^{\theta_1\|v_0\|k(t)} \quad \text{for all} \quad t \ge 0, \tag{11}$$

where

$$k(t) = \begin{cases} \frac{1}{\eta_2}(e^{\eta_2 t} - 1), & \eta_2 > 0,\\ t, & \eta_2 = 0.\end{cases}$$

Results (10) and (11) show that the solutions are global ($\tau_{max} = +\infty$).

Remark 2.1 Theorem 2.1 interprets that if the capital productivity is greater than the sum of the growth rates of labor supply and labor productivity, then the solution (u, v) (wage-employment) of (3)-(4) is positive. This means that the employment and labor power depend on the amount of national income generated by the invested capital.

3 Boundedness of Solution

The solution of the problem (3)-(4) constructed in Theorem 2.1 is not always bounded as is shown in the following lemma.

Lemma 3.1 *If $v_0 \neq 0$ and η_2 is sufficiently large, then the solution (u, v) in Theorem 2.1 is unbounded.*

Proof. Suppose (u, v) is a globally bounded solution, there is a constant $M > 0$ such that $\|u(t)\| \leq M$ and $\|v(t)\| \leq M$ for all $t \geq 0$. Since $v_0 \neq 0$, there exists $\omega > M^2$ such that $T_2(t)v_0 > \omega$ for all $t \geq 0$. By the nonnegativity of u, v, (9) gives

$$v(t) \geq \left(\omega - \frac{M^2(\eta_2 + \theta_2)}{\eta_2}\right) e^{\eta_2 t} + \frac{M^2(\eta_2 + \theta_2)}{\eta_2}.$$

Getting $\eta_2 > \frac{M^2\theta_2}{\omega - M^2}$ gives $\|v(t)\| \to +\infty$ as $t \to +\infty$. We have a contradiction.

Lemma 3.1 states that to get bounded solutions, we need some restrictions either on the coefficients of the system or on the initial data.

Theorem 3.1 *If $u_0, v_0 \in X$ and $\eta_2 \geq 0$, then*

$$\|v(t)\| \leq \|v_0\| e^{\eta_2 t} \quad \text{for all} \quad t \geq 0, \tag{12}$$

$$\|u(t)\| \leq e^{(\theta_1 \|v_0\| c(\tau) - \eta_1)t} \|u_0\| \quad \text{for all} \quad t \in [0, \tau], \tag{13}$$

where $c(t) := \frac{a e^{\eta_2 t}}{a + \eta_2}$. Further, if $\eta_2 = 0$ and $\eta_1 > \theta_1 \|v_0\|$, then

$$\lim_{t \to \infty} \|u(t)\| = 0.$$

Proof. Substituting $u = \phi e^{-\eta_1 t}$ and $v = \varphi e^{\eta_2 t}$ into (3) and (4), respectively, gives

$$\phi_t - \delta_1 \phi_{xx} = \theta_1 \phi (h * e^{\eta_2 t} \varphi), \tag{14}$$

$$\varphi_t - \delta_2 \varphi_{xx} = -\eta_2 \varphi^2 e^{\eta_2 t} - \theta_2 e^{-\eta_1 t} \phi \varphi \tag{15}$$

with the initial data

$$\phi_0(x) = u_0(x), \qquad \varphi_0(x) = v_0(x). \tag{16}$$

By the nonnegativity of ϕ and φ, (15) with (16) give

$$\varphi(t) = T_2(t)v_0 - \int_0^t T_2(t-s)[\eta_2 \varphi^2(s) e^{\eta_2 s} + \theta_2 e^{-\eta_1 s} \phi(s) \varphi(s)]\, ds \leq T_2(t) v_0 \tag{17}$$

for all $(x, t) \in \Omega \times [0, \infty)$. This implies that

$$\|v(t)\| = \|\varphi(t)\| e^{\eta_2 t} \leq \|v_0\| e^{\eta_2 t}, \quad \text{for all} \quad t \geq 0.$$

Next, by (17) and (14), we obtain

$$\phi_t - \delta_1 \phi_{xx} \leq \theta_1 \|v_0\| c(t) \phi.$$

Transforming $\phi = e^{\theta_1 \|v_0\| c(\tau) t} z$ on $\Omega \times [0, \tau]$ gives

$$z_t - \delta_1 z_{xx} \leq 0, \quad z(0) = \phi(0) = u_0.$$

This implies that

$$z(t) = T_1(t) u_0, \qquad t \geq 0.$$

Therefore, $\|\phi(t)\| \leq e^{\theta_1 \|v_0\| c(\tau) t} \|u_0\|$ and

$$\|u(t)\| = \|\phi(t)\| e^{-\eta_1 t} \leq e^{(\theta_1 \|v_0\| c(\tau) - \eta_1) t} \|u_0\| \quad \text{for all} \quad t \in [0, \tau]. \tag{18}$$

Further, for $\eta_2 = 0$ and $\eta_1 > \theta_1 \|v_0\|$, (18) implies that

$$\lim_{t \to \infty} \|u(t)\| = 0.$$

Theorem 3.2 *If $\eta_2 = 0$ and $\delta_1 \leq \delta_2$, then the solution (u, v) of (3)-(4) is globally bounded. Moreover,*

$$\|v(t)\| \leq \|v_0\| \quad \textit{for all} \quad t \geq 0, \tag{19}$$

$$\|u(t)\| \leq \|u_0\| + \frac{\theta_1}{\theta_2} \sqrt{\frac{\delta_2}{\delta_1}} \|v_0\| \quad \textit{for all} \quad t \geq 0. \tag{20}$$

Proof. The nonnegativity of v gives $(h * v)(s) \leq v(s)$ for all $s \geq 0$. If $\eta_2 = 0$, (12) gives (19). Moreover, from (8) and (9), we have

$$u(t) = e^{-\eta_1 t} T_1(t) u_0 + \theta_1 U(t), \tag{21}$$

$$v(t) = T_2(t) v_0 - \theta_2 V(t), \tag{22}$$

where

$$\begin{aligned} U(t) &= \int_0^t e^{-\eta_1 (t-s)} T_1(t-s) u(s) (h * v)(s) \, ds \leq \int_0^t T_1(t-s) u(s) v(s) \, ds, \\ V(t) &= \int_0^t T_2(t-s) u(s) v(s) \, ds. \end{aligned} \tag{23}$$

Conditions $\delta_1 \leq \delta_2$ and (5) provide

$$T_1(t) w \leq \sqrt{\frac{\delta_2}{\delta_1}} T_2(t) w \qquad \text{for all} \quad w \in X, \quad t \geq 0. \tag{24}$$

Moreover, by the nonnegativity of v, (22) implies that

$$V(t) \leq \frac{1}{\theta_2} T_2(t) v_0 \qquad \text{for all} \quad t \geq 0. \tag{25}$$

Equations (23), (24) and (25) give

$$U(t) \leq \sqrt{\frac{\delta_2}{\delta_1}} V(t) \leq \frac{1}{\theta_2} \sqrt{\frac{\delta_2}{\delta_1}} T_2(t) v_0 \qquad \text{for all} \quad t \geq 0. \tag{26}$$

Finally, (26) together with (21) imply (20).

Theorem 3.3 *Let* $\eta_1 = 0$*,* $\delta_1 \leq \delta_2$ *and* $0 \leq \eta_2 \leq H(t)$ *for all* $t \geq \tau$*, where* H *is a positively continuous function such that* $\lim_{t\to\infty} tH(t) = 0$ *for some* $\tau > 0$*. The solution* (u, v) *of* (3)-(4) *is globally bounded. Moreover,*

$$\|u(t)\| \leq \|u_0\| + \frac{\theta_1}{\theta_2}\sqrt{\frac{\delta_2}{\delta_1}}\|v_0\| \quad \textit{for all} \quad t \geq 0, \tag{27}$$

$$\|v(t)\| \leq c\|v_0\| \quad \textit{for all} \quad t \geq 0, \quad \textit{for some} \quad c > 0. \tag{28}$$

Proof. For $\eta_1 = 0$, (8) and (9) give

$$u(t) = T_1(t)u_0 + \theta_1 \int_0^t T_1(t-s)u(s)v(s)\,ds, \tag{29}$$

$$v(t) = e^{\eta_2 t}\left[T_2(t)v_0 - \int_0^t e^{-\eta_2 s}T_2(t-s)[\eta_2 v^2(s) + \theta_2 u(s)v(s)]\,ds\right], \tag{30}$$

respectively. Since v is nonnegative, (30) implies that

$$\int_0^t e^{-\eta_2 s}T_2(t-s)[\eta_2 v^2(s) + \theta_2 u(s)v(s)]\,ds \leq T_2(t)v_0. \tag{31}$$

Further, since $\eta_2, \theta_2 > 0$ and the function $f(s) = e^{-\eta_2 s}$ is decreasing on $[0, t]$, (31) gives

$$\int_0^t T_2(t-s)u(s)v(s)\,ds \leq \frac{T_2(t)v_0}{\theta_2}.$$

Therefore, inserting (24) into (29), we obtain

$$u(t) \leq T_1(t)u_0 + \frac{\theta_1}{\theta_2}\sqrt{\frac{\delta_2}{\delta_1}}T_2(t)v_0.$$

This proves (27).

Next, if there exists $\tau > 0$ such that $\eta_2 \leq H(t)$ for all $t \geq \tau$, where H is a positively continuous function such that $\lim_{t\to\infty} tH(t) = 0$, then (12) gives (28), where $c = e^{\tau H(\tau)}$.

Remark 3.1 Theorem 3.2 clarifies that the solution (u, v) of (3)-(4) is globally bounded when the capital productivity is equal to the sum of the growth rates of labor supply and labor productivity. Further, Theorem 3.3 is valid if the rate of labor productivity and the intercept of the linear Phillips curve negate each other. This may occur when the rate of labor productivity is negative.

In particular, if the employment is unlimited, the system (3) has the form

$$\begin{aligned} u_t &= \delta_1 \Delta u - \eta_1 u + \theta_1 uv, \\ v_t &= \delta_2 \Delta v + \eta_2 v - \theta_2 uv \end{aligned} \tag{32}$$

subject to the initial conditions (4), and we have the following theorem.

Theorem 3.4 *If* $\eta_1 = 0$ *and* $u_0(x) > \eta_2/\theta_2$ *for all* $x \in \Omega$*, then the solution* (u, v) *of* (32)-(4) *satisfies*

$$\|v(t)\| \leq \|v_0\| \quad \textit{for all} \quad t \geq 0. \tag{33}$$

Moreover, if there exists $\kappa > \eta_2/\theta_2$ *such that* $u_0(x) > \kappa$ *for all* $x \in \Omega$*, then*

$$\|u(t)\| \leq e^{\frac{\theta_1}{\kappa\theta_2 - \eta_2}\|v_0\|}\|u_0\| \quad \textit{for all} \quad t \geq 0, \tag{34}$$

$$\|v(t)\| \leq e^{-(\kappa\theta_2 - \eta_2)t}\|v_0\| \quad \textit{for all} \quad t \geq 0. \tag{35}$$

Proof. Since $u_0 > \eta_2/\theta_2$, (29) implies that

$$u(t) \geq T_1(t)(\eta_2/\theta_2) \geq \eta_2/\theta_2 \quad \text{for all} \quad t \geq 0.$$

We define a linear operator $B(t) := \eta_2 - \theta_2 u(t)$ on X. From (32), we have

$$v_t(t) = [\delta_2 \Delta + B(t)]v(t). \tag{36}$$

The dissipativity of $B(t)$ for all $t \geq 0$ implies that there exists a contraction quasi semigroup $R(t,s)$ on X generated by $\delta_2\Delta + B(t)$, [19]. Moreover, the problem (36)-(4) has a solution

$$v(t) = R(0,t)v_0 \quad \text{for all} \quad t \geq 0.$$

This proves (33).

If $u_0 \geq \kappa > \eta_2/\theta_2$, again, from (29), we have $u(t) \geq \kappa$. Further, $\eta_2 - \theta_2 u(t) < \eta_2 - \kappa\theta_2 < 0$ for all $t \geq 0$. Therefore, (36) can be rewritten as

$$v_t(t) = [\delta_2\Delta + B(t) + \omega I]v(t) - \omega v(t), \tag{37}$$

where $\omega := \kappa\theta_2 - \eta_2 > 0$. Since $B(t) + \omega I$ is a dissipative operator on X, operator $\delta_2\Delta + B(t) + \omega I$ generates a contraction quasi semigroup $G(t,s)$. Therefore, the contraction quasi semigroup $R(t,s)$ generated by $\delta_2\Delta + B(t)$ has a representation

$$R(t,s) = e^{-\omega s}G(t,s) \quad \text{for all} \quad t,s \geq 0.$$

Thus, the solution of (37)-(4) is given by

$$v(t) = K(0,t)v_0 = e^{-\omega t}G(0,t)v_0 \quad \text{for all} \quad t \geq 0. \tag{38}$$

Equation (38) implies (35). Further, substituting (38) into (29) gives

$$u(t) = T_1(t)u_0 + \theta_1 \int_0^t T_1(t-s)u(s)e^{-\omega s}G(0,s)v_0\, ds.$$

Finally, Gronwall's equation implies (34).

Remark 3.2 Besides Theorem 3.4, we can prove that all the results on the positiveness and (globally) boundedness of solutions in Theorems 2.1, 3.1, 3.2 and 3.3 are valid for the system (32)-(4). The proofs are left to the reader.

4 Stability of Solution

We focus on the system (3)-(4) subject to the no-flux boundary on the regular boundary $\partial\Omega$. To begin with, we will analyze the stability of the equilibrium solution to disclose its vulnerability at parameter variations. System (3) is equivalent to the three-dimensional system

$$\begin{aligned} u_t &= \delta_1\Delta u - \eta_1 u + \theta_1 uw, \\ v_t &= \delta_2\Delta v + \eta_2(1-v)v - \theta_2 uv, \\ w_t &= a(v-w), \end{aligned} \tag{39}$$

where w stands for the expectations of the future employment levels based on the past employment levels. The third equation in (39) shows that the expectations change continuously and correct themselves.

Straightforward computation shows that system (39) has three equilibrium points:

$$S_1 = (0,0,0), \qquad S_2 = (0,1,1), \qquad S_3 = \left(\frac{(\theta_1 - \eta_1)\eta_2}{\theta_1\theta_2}, \frac{\eta_1}{\theta_1}, \frac{\eta_1}{\theta_1} \right).$$

After translating the equilibrium point (u^*, v^*, w^*) to the origin by the translation $\bar{u} = u - u^*, \bar{v} = v - v^*$, $\bar{w} = w - w^*$ and still denoting $\bar{u}$, $\bar{v}$ and $\bar{w}$ by u, v and w, respectively, the system (39) reduces to the following system:

$$\begin{aligned} u_t &= \delta_1 \Delta u + (\theta_1 - \eta_1)u + \theta_1 u^* w + f(u,v,w), \\ v_t &= \delta_2 \Delta v - \theta_2 v^* u + (\eta_2 - \theta_2 u^* - 2\eta_2 v^*)v + g(u,v,w), \\ w_t &= a(v - w), \end{aligned} \tag{40}$$

where

$$f(u,v,w) = \theta_1 uw, \qquad g(u,v,w) = -\eta_2 v^2 - \theta_2 uv,$$

subject to the no-flux boundary conditions

$$\partial_\nu u = \partial_\nu v = \partial_\nu w = 0, \quad x \in \partial\Omega, \quad t \geq 0. \tag{41}$$

Henceforth, we will only focus on the special case when $\Omega := (0,\pi)$ and $X := H^2(\Omega)$ is the standard Sobolev space, so we consider the following system:

$$\begin{aligned} u_t &= \delta_1 u_{xx} + (\theta_1 - \eta_1)u + \theta_1 u^* w + f(u,v,w), \\ v_t &= \delta_2 v_{xx} - \theta_2 v^* u + (\eta_2 - \theta_2 u^* - 2\eta_2 v^*)v + g(u,v,w), \\ w_t &= a(v - w) \end{aligned} \tag{42}$$

subject to the Neumann boundary condition

$$u_x(0,t) = u_x(\pi,t) = 0, \quad v_x(0,t) = v_x(\pi,t) = 0, \quad w_x(0,t) = w_x(\pi,t) = 0, \quad t \geq 0. \tag{43}$$

The linearized system (42) at (u^*, v^*, w^*) can be written as

$$\begin{pmatrix} u_t \\ v_t \\ w_t \end{pmatrix} = L \begin{pmatrix} u \\ v \\ w \end{pmatrix},$$

where

$$L = \begin{pmatrix} \delta_1 \dfrac{\partial^2}{\partial x^2} + \theta_1 - \eta_1 & 0 & \theta_1 u^* \\ -\theta_2 v^* & \delta_2 \dfrac{\partial^2}{\partial x^2} + \eta_2 - \theta_2 u^* - 2\eta_2 v^* & 0 \\ 0 & a & -a \end{pmatrix}$$

on the domain

$$\mathcal{D}(L) = \{(u,v,w) \in [H^2(\Omega)]^3 : u'(0) = u'(\pi) = 0,\ v'(0) = v'(\pi) = 0,\ w'(0) = w'(\pi)\}.$$

It is well-known that the eigenvalue problem

$$z'' = \mu z, \quad x \in (0,\pi), \quad z'(0) = z'(\pi) = 0,$$

has the eigenvalues $\mu_n = -n^2$, $n \in \mathbb{N}_0 := \mathbb{N} \cup \{0\}$, with the corresponding eigenfunctions $\phi_n(x) = \cos nx$. Let

$$\begin{pmatrix} \phi \\ \psi \\ \varphi \end{pmatrix} = \sum_{n=0}^{\infty} \begin{pmatrix} a_n \\ b_n \\ c_n \end{pmatrix} \cos nx,$$

where a_n, b_n, c_n are constants, be an eigenfunction of L with the eigenvalue λ, that is,

$$L \begin{pmatrix} \phi \\ \psi \\ \varphi \end{pmatrix} = \lambda \begin{pmatrix} \phi \\ \psi \\ \varphi \end{pmatrix}.$$

The orthogonality of the function sequence (ϕ_n) implies that

$$L_n \begin{pmatrix} a_n \\ b_n \\ c_n \end{pmatrix} = \lambda \begin{pmatrix} a_n \\ b_n \\ c_n \end{pmatrix}, \quad n \in \mathbb{N}_0,$$

where

$$L_n = \begin{pmatrix} -n^2\delta_1 + \theta_1 - \eta_1 & 0 & \theta_1 u^* \\ -\theta_2 v^* & -n^2\delta_2 + \eta_2 - \theta_2 u^* - 2\eta_2 v^* & 0 \\ 0 & a & -a \end{pmatrix}.$$

Lemma 3.1 of [13] implies that λ is an eigenvalue for L if and only if λ is an eigenvalue for L_n for some $n \in \mathbb{N}_0$. The characteristic equation of L_n at (u^*, v^*, w^*) is

$$\lambda^3 + \alpha_n \lambda^2 + \beta_n \lambda + \gamma_n = 0, \quad n \in \mathbb{N}_0, \tag{44}$$

where

$$\begin{aligned} \alpha_n &= n^2(\delta_1 + \delta_2) + a + \eta_1 - \eta_2 - \theta_1 + u^*\theta_2 + 2v^*\eta_2, \\ \beta_n &= n^4\delta_1\delta_2 + n^2(a(\delta_1 + \delta_2) + \delta_2\eta_1 - \delta_1\eta_2 - \delta_2\theta_1) + a(\eta_1 - \eta_2 - \theta_1) \\ &\quad + \eta_2(\theta_1 - \eta_1) + (n^2\delta_1 + a + \eta_1 - \theta_1)(\theta_2 u^* + 2\eta_2 v^*), \\ \gamma_n &= an^4\delta_1\delta_2 + an^2(\delta_2\eta_1 - \delta_1\eta_2 - \delta_2\theta_1) + a\eta_2(\theta_1 - \eta_1) \\ &\quad + (n^2\delta_1 + \eta_1 - \theta_1)(a\theta_2 u^* + 2a\eta_2 v^*) + au^*v^*\theta_1\theta_2. \end{aligned} \tag{45}$$

The standard linear operator theory provides that if all the eigenvalues of the operator L have negative real parts, then (u^*, v^*, w^*) is asymptotically stable, and if some eigenvalues have positive real parts, then (u^*, v^*, w^*) is unstable. For (44), we have the following lemma.

Lemma 4.1 *[20] The real parts of the roots of the equation $x^3 + \alpha x^2 + \beta x + \gamma = 0$ are all negative if and only if $\alpha > 0$, $\alpha\beta - \gamma > 0$ and $\gamma > 0$.*

Evaluation (44) at the equilibrium S_1 together with Lemma 4.1 give that S_1 is asymptotically stable if $\eta_2 < n^2\delta_2$ for some n. However, this stability is not significant in the economic sense since S_1 provides the absence of wages and employment. The equilibrium S_2 is asymptotically stable if $\eta_1 + n^2\delta_1 > \theta_1$ for some n implying a decrease in wages. Since S_2 represents the absence of wages corresponding to full employment, it is meaningless in this case.

We note that the position of the equilibrium S_3 does not depend on the delay μ, but its stability does. The stability conditions of the equilibrium S_3 are summarized in the following theorem.

Theorem 4.1 *Let $\mu = 1/a$ be a delay and $\delta_n = n^2(\delta_1 + \delta_2)$. The stability of S_3 is considered in three cases:*

(a) If $\theta_1(\theta_1 - \eta_1 - \delta_n) - \eta_1\eta_2 < 0$ for some n, then S_3 is asymptotically stable, regardless of the delay.

(b) If $\theta_1(\theta_1 - \eta_1 - \delta_n) - \eta_1\eta_2 > 0$ and $\mu(\theta_1 - \eta_1 - \delta_n - \frac{\eta_1\eta_2}{\theta_1}) < 1$ for some n, then S_3 is asymptotically stable.

(c) If $\mu(\theta_1 - \eta_1 - \delta_n - \frac{\eta_1\eta_2}{\theta_1}) > 1$ for some n, then S_3 is unstable.

Proof. An application of Lemma 4.1 to the roots of (44) at S_3 implies that S_3 is asymptotically stable if

$$\theta_1 - \eta_1 - \delta_n - \frac{\eta_1\eta_2}{\theta_1} < a, \tag{46}$$

where $\delta_n = n^2(\delta_1 + \delta_2)$ for some $n \in \mathbb{N}_0$.

(a) Since $a > 0$, the inequality in (46) is valid if the left-hand side of (46) is negative (regardless of μ), i.e.,

$$\theta_1(\theta_1 - \eta_1 - \delta_n) - \eta_1\eta_2 < 0. \tag{47}$$

Since $\delta_n > 0$ for all $n \in \mathbb{N}_0$, the left-hand side of (47) is valid if $\eta_1 > \theta_1$ or $\eta_1 + \delta_n < \theta_1$ for some n and η_2 is large enough.

(b) For a small delay μ, inequality (46) gives that $\mu(\theta_1 - \eta_1 - \delta_n - \frac{\eta_1\eta_2}{\theta_1}) < 1$ and the left-hand side is positive.

(c) The condition $\mu(\theta_1 - \eta_1 - \delta_n - \frac{\eta_1\eta_2}{\theta_1}) > 1$ for some n negates the inequality in (46). This implies that characteristic equation (44) may have eigenvalues with positive real parts.

Remark 4.1 (a) The condition (47) is valid if $\eta_1 > \theta_1$ or $\eta_1 + \delta_n < \theta_1$ for some n together with η_2 being large enough. The stability due to both conditions is regardless of the delay μ and this case rarely happens in real economic life. The first hypothesis confirms that wage-employment system (42)-(43) is stable if the growth rate of the labor productivity is greater than the difference from the slope of the linear Phillips curve to its intercept. At this point, all solutions must approach the positive stable equilibrium when $t \to \infty$.

(b) In particular, for $n = 0$, S_3 is a locally asymptotically stable equilibrium for system (42)-(43) without the diffusion Δ (or system (1)).

(c) If $\eta_2 = 0$ and $\delta_1 \leq \delta_2$, Theorem 3.2 implies that the equilibrium $\left(0, \frac{\eta_1}{\theta_1}\right)$ is global asymptotically stable on the uv-plane. However, similar to the equilibrium S_2, the equilibrium is not meaningful in economic sense.

5 Conclusions

In this paper, we extend the original wage-employment system to the diffusive system. The system is of a diffusive predator-prey type. The properties of solutions to the system including global existence, positivity, uniform boundedness and decay estimates depend on the parameters being varied. The system has three equilibrium points, one of which is asymptotically stable for the appropriate parameters and the stability is economically meaningful.

Acknowledgments

The authors would like to thank the referees for their valuable comments which have significantly improved this paper and Sebelas Maret University for the funding provided. This work was fully supported by the Research Group Funds of the Sebelas Maret University under Grant No. 228/UN27.22/PT.01.03/2023.

References

[1] R.M. Goodwin. *A Growth Cycle*. Cambridge University Press, Cambridge, 1967.

[2] M.O.M. Bastos de Almeida. *The Lotka-Volterra Equations in Finance and Economics*. Master's Final Work Dissertation, Universidade de Lisboa, 2017.

[3] D. Harvie. Testing Goodwin: growth cycles in ten OECD countries. *Camb. J. Econ.* **24** (2000) 349–376.

[4] V. Vadasz. Economic motion: An economic application of the Lotka-Volterra predator-prey model. Franklin and Marshall College Archives, Undergraduate Honors Thesis, 2007.

[5] C.A. Comes. Banking system: Three level Lotka-Volterra model. *Procedia Econ. Financ.* **3** (2012) 251–255.

[6] H.C. Hung, Y.C. Chiu, H.C. Huang and M.C. Wu. An enhanced application of Lotka-Volterra model to forecast the sales of two competing retail formats. *Comput. Ind. Eng.* **109** (2017) 325–334.

[7] T.K. Kar. Stability analysis of a prey-predator model incorporating a prey refuge. *Commun. Nonlinear Sci. Numer. Simul.* **10** (2005) 681–691.

[8] C. Michalakelis, C. Christodoulos, D. Varoutas and T. Sphicopoulos. Dynamic estimation of markets exhibiting a prey-predator behavior. *Expert Syst. Appl.* **39** (2012) 7690–7000.

[9] O. Nikolaieva and Y. Bochko. Application of the "predator-prey" model for analysis and forecasting the share of the market of mobile operating systems. *Int. J. Innov. Technol. Econ.* **4** (24) (2019) 3–11.

[10] R.C. Casten and C.J. Holland. Stability properties of solution to systems of reaction-diffusion equations. *SIAM J. Appl. Math.* **33** (2) (1977) 353–364.

[11] A.W. Wijeratne, F. Yi and J. Wei. Bifurcation analysis in the diffusive Lotka-Volterra system: An application to market economy. *Chaos Solit. Fractals* **40** (2009) 902–911.

[12] S. Yan and S. Guo. Dynamics of a Lotka-Volterra competition-diffusion model with stage structure and spatial heterogeneity. *Discrete Contin. Dyn. Syst.-B* **23** (4) (2018) 1559–1579.

[13] X.P. Yan and C.H. Zhang. Stability and turing instability in a diffusive predator-prey system with Beddington-DeAngelis functional response. *Nonlinear Anal. Real World Appl.* **20** (2014) 1–13.

[14] P. Zhou and D. Xiao D. Global dynamics of a classical Lotka-Volterra competition-diffusion-advection system. *J. Funct. Anal.* **275** (2) (2018) 356–380.

[15] M. Mardiyana, S. Sutrima, R. Setiyowati and R. Respatiwulan. Solvability of equations with time-dependent potentials. *Nonlinear Dyn. Syst. Theory* **22** (3) (2022) 291–302.

[16] S. Sutrima and R. Setiyowati. Equivalent conditions and persistence for uniformly exponential dichotomy. *Nonlinear Dyn. Syst. Theory* **22** (3) (2022) 341–354.

[17] M. Kirane, S. Badraoui and M. Guedda. Uniform boundedness and extinction results of solutions to a predator-prey system. *Electron. J. Qual. Theory Differ. Equ.* **11** (2020) 1–11.

[18] A. Friedman. *Partial Differential Equations of Parabolic Type*. Robert E. Krieger Publishing Company, Florida, 1983.

[19] S. Sutrima, C.R. Indrati and L. Aryati. Exact null controllability, stabilizability, and detectability of linear nonautonomous control systems: A quasisemigroup approach. *Abstr. Appl. Anal.* **3791609** (2018) 1–12.

[20] K. Kishimoto. The diffusive Lotka-Volterra system with three species can have a stable non-constant equilibrium solution. *J. Math. Biology* **10** (1982) 103–112.

Nonlinear Dynamics and Systems Theory, **23** (4) (2023) 447–460

Multiple Well-Posedness of Higher-Order Abstract Cauchy Problem

Habiba Toumi [1*] and Ahmed Nouar [2]

[1] *Laboratory LAMAHIS, University of Badji Mokhtar, Annaba 23000, Algeria.*
[2] *Laboratory of LAMAHIS, University of 20 Août 1955, Skikda 21000, Algeria.*

Received: April 26, 2023; Revised: September 22, 2023

Abstract: In this paper, we fulfill some conditions to examine the multiple well-posedness conditions that define the continuous dependence of the solutions and their derivatives on the initial data of the Cauchy problem. Indeed, for the differential operator equation of arbitrary order in a Hilbert space, an appropriate condition is given for the two main operators that assert the multiple well-posedness. Our results are new and complement some previous ones in the literature.

Keywords: *abstract Cauchy problems; asymptotic stability; integrated semi-groups; stability of nonlinear problems in mechanics; well-posedness.*

Mathematics Subject Classification (2010): 47D09, 70K20, 47D60, 93D20, 34G10.

1 Introduction

In [21], Vlasenko *et al.* studied the p-fold well-posedness of the higher-order abstract Cauchy problem of the following form:

$$\sum_{j=0}^{n} A_j \frac{d^j u}{dt^j} = 0, \qquad t > 0, \tag{1}$$

$$u^j(0) = u_j, \qquad j = 0, ..., n-1, \tag{2}$$

where A_j $(j = 0, ..., n)$ are linear closed operators from a complex Banach space $\mathcal{E}$ into

* Corresponding author: mailto:habiba.toumi@yahoo.com

another complex Banach space $\mathcal{F}$ with the domain of definition $\mathcal{D}(A_j) \subset \mathcal{E}$, A_n can be a degenerate operator.

Many real phenomena can be modeled using problems of the form of $(1),(2)$. For example, many initial-value or initial-boundary value problems for partial differential equations arise in mechanics, physics, engineering, control theory, etc., in particular, the description of vibrations (see [5], [13], [2]) or the vibrations of a viscoelastic pipeline [14]. The theory of problems of this kind is also connected with many other branches of mathematics, which translates the importance of their study for both theoretical investigations and practical applications.

Over the past half-century, $(1),(2)$ has been studied extensively by many scholars. Especially, for the first-order abstract Cauchy problem, the theory (or closely related operator semigroup theory) has evolved relatively well since the well-known Hille-Yosida theorem was presented in 1948, and is well documented in the monographs (see [6], [15] and other), the study of the second-order abstract Cauchy problem has also received much attention. For more information, we can refer to [10], [18], [20], and references cited therein. Since integrated semi-groups were introduced at the end of the eighties of the last century, it has become possible to deal with the ill-posed first-order abstract Cauchy problems (see [16], [11], [8]).

In 2004, Vlasenko *et al.* [21] carried out one of the latest and significant research on establishing conditions that ensure the p-fold well-posedness of the Cauchy problem $(1),(2)$. The study imposed that A_n is a bounded operator and $A_{n-1} = F + B$, where F and B are two operators fulfilling certain criteria that lead to guarantee the p-fold well-posedness in the case of the Hilbert space.

Motivated by the aforementioned works, this paper aims to establish new sufficient conditions that ensure the p-fold well-posedness of the problem $(1),(2)$ even when A_n is a non bounded operator and when the requirements on the two main operators A_n and A_{n-1} are different from those in [21]. The theorem presented in this paper is new and extends and improves previously known results.

Due to its great importance and its many applications in various mathematical fields such as nonlinear dynamics and systems theory (see [1], [22], [3]), many scholars have devoted a great deal of attention to this topic. For example, Vlasenko and his collaborators have published several works in this direction, notably in the case of nonlinear operators. As a result, their interesting outcomes inspired us to find new criteria that guarantee the stability of nonlinear dynamics.

The paper is organized as follows. In Section 2, we introduce some necessary definitions and preliminary results that play a crucial role in establishing our main outcomes. In Section 3, we present some previous global existence results which inspired us to investigate problem $(1),(2)$. Finally, we state and prove our main results in Section 4.

2 Preliminaries

Definition 2.1 (see [21]) We call a solution of problem $(1),(2)$ any function u satisfying condition (2) and

$$u \in C^n((0,\infty),\mathcal{E}) \bigcap C^{n-1}([0,\infty),\mathcal{E})$$

so that

$$A_j u \in C^j((0,\infty),\mathcal{F})\bigcap C^{j-1}([0,\infty),\mathcal{F}),\ \ j=1,...,n.$$

Definition 2.2 (see [21]) The Cauchy problem (1), (2) is $p-$fold well-posed $(p \in \{1,...,n\})$ if and only if for any of its solutions u, the following estimate is true:

$$\left\|u^{p-1}(t)\right\| \leq F(t)\sum_{j=0}^{n-1}\|u_j\|,\ \ t \geq 0, \tag{3}$$

where F is a non-negative function from $\mathbb{R}_+$ to $\mathbb{R}_+$.

Definition 2.3 (see [21]) If F is a locally bounded function on $\mathbb{R}_+$ the problem (1), (2) is $p-$fold uniformly well-posed.

Definition 2.4 (see [21]) The problem (1), (2) is said to be $p-$fold exponentially well-posed if $F(t) = Ce^{\omega t}$, where $C \geq 0$ and $\omega \geq 0$.

Remark 2.1 (see [21]) If $p = n$, the problem (1), (2) is full-fold well-posed.

Examples. Consider the problem of the vibrating string

$$\frac{\partial^2 u}{\partial x^2} - C^2\frac{\partial^2 u}{\partial t^2} = 0,\ \ t>0,\ -\infty < x < \infty,$$

$$u(x,0) = f(x),\quad u_t(x,0) = 0.$$

The solution of this problem is given by

$$u(x,t) = \frac{1}{2}\left[f(x-Ct) + f(x+Ct)\right].$$

Then

$$u(x,t) = \frac{1}{2}\left[G(-Ct)f(x) + G(Ct)f(x)\right],$$

where $\{G(t)\}$ is a semigroup of the operator $\frac{d}{dx}$. We have

$$\begin{aligned}\|u(x,t)\| &= \left\|\frac{1}{2}\left[G(-Ct)f(x) + G(Ct)f(x)\right]\right\| \\ &\leq \frac{1}{2}\|G(-Ct)\|\|f(x)\| + \|G(Ct)\|\|f(x)\|.\end{aligned}$$

$G(-Ct)$ is strongly continuous, then there exist M and ω such that

$$\|G(-Ct)\| \leq M\exp(-\omega Ct),$$

also

$$\|G(Ct)\| \leq M\exp(\omega Ct),$$

which implies that

$$\|u(x,t)\| \leq \tfrac{1}{2}\left(\exp(\omega Ct) + \exp(-\omega Ct)\right)\|f(x)\|.$$

For

$$F(t) = \max\left(\tfrac{1}{2}\left(\exp(\omega C t) + \exp(-\omega C t)\right), 1\right),$$

we have

$$\|u(x,t)\| \leq F(t) \sum_{j=0}^{1} \|u_j\|,$$

$$\begin{aligned} u_t(x,t) &= \frac{1}{2}\left[\frac{dG(-Ct) f(x)}{dt} + \frac{dG(Ct) f(x)}{dt}\right] \\ &= \frac{1}{2}\left[AG(-Ct) f(x) + AG(Ct) f(x)\right]. \end{aligned}$$

As the operator A is unbounded, then there is no nonnegative function F such that

$$\|u_t(x,t)\| \leq K(t) \sum_{j=0}^{1} \|u_j\|.$$

Hence, the problem of the vibrating string is well-posed but is not 2-fold well-posed.

Equation (1) is associated with the characteristic polynomial

$$L(\lambda) = \sum_{j=0}^{n} \lambda^j A_j$$

and its resolvent $\mathcal{R}(\lambda) = L^{-1}(\lambda)$. Let $\mathcal{G}$ be the angle in the complex plane given by

$$\mathcal{G} = \mathcal{G}(b,\theta) = \left\{\lambda = b + re^{i\gamma},\ \ |\gamma| \leq \pi - \theta,\ \ r \geq 0\right\}, \quad 0 < \theta < \frac{\pi}{2},$$

and bounded by a pair of rays. The orientation of the boundary contour Λ should be such that the area $\mathcal{G}$ is located on its left side when bypassing below see Figure **A**.

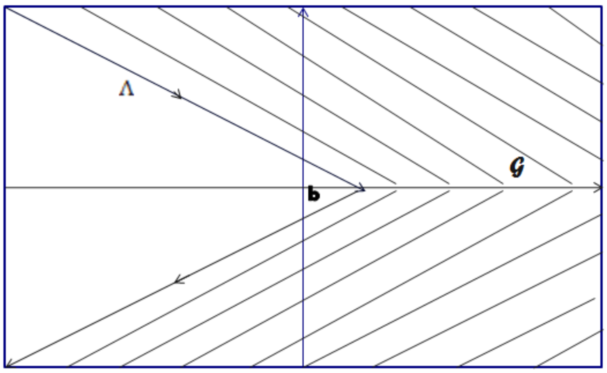

A

Here, the joint properties of the two leading operators A_{n-1} and A_n in terms of the following linear bundle of operators $\mathcal{P}(\lambda)$ and its resolvent $\mathcal{S}(\lambda)$ are

$$\mathcal{P}(\lambda) = \lambda A_n + A_{n-1},$$

$$\mathcal{S}(\lambda) = \mathcal{P}^{-1}(\lambda).$$

Theorem 2.1 *(see [9], [12], [19]) A is a closed linear operator from $\mathcal{E}$ into $\mathcal{E}$ so that $\|A\| \leq q < 1$. Then $(I + A)$ is a reversible and $(I + A)^{-1}$ is a bounded operator.*

Corollary 2.1 *Suppose that $n > 1$, the linear $\mathcal{D}(L)$ is dense in $\mathcal{E}$, the number p belongs to the set $\{1, ..., n\}$ and, in a certain angle $\mathcal{G}(b, \theta)$, $b > 0$, the resolvent $\mathcal{S}(\lambda)$ of the bundle of leading operators satisfies the estimates*

$$\|\mathcal{S}(\lambda) A_j\| \leq C |\lambda|^{n-p}, \quad j = 0, ..., n-1, \tag{4}$$

and

$$\|\mathcal{S}(\lambda) A_j\| \leq C |\lambda|^{q_j}, \quad j = 0, ..., n-2, \tag{5}$$

with the constants $q_j < n - j - 1$. Then the Cauchy problem $(1), (2)$ is full-fold well-posed and $p-$fold exponentially well-posed.

In [21], for the proof, the authors postulated another Cauchy problem and presented the proof without that assumption. The proof is as follows.

Proof. For $\lambda \in \mathcal{G}(a, \theta)$,

$$\begin{aligned} L(\lambda) &= \lambda^n A_n + \lambda^{n-1} A_{n-1} + \sum_{j=0}^{n-2} \lambda^j A_j \\ &= \lambda^{n-1}(\lambda A_n + A_{n-1}) + \sum_{j=0}^{n-2} \lambda^j A_j \\ &= \lambda^{n-1} P(\lambda) + \sum_{j=0}^{n-2} \lambda^j A_j \\ &= \lambda^{n-1} P(\lambda)(I + \sum_{j=0}^{n-2} \lambda^{j-n+1} P^{-1}(\lambda) A_j), \end{aligned}$$

so

$$L(\lambda) = \lambda^{n-1} P(\lambda)(I + \sum_{j=0}^{n-2} \lambda^{j-n+1} S(\lambda) A_j).$$

As the estimate (5) is verified, then

$$\begin{aligned} \left\| \sum_{j=0}^{n-2} \lambda^{j-n+1} S(\lambda) A_j \right\| &\leq \sum_{j=0}^{n-2} |\lambda|^{j-n+1} \|S(\lambda) A_j\| \\ &\leq \sum_{j=0}^{n-2} |\lambda|^{j-n+1} C |\lambda|_j^q \\ &\leq C \sum_{j=0}^{n-2} |\lambda|^{j-n+1+q_j}, \end{aligned}$$

we have $q_j < n - j - 1$, so $j - n + 1 + q_j < 0$, and as $\lambda \in \mathcal{G}(a, \theta)$, this implies that $\left(\frac{1}{|\lambda|}\right)^{-j+n-1-q_j} < \left(\frac{1}{a_0 \sin\theta}\right)^{-j+n-1-q_j}$, $j = 0, \cdots, n-2$. So

$$\begin{aligned}\left\|\sum_{j=0}^{n-2}\lambda^{j-n+1}S(\lambda)A_j\right\| &< C((\frac{1}{|\lambda|})^{n-1-q_0}+(\frac{1}{|\lambda|})^{n-2-q_1}+\cdots+(\frac{1}{|\lambda|})^{1-q_{n-2}})\\ &< C((\frac{1}{a_0\sin\theta})^{n-1-q_0}+(\frac{1}{a_0\sin\theta})^{n-2-q_1}+\cdots\\ &+ (\frac{1}{a_0\sin\theta})^{1-q_{n-2}}),\end{aligned}$$

for $a_0\sin\theta\leq 1$, we let

$$h=\max\left\{n-1-q_0,n-2-q_0,\cdots,1-q_{n-2}\right\},$$

and if $a_0\sin\theta\geq 1$, we let

$$h=\min\left\{n-1-q_0,n-2-q_0,\cdots,1-q_{n-2}\right\},$$

in any case, we have

$$\left\|\sum_{j=0}^{n-2}\lambda^{j-n+1}S(\lambda)A_j\right\|<C((n-1)(\tfrac{1}{a_0\sin\theta})^h).$$

For $a_0=\frac{(C(n-1))^{\frac{1}{h}}}{\sin\theta}$, we get

$$C((n-1)(\tfrac{1}{a_0\sin\theta})^h)=1,$$

therefore $\mathcal{G}_0=\mathcal{G}\left(\frac{(C(n-1))^{\frac{1}{h}}}{\sin\theta},\theta\right)\subset\mathcal{G}(a,\theta)$ so that

$$\left\|\sum_{j=0}^{n-2}\lambda^{j-n+1}S(\lambda)A_j\right\|<1.$$

According to Theorem 2.6, we conclude that

$$\gamma(\lambda)=\left(I+\sum_{j=0}^{n-2}\lambda^{j-n+1}S(\lambda)A_j\right)^{-1}$$

exists and is bounded in $\mathcal{G}_0$. We have also

$$\begin{aligned}\left\|L^{-1}(\lambda)A_jx\right\| &= \left\|(\lambda^{n-1}P(\lambda)(I+\sum_{j=0}^{n-2}\lambda^{j-n+1}P^{-1}(\lambda)A_j))^{-1}A_jx\right\|\\ &= \left\|(I+\sum_{j=0}^{n-2}\lambda^{j-n+1}P^{-1}(\lambda)A_j)^{-1}\lambda^{1-n}P^{-1}(\lambda)A_jx\right\|\\ &\leq \left\|(I+\sum_{j=0}^{n-2}\lambda^{j-n+1}P^{-1}(\lambda)A_j)^{-1}\right\||\lambda|^{1-n}\left\|P^{-1}(\lambda)A_j\right\|\|x\|\\ &\leq \left\|(I+\sum_{j=0}^{n-2}\lambda^{j-n+1}P^{-1}(\lambda)A_j)^{-1}\right\||\lambda|^{1-n}\|S(\lambda)A_j\|\|x\|\\ &\leq \left\|(I+\sum_{j=0}^{n-2}\lambda^{j-n+1}P^{-1}(\lambda)A_j)^{-1}\right\||\lambda|^{1-n}C|\lambda|^{n-p}\|x\|,\end{aligned}$$

and as $(I + \sum\limits_{j=0}^{n-2} \lambda^{j-n+1} S(\lambda) A_j)^{-1}$ exists and is bounded in $\mathcal{G}_0$, then there is $K > 0$ such that

$$\left\| (I + \sum_{j=0}^{n-2} \lambda^{j-n+1} S(\lambda) A_j)^{-1} \right\| \leq K$$

so that

$$\left\| L(\lambda)^{-1} A_j x \right\| \leq KC \left| \lambda \right|^{1-n+n-p} \left\| x \right\|.$$

This implies that there exists $K_1 = CK$ such that

$$\left\| L(\lambda)^{-1} A_j x \right\| \leq K_1 \left| \lambda \right|^{1-p} \left\| x \right\|,$$

and hence

$$\left\| R(\lambda) A_j x \right\| \leq \frac{K_1}{\left| \lambda \right|^{1-p}} \left\| x \right\|.$$

According to Theorem 4 in [21], the result is proved.

We conclude that two conditions (4), (5) are substitutes for condition (19) in [21]. By this corollary, we get the full-fold uniform well-posedness of the initial boundary-value problems that describe small vibrations of an elastic bar in [13].

Theorem 2.2 *(see [9], [12], [19]) A is a self-adjoint operator and A^{-1} exists and is a bounded operator on $R(A)$. Then $\overline{R(A)} = \mathcal{H}$ and A^{-1} is a self-adjoint operator.*

Theorem 2.3 *(see [9], [12], [19]) Suppose $\mathcal{D}(A)$ and $R(A)$ are dense in $\mathcal{H}$ and A^{-1} exists. Then $(A^*)^{-1}$ exists and $(A^*)^{-1} = \left(A^{-1}\right)^*$.*

3 Global Existence Result

In this part, we display some existing theorems [21] that set some conditions which guarantee two inequalities (4) and (5) so that to achieve the full-fold exponentially well-posedness in the case of the Hilbert space $\mathcal{E} = \mathcal{F} = \mathcal{H}$ and for the closed operators A_j with the domains of definitions $\mathcal{D}(A_j)$ being dense in $\mathcal{H}$.

Theorem 3.1 *Suppose that $n > 1$, A_n is a nonnegative bounded operator and $A_{n-1} = F + B$, where F is a self-adjoint operator and B is a symmetric or skew-symmetric operator. Suppose that the linear $\bigcap\limits_{j=0}^{n-1} \mathcal{D}(A_j)$ is dense in H, $\mathcal{D}F \subset \bigcap\limits_{j=0}^{n-2} \mathcal{D}\left(A_j^*\right) \cap \mathcal{D}(B)$, for certain $b \geq 0$, the operator $F + bA_n$ is positive-definite (with a positive lower bound), and*

$$q = \left\| B\left(F + bA_n\right)^{-1} \right\| < 1. \tag{6}$$

Then the Cauchy problem (1), (2) is full-fold well-posed and (n-1)-fold exponentially well-posed. In addition, if A_n is positive-definite, then the problem is full-fold exponentially well-posed.

We can find another condition that guarantees the same results as the previous theorem.

Theorem 3.2 *Suppose that $n > 1$, $D(L)$ is dense in $\mathcal{H}$, $A_n = A_n^* \geq 0$, $A_{n-1} = F + B$, where $F = F^*$, B is a symmetric or skew-symmetric operator, and for a certain number $b \geq 0$, estimate (6) is true, furthermore, $F + bA_n \geq mI > 0$,*

$$\mathcal{D}\left((F + bA_n)^{\frac{1}{2}}\right) \subset \mathcal{D}(A_n) \cap \mathcal{D}(B) \cap \left(\bigcap_{j=0}^{n-2} \mathcal{D}(A_n^*)\right).$$

Then the Cauchy problem (1), (2) is full-fold well-posed and (n-1)-fold exponentially well-posed. In addition, if the operator A_n is positive-definite and bounded, then the problem is full-fold exponentially well-posed.

4 Main Result

In this section, we give the main result of the paper. We will study the case where A_n is an unbounded and non self-adjoint operator.

Theorem 4.1 *Suppose that $n > 1$, $A_n = K + C$, where K is a positive self-adjoint operator and C is a symmetric operator, and A_{n-1} is a symmetric operator such that the linear $\bigcap_{j=0}^{n-1} \mathcal{D}(A_j)$ is dense in $\mathcal{H}$ so that*

$$\mathcal{D}(C^*) \subset \bigcap_{j=0}^{n-2} \mathcal{D}\left(A_j^*\right) \cap \mathcal{D}(A_{n-1}), \ \mathcal{D}(K) \subset \mathcal{D}(C), \tag{7}$$

and for a certain $b \geq 0$, the operator $A_{n-1} + bK$ is positive-definite, we have

$$q = \left\| C(A_{n-1} + bK)^{-1} \right\| \leq \frac{1}{|\lambda|} \tag{8}$$

and

$$\left\| (A_{n-1} + bK) K^{-1} \right\| \leq \frac{1}{b}. \tag{9}$$

Then the Cauchy problem (1), (2) is full-fold well-posed and full-fold exponentially well-posed.

Proof. For $\lambda \in G(b, \theta)$, we have

$$\begin{aligned} \mathcal{D}\left((\lambda A_n + A_{n-1})^*\right) &= \mathcal{D}\left((\lambda K + \lambda C + A_{n-1})^*\right) \\ &= \mathcal{D}(\lambda K) \cap \mathcal{D}(\lambda C) \cap \mathcal{D}\left(A_{n-1}^*\right). \end{aligned} \tag{10}$$

Because C is a symmetric operator, we have $\mathcal{D}(C) \subset \mathcal{D}(C^*)$ and $\mathcal{D}(K) \subset \mathcal{D}(C)$, which means that

$$\mathcal{D}(K) \subset \mathcal{D}(C) \subset \mathcal{D}(C^*).$$

Then

$$\mathcal{D}\left((\lambda K + \lambda C + A_{n-1})^*\right) = \mathcal{D}(K) \cap \mathcal{D}\left(A_{n-1}^*\right)$$

and

$$\mathcal{D}(K) \subset \mathcal{D}(C^*) \subset \mathcal{D}\left(A_{n-1}^*\right).$$

Thus, we have

$$\mathcal{D}\left((\lambda K + \lambda C + A_{n-1})^*\right) = \mathcal{D}(K) \tag{11}$$

and

$$\begin{aligned} \mathcal{D}\left((\lambda K + \lambda C^* + A_{n-1})\right) &= \mathcal{D}(K) \cap \mathcal{D}(C^*) \cap \mathcal{D}(A_{n-1}) \\ &= \mathcal{D}(K) \cap \mathcal{D}(A_{n-1}). \end{aligned}$$

As C is a symmetric operator and using (7), we have

$$\mathcal{D}(K) \subset \mathcal{D}(C) \subset \mathcal{D}(C^*) \subset \mathcal{D}(A_{n-1}),$$

which implies

$$\mathcal{D}\left((\lambda K + \lambda C^* + A_{n-1})\right) = \mathcal{D}(K). \tag{12}$$

Furthermore, according to (11) and (12), we have

$$\mathcal{D}\left((\lambda K + \lambda C + A_{n-1})^*\right) = \mathcal{D}(\lambda K + \lambda C^* + A_{n-1}).$$

In addition, $\forall x \in \mathcal{D}(\lambda K + \lambda C^* + A_{n-1})$, C and A_{n-1} are symmetric operators and K is a self-adjoint operator, we can therefore write

$$\begin{aligned} \langle (\lambda K + \lambda C^* + A_{n-1})\, x, x\rangle &= \left\langle \left(\lambda K + \lambda C^* + A_{n-1}^*\right) x, x\right\rangle \\ &= \left\langle (\lambda K + \lambda C + A_{n-1})^*\, x, x\right\rangle. \end{aligned}$$

As $A_{n-1} + bK$ is a positive operator, we have

$$\begin{aligned} \mathcal{D}\left((A_{n-1} + bK)^*\right) &= \mathcal{D}\left(A_{n-1}^*\right) \cap \mathcal{D}(K) \\ &= \mathcal{D}(K). \end{aligned}$$

We have also

$$\begin{aligned} \mathcal{D}\left((A_{n-1} + bK)\right) &= \mathcal{D}(A_{n-1}) \cap \mathcal{D}(K) \\ &= \mathcal{D}(K). \end{aligned}$$

Therefore

$$\mathcal{D}((A_{n-1} + bK)^*) = \mathcal{D}(A_{n-1} + bK).$$

Let us remind that A_{n-1} are symmetric operators and K is a self-adjoint operator, then $\forall x,\, y \in \mathcal{D}\left((A_{n-1} + bK)^*\right)$,

$$\langle (A_{n-1} + bK)\, x, y\rangle = \langle x, (A_{n-1} + bK)\, y\rangle.$$

This implies that $A_{n-1} + bK$ is a self-adjoint operator, and as C is a symmetric operator, we get

$$\mathcal{D}\left((A_{n-1} + bK)\right) = \mathcal{D}(K).$$

As $\mathcal{D}(K) \subset \mathcal{D}(C)$, we have

$$\mathcal{D}\left(\left(A_{n-1}+bK\right)\right)\subset\mathcal{D}\left(C\right)$$

and

$$\begin{aligned}\|C\| &= \left\|C\left(A_{n-1}+bK\right)^{-1}\left(A_{n-1}+bK\right)\right\| \\ &\leq \left\|C\left(A_{n-1}+bK\right)^{-1}\right\|\left\|\left(A_{n-1}+bK\right)\right\| \\ &\leq q\left\|\left(A_{n-1}+bK\right)\right\|.\end{aligned}$$

As K is a self-adjoint operator, $\mathcal{D}\left(A_{n-1}+bK\right)=\mathcal{D}\left(K\right)$ and

$$\begin{aligned}\left\|\left(A_{n-1}+bK\right)\right\| &= \left\|\left(A_{n-1}+bK\right)K^{-1}K\right\| \\ &\leq \left\|\left(A_{n-1}+bK\right)K^{-1}\right\|\left\|K\right\| \\ &\leq \frac{1}{b}\left\|K\right\| \\ &\leq \left\|bK\right\|.\end{aligned}$$

Then, according to Theorem 4.12 in [9], we obtain

$$\left|\left\langle Cx,x\right\rangle\right|\leq q\left\langle\left(A_{n-1}+bK\right)x,x\right\rangle, \tag{13}$$

$$\left\langle\left(A_{n-1}+bK\right)x,x\right\rangle\leq\left\langle bKx,x\right\rangle \tag{14}$$

for all $x\in\mathcal{D}\left(K\right)$ and $\lambda\in G\left(b,\theta\right).$

Using (13) and (14), for all $x\in\mathcal{D}\left(K\right)$ and for all $\lambda\in G\left(b,\theta\right)$, we get

$$\begin{aligned}&\left|\left\langle\left(\lambda A_{n}+A_{n-1}\right)x,x\right\rangle\right| \\ &\quad= \left|\left\langle\left(\lambda K+\lambda C+A_{n-1}\right)x,x\right\rangle\right| \\ &\quad\geq \left|\left\langle\left(\lambda K+A_{n-1}\right)x,x\right\rangle\right|-\left|\lambda\right|\left|\left\langle Cx,x\right\rangle\right| \\ &\quad\geq \left|\left\langle\left(\lambda K+A_{n-1}-bK+bK\right)x,x\right\rangle\right|-\left|\lambda\right|q\left\langle\left(A_{n-1}+bK\right)x,x\right\rangle \\ &\quad\geq \left|\left\langle\lambda Kx,x\right\rangle\right|-\left\langle\left(bK-\left(A_{n-1}+bK\right)\right)x,x\right\rangle-\left|\lambda\right|q\left\langle\left(A_{n-1}+bK\right)x,x\right\rangle \\ &\quad\geq \left|\left\langle\lambda Kx,x\right\rangle\right|-\left\langle bKx,x\right\rangle+\left\langle\left(A_{n-1}+bK\right)x,x\right\rangle-\left|\lambda\right|q\left\langle\left(A_{n-1}+bK\right)x,x\right\rangle.\end{aligned}$$

As $\left|\lambda\right|\geq b$, then $-\left\langle bKx,x\right\rangle\geq-\left|\lambda\right|\left\langle Kx,x\right\rangle$, which implies that

$$\begin{aligned}&\left|\left\langle\left(\lambda A_{n}+A_{n-1}\right)x,x\right\rangle\right| \\ &\quad\geq \left|\lambda\right|\left\langle Kx,x\right\rangle-\left|\lambda\right|\left\langle Kx,x\right\rangle+\left\langle\left(A_{n-1}+bK\right)x,x\right\rangle-\left|\lambda\right|q\left\langle\left(A_{n-1}+bK\right)x,x\right\rangle \\ &\quad\geq \left(1-\left|\lambda\right|q\right)\left\langle\left(A_{n-1}+bK\right)x,x\right\rangle.\end{aligned}$$

Since $q<\frac{1}{\left|\lambda\right|}$, we have $q\left|\lambda\right|<1$, this gives $0<1-q\left|\lambda\right|<1$, hence $\exists\alpha_{0}\in\left]0,1\right[$ with

$$1-q\left|\lambda\right|\geq\alpha_{0},$$

$A_{n-1}+bK$ is a positive-definite operator, i.e.,

$$\forall x\in\mathcal{D}\left(A_{n-1}+bK\right),\ \exists C_{0}>0:\ \left\langle\left(A_{n-1}+bK\right)x,x\right\rangle\geq C_{0}\left\langle x,x\right\rangle,$$

which implies

$$\begin{aligned}\left|\left\langle\left(\lambda A_{n}+A_{n-1}\right)x,x\right\rangle\right| &\geq \left(1-\left|\lambda\right|q\right)\left\langle\left(A_{n-1}+bK\right)x,x\right\rangle \\ &\geq \alpha_{0}C_{0}\left\langle x,x\right\rangle.\end{aligned}$$

Hence

$$\left|\left\langle\left(\lambda A_{n}+A_{n-1}\right)x,x\right\rangle\right|\geq C_{1}\left\langle x,x\right\rangle, \tag{15}$$

$$\lambda \in \mathcal{G}, \quad x \in \mathcal{D}(K),$$

with $C_1 = 0 + \alpha_0 C_0$. Now, we have

$$(\lambda A_n + A_{n-1})^* = \lambda K + \lambda C^* + A_{n-1}.$$

Then $A_{n-1} + bK$ is a positive self-adjoint operator and C^* is a symmetric operator, therefore

$$\mathcal{D}(A_{n-1} + bK) = \mathcal{D}(K) \subset \mathcal{D}(C^*)$$

and

$$\begin{aligned} \|C^*\| &= \left\| C^* (A_{n-1} + bK)^{-1} (A_{n-1} + bK) \right\| \\ &\leq \left\| C^* (A_{n-1} + bK)^{-1} \right\| \|(A_{n-1} + bK)\| \\ &\leq q \|(A_{n-1} + bK)\|. \end{aligned}$$

Using Theorem 4.12 in [9], we can easily get

$$|\langle C^* x, x\rangle| \leq q \langle (A_{n-1} + bK) x, x\rangle. \tag{16}$$

In the same way as in the proof of inequality (15) and using the relation (16), we can prove the following:

$$\left|\left\langle (\lambda A_n + A_{n-1})^* x, x\right\rangle\right| \geq C_2 \langle x, x\rangle, \quad \lambda \in \mathcal{G}, \ x \in \mathcal{D}(K). \tag{17}$$

In addition, using (15) and (17), we get the existence and the boundedness of $(\lambda A_n + A_{n-1})^{-1}$.

Furthermore, we have

$$\mathcal{D}\left((\lambda A_n + A_{n-1})^*\right) = \mathcal{D}(K)$$

and

$$\mathcal{D}(\lambda A_n + A_{n-1}) = \mathcal{D}(K)$$

with

$$\mathcal{D}\left((\lambda A_n + A_{n-1})^*\right) = \mathcal{D}(\lambda A_n + A_{n-1}).$$

So, $\forall x \in \mathcal{D}(\lambda A_n + A_{n-1})$,

$$\begin{aligned} \langle (\lambda A_n + A_{n-1}) x, x\rangle &= \langle (\lambda K + \lambda C + A_{n-1}) x, x\rangle \\ &= |\lambda| \langle Kx, x\rangle + |\lambda| \langle Cx, x\rangle + \langle A_{n-1} x, x\rangle. \end{aligned}$$

As K is a self-adjoint operator and A_{n-1} is a symmetric operator, we can write

$$\begin{aligned} \langle (\lambda A_n + A_{n-1}) x, x\rangle &= |\lambda| \langle x, Kx\rangle + |\lambda| \langle x, Cx\rangle + \langle x, A_{n-1} x\rangle, \\ &= \langle x, (\lambda A_n + A_{n-1}) x\rangle. \end{aligned}$$

This implies that $(\lambda A_n + A_{n-1})$ is a self-adjoint operator and $(\lambda A_n + A_{n-1})^{-1}$ exists and is bounded on $R(\lambda A_n + A_{n-1})$. According to Theorem 2.9, we conclude that

$R(\lambda A_n + A_{n-1})$ is dense in H and $\mathcal{D}(\lambda A_n + A_{n-1})$ is dense in H. From Theorem 2.9, we find that $\left((\lambda A_n + A_{n-1})^*\right)^{-1}$ exists with

$$\left((\lambda A_n + A_{n-1})^*\right)^{-1} = \left((\lambda A_n + A_{n-1})^{-1}\right)^* = (\lambda A_n + A_{n-1})^{-1}. \tag{18}$$

According to (15), (17) and (18), and for $\mathcal{Q}(\lambda) = \left((\lambda A_n + A_{n-1})^*\right)^{-1}$, there exists a constant $C_3 > 0$ such that

$$\|\mathcal{Q}(\lambda)\| \leq C_3, \quad \lambda \in \mathcal{G}. \tag{19}$$

Use $\mathcal{D}(C^*) \subset \bigcap_{j=0}^{n-2} \mathcal{D}(A^*)_j$ and $\mathcal{D}(K) \subset \mathcal{D}(C)$, where C is a symmetric operator and any $C \subset C^*$, so $\mathcal{D}(K) \subset \bigcap_{j=0}^{n-2} \mathcal{D}(A^*)_j$ and

$$\mathcal{D}(\mathcal{P}^*(\lambda)) = \mathcal{D}(\lambda K + \lambda C + A_{n-1})^* = \mathcal{D}(\lambda K + \lambda C^* + A_{n-1}) = \mathcal{D}(K).$$

Hence

$$\mathcal{D}(\mathcal{P}^*(\lambda)) \subset \bigcap_{j=0}^{n-2} \mathcal{D}(A^*)_j.$$

As $\mathcal{P}^*(\lambda)$ and A_j^* are closed, and according to Remark 1.5 in [9], we have A_j^* are $\mathcal{P}^*(\lambda)$-bounded, where $j = 0, ..., n-2$, this gives

$$\left\|A_j^*\right\| \leq a + b\,\|\mathcal{P}^*(\lambda)\|. \quad \lambda \in \mathcal{G} \;\; a > 0, \;\; b > 0, \;\; j = 0, ..., n-2, \tag{20}$$

and thus

$$\begin{aligned} \left\|A_j^* \mathcal{Q}(\lambda)\right\| &\leq \left\|A_j^*\right\| \|\mathcal{Q}(\lambda)\| \\ &\leq (a + b\,\|\mathcal{P}^*(\lambda)\|)\|\,\mathcal{Q}(\lambda)\|, \\ &\leq a\,\|\mathcal{Q}(\lambda)\| + b\,\|\mathcal{P}^*(\lambda)\|\,\|\mathcal{Q}(\lambda)\|, \end{aligned}$$

where $j = 0, ..., n-2$. We have

$$\mathcal{Q}(\lambda) = (\mathcal{P}^*(\lambda))^{-1},$$

so

$$\|\mathcal{P}^*(\lambda)\|\,\|\mathcal{Q}(\lambda)\| = 1.$$

Therefore

$$\left\|A_j^* \mathcal{Q}(\lambda)\right\| \leq a\,\|\mathcal{Q}(\lambda)\| + b, \quad \lambda \in \mathcal{G}. \tag{21}$$

From (19) and (21), we find that $\exists C_4 > 0$, where

$$\left\|A_j^* \mathcal{Q}(\lambda)\right\| \leq C_4, \quad \lambda \in \mathcal{G} \quad j = 0, ..., n-2, \tag{22}$$

and

$$\left\|A_j^* \mathcal{Q}(\lambda)\right\| = \left\|A_j^* \left(\mathcal{P}^{-1}(\lambda)\right)^*\right\| = \left\|\left(\mathcal{P}^{-1}(\lambda) A_j\right)^*\right\| = \left\|\left(\mathcal{P}^{-1}(\lambda) A_j\right)\right\|$$

so that

$$\left\|\left(\mathcal{P}^{-1}(\lambda) A_j\right)\right\| \leq C_4,\ \ \lambda \in \mathcal{G}(b,\theta),\ j=0,...,n-2. \tag{23}$$

We have $\mathcal{D}(K) \subset \mathcal{D}(A_{n-1})$ and $\mathcal{D}(\mathcal{P}^*(\lambda)) = \mathcal{D}(K)$. If A_{n-1} is a symmetric operator, then

$$\mathcal{D}(\mathcal{P}^*(\lambda)) \subset \mathcal{D}(A_{n-1}) \subset \mathcal{D}\left(A_{n-1}^*\right).$$

As A_{n-1}^* is closable, so A_{n-1}^* is $\mathcal{P}^*(\lambda)$-bounded, therefore

$$\left\|A_{n-1}^*\right\| \leq c + d\left\|\mathcal{P}^*(\lambda)\right\|,\ \ \ \lambda \in \mathcal{G}, c>0,\ d>0. \tag{24}$$

This implies

$$\begin{aligned}
\left\|A_{n-1}^*\mathcal{Q}(\lambda)\right\| &\leq \left\|A_{n-1}^*\right\|\left\|\mathcal{Q}(\lambda)\right\| \\
&\leq (c + d\left\|\mathcal{P}^*(\lambda)\right\|)\left\|\mathcal{Q}(\lambda)\right\|, \\
&\leq c\left\|\mathcal{Q}(\lambda)\right\| + d\left\|\mathcal{P}^*(\lambda)\right\|\left\|\mathcal{Q}(\lambda)\right\|,
\end{aligned}$$

which we can rewrite as

$$\left\|A_{n-1}^*\mathcal{Q}(\lambda)\right\| \leq C_5,\ \ \ \lambda \in \mathcal{G},$$

where $C_5 = c\left\|\mathcal{Q}(\lambda)\right\| + d$. Therefore $\lambda \in G(b,\theta)$, and we have

$$\left\|\mathcal{P}^{-1}(\lambda) A_{n-1}\right\| \leq C_5,\ \ \lambda \in \mathcal{G}. \tag{25}$$

Using (23) and (25), we find that

$$\left\|\left(\mathcal{P}^{-1}(\lambda) A_j\right)\right\| \leq C_6,\ \ \lambda \in G(b,\theta),\ j=0,...,n-1, \tag{26}$$

where $C_6 = \max(C_4, C_5)$. Moreover, the use of (23) leads to the estimate

$$\left\|\left(\mathcal{P}^{-1}(\lambda) A_j\right)\right\| \leq C_4\left|\lambda\right|^{q_j},\ \ \lambda \in G(b,\theta),\ j=0,...,n-2, \tag{27}$$

where $q_j = 0$. Using (26), we get the estimate

$$\left\|\left(\mathcal{P}^{-1}(\lambda) A_j\right)\right\| \leq C_6\left|\lambda\right|^{n-p},\ \ \lambda \in G(b,\theta),\ j=0,...,n-1. \tag{28}$$

For $n=p$, according to (27), (28) and Corollary 2.4, we obtain the full-fold exponential well-posedness and full-fold well-posedness of the Cauchy problem.

5 Conclusion

In this paper, we found the sufficient conditions for the operators Aj in (1), in the case of the Hilbert space, that guarantee the conditions (4), (5) even if A_n is not bounded and self-adjoint. As a result, the problem (1), (2) is full-fold exponentially well-posed. There will always be attempts to find the least possible sufficient conditions to fulfill the multi well-posedness.

References

[1] A. Abbassi, C. Allalou and A. Kassidi. Existense of weak solution for nonlinear p-elliptic problem by topological degree. *Nonlinear Dynamics and Systems Theory* **20** (3) (2021) 229–241.

[2] V. Adamjan, V. I. Pivovarchik and C. Tretter. *On a class of non-selfadjoint quadratic matrix operator pencils arising in elasticity theory.* J. Operator Theory **47** (2) (2002) 325–341.

[3] R. Benterki, L. Damene and L. Baymout. The solution of the second part of the 16th Hilbert problem for a class of piecewise linear hamiltonian saddles separated by conics. *Nonlinear Dynamics and Systems Theory* **22** (3) (2022) 231–242.

[4] P. Colli and A. Favini. On some degenerate second order equations of mixed type. *Funks. Ekvacioj* **38** (1995) 473–489.

[5] H. O. Fattorini. Extension and behavior at infinity of solutions of certain linear operational differential equations. *Pacif. J. Math.* **33** (3) (1970) 583–615.

[6] H. O. Fattorini. *The Cauchy Problem.* Addison-Wesley, Reading, Mass. (1983).

[7] J. A. Goldstein. *Semigroups of Linear Operators and Applications [Russian translation].* Vyshcha Shkola, Kiev, 1989.

[8] L. Jin. Integrated semi-groups and higher-order abstract equations. *J. Math. Ana. App.* **222** (1) (1998) 110–125.

[9] T. Kato. *Perturbation theory for linear operators* [Russian translation]. Mir, Moscow, 1972.

[10] T. D. Ke, V. Obukhovskii, N.-C. Wong and J.-C. Yao. An abstract Cauchy problem for higher-order functional differential inclusions with infinite delay. *Di. Math. Ana. App.* **31** (2) (2011) 199–229.

[11] H. Kellermann and M. Hieber. Integrated semigroups. *J. Funct. Anal.* **84** (1989) 160–180.

[12] N. D. Kopatchevsky. Spectral Theory of Operator Pencils. V.l. Vernadsky Tavrida National University. Simferopol, 2009.

[13] P. Lancaster and A. Shkalikov. Damped vibrations of beams and related spectral problems. *Can. Appl. Math. Quart.* **2** (1) (1994) 45–90.

[14] A. I. Miloslavskii. On the substantiation of the spectral approach to nonconservative problems of the theory of elastic stability. *Funkts. Anal. Prilozhen.* **17** (3) (1983) 83–84.

[15] R. Nagel. One-parameter Semi-groups of Positive Operators (ed). Lecture Notes Math. 1184, Springer-Verlag, Berlin (**1986**).

[16] F. Neubrander. Integrated semigroups and their applications to the abstract Cauchy problem. *Pacif. J. Math.* **135** (1) (1996) 111–155.

[17] F. Neubrander. Well posedness of higher order abstract Cauchy problems. *Trans. Amer. Math. Soc.* **295** (1) (1989) 257–290.

[18] J. C. Saut and N. Tzverkov. The Cauchy problem for of higher-order KP equations. *J. Diff. Equa.* **5** (153) (1998) 32–37.

[19] V. I. Smirnov. *Cour de mathématiques supérieures.* Tome V, Mir, Moscou, 1975.

[20] X. Tijun and L. Jin. Differential operators and C-well-posedness of complete second order abstract Cauchy problems. *Pacific Journal of Mat.* **186** (1) (1998) 167–200.

[21] L. A. Vlasenko, A. L. Piven' and A. G. Rutkas. Criteria for the well-posedness of the Cauchy problem for differential operator equations of arbitrary order. *Ukrain. Math. J.* **56** (2004) 1766–1781.

[22] A. Yu. Aleksandrov. Delay-independent stability conditions for a class of nonlinear mechanical systems. *Nonlinear Dynamics and Systems Theory* **21** (3) (2021) 447–456.